Limiting land subsidence of an island polder with a clay - peat subsurface

Laura Nougues

How can land subsidence be limited in a clay - peat polder through the implementation of water management practices in order to reduce greenhouse gas emissions, improve (ground)water quality and stimulate biodiversity?

TU Delft
Delft University of Technology
DE EENZAAMHEID
Deltares
Hoogheemraadschap van Rijnland
H+N+S+

Limiting land surface subsidence of an island polder with a clay - peat subsurface

by

Laura Nougues

in partial fulfilment of the requirements for the degree of Master of Science
in Civil Engineering, MSc Track: Water Management
at the Delft University of Technology,
to be defended publicly on Friday November 19, 2021 at 15:30.

Student number:	4356233	
Project duration:	March 15, 2021 – November 19, 2021	
Thesis committee:	Prof. dr. ir. R. Uijlenhoet,	TU Delft, Water Management, chair
	Dr. ir. O. Hoes,	TU Delft, Water Management, daily supervisor
	Ir. R. Stuurman,	Deltares, company supervisor
	Dr. ir. F. J. van Leijen,	TU Delft, Geoscience and Remote Sensing, supervisor

TU Delft Delft University of Technology

Preface

This thesis is the result of an eight month long graduation trajectory in which I learned a great deal about peatlands, groundwater modelling and cows. I'm proud of the work I did both in the field and behind my laptop and a large part of what I achieved would not have been possible without the help and support of the following people.

To start off, I would like to thank my graduation committee. Roelof, thank you for making this project possible. I am super grateful that I got to go into the field so much and get my first real taste of the practical side of water management. Olivier, thank you for the continuous support and all the weekly meetings we had to brainstorm about any issue, large or small. Freek, thank you for all your help and tips within the Geoscience and Remote Sensing field, a field I am glad I got to brush the surface of during this project. Lastly, Remko, thank you for the great and helpful feedback and for the time you took to help me figure out the puzzle that was the structure of this report.

Next to my committee, I would like to thank Joost van Schie. Thank you Joost for your hospitality, being so enthusiastic about this project the past eight months and for the amazing opportunity to get to do so many tests at the Eenzaamheid.

Marinus Bogaard, Jaap van der Salm, Dick Melman, Nico Jonker and Jakkus van der Salm. Thank you for all the knowledge you gathered about the Zwanburgerpolder and shared with me. It was a huge addition to this thesis.

From Deltares, I would like to thank Erik van Vilsteren, Frans Roelofsen, André Cinjee, Martine Kox, Henk Kooi, Daan Rooze and Roel Melman. Thank you all for your help with all the lab and field experiments, figuring out iMOD and FlexPDE and making boreholes in the Zwanburgerpolder.

Rui Lima, thank you for coming along to the Zwanburgerpolder for the ditch routing. I am glad I got to see the drone in action and am super happy with the obtained results.

Hans de Graaf and Henk Kooi, thank you for the extensive and very enjoyable tour of the windmill. From our conversations, I was able to get a good understanding of the Zwanburgerpolder, including its history.

I would like to thank my proof-reading committee: my parents, Victor, Jasper and Simone. Thank you for taking the time to dive into my report. Thank you also for all the study breaks you offered in which you pulled me out of my graduation bubble.

Lastly, I would like to thank my fellow graduates from the *afstudeerhok*. Since September, you guys have made the graduation process a lot more fun, especially after working from home for so long. Thank you for all the coffee breaks, ping-pong energizers and the occasional drink to unwind.

Laura Nougues
The Hague, November 2021

Abstract

For hundreds of years, ditch water levels in Dutch agricultural peatlands have been lowered to increase the loading capacity of farming parcels. This lowering results in groundwater levels in the middle of the parcels that fall a few decimeters under the ditch levels. When the groundwater level in a peat soil is lowered, newly uncovered peat is exposed to oxygen and begins to oxidise. This process emits greenhouse gasses (GHG), releases nutrients; like nitrogen and phosphorus that stimulate eutrophication, dries out the top subsurface layer and causes the land to subside.

This study focuses on an island polder in Warmond, the Zwanburgerpolder, with a clay - peat subsurface. Half of the Zwanburgerpolder belongs to the Eenzaamheid, a biological cheese farm with the ambition to transition to a regenerative cheese farm. One of the key objectives to achieve this regenerative goal is to limit the GHG emitted from the farm. An analysis of the current (ground)water system of the Zwanburgerpolder was done which focused on limiting land subsidence by raising the groundwater level and thereby reducing the emission of GHG, improving (ground)water quality and stimulating biodiversity.

First, four research components were examined through field experiments and literature studies: 1) water quantity, 2) water quality, 3) GHG emissions and 4) land surface displacements. The obtained results were used to understand how the Zwanburgerpolder works and identify the relationships between the four components. Then, two groundwater models were developed to represent the current groundwater level and flows in the Zwanburgerpolder: one in iMOD and one in FlexPDE. The iMOD model was used to get a visual representation of the groundwater level variations across the island and to see the groundwater response to precipitation and evaporation. The FlexPDE model was used to get an overview of the phreatic groundwater level drop between two ditches over the summer.

To find the most suitable way to limit land subsidence in the Zwanburgerpolder, the models were adjusted to represent possible future situations. Instead of using the collected climate data of 2021 as input parameter, the projected climate data of 2065 was used. The future models consisted of a base scenario, in which no changes were made to the polder compared to the current situation and adapted scenarios, in which the following five water management measures were tested:

1. Adding ditches,
2. Installing horizontal drains,
3. Temporarily inundating parcels,
4. Installing vertical drains and
5. Raising the summer ditch water level.

Temporarily inundating parcels performed the best quantitatively and qualitatively during the comparison of the measures. However, this measure is agriculturally unfavourable because as a consequence, parcels cannot be used for grazing during a significantly long period of time. For the Eenzaamheid, where regenerative practices and agricultural capacity take center stage, the recommendation for limiting land subsidence is to combine and adjust two measures: temporarily inundating parcels and adding ditches.

Gutters that currently run down the center of the parcels should be enlarged and inundated during the summer period, by siphoning water from the boezem. Inundation can take place during the whole summer, since grazing is still possible alongside the gutters.

It is recommended to start off by only applying the measures in the most critical parcels in order to use it as a testing ground to check the possibly negative effects of the measures besides the desired positive effects of

limiting land subsidence, reducing GHG emissions and improving the (ground)water quality.

Further, the results discussed in this report provide an interesting addition to peatland subsidence studies. They were obtained through field experiments done on a much smaller budget than other studies done so far with expensive measurement setups. The recommendation towards such peatland subsidence studies is therefore to apply a large network of lower cost measurement setups, instead of a few costly ones, in order to get an extensive representation of the behaviour of different Dutch peatlands.

The main limitations in this study are the uncertainties linked to the parameters used to build the iMOD and FlexPDE models and the time constraint on the field experiments. The parameter uncertainties mean that the final model outputs fall within a certain error range. To minimize the error range, a model sensitivity and uncertainty analysis should be done. Without the field work time constraint, it would have been possible to identify the seasonal patterns in the groundwater level fluctuations compared to the other water bodies and in the land surface displacements.

Abbreviations and glossary

Actueel Hoogtebestand Nederland - AHN

Carbon dioxide - CO_2

Dissolved oxygen - DO

Electrical conductivity - EC

Food and Agriculture Organization of the United Nations - FAO

Global Navigation Satellite System - GNSS

Greenhouse gas - GHG

Inductively Coupled Plasma - Optical Emission Spectrometery - ICP-OES

Interferometric Synthetic Aperture Radar - InSAR

Ion Chromatography - IC

Kader Richtlijn Water - KRW

Landelijk Hydrologisch Model - LHM

Lowest groundwater level - LGL

Methane - CH_4

Micro-portable greenhouse gas analyzer - MGGA

Nationaal Onderzoeksprogramma Broeikasgassen Veenweide - NOBV

Nitrous oxide - N_2O

Surface elevation table - SET

Auger - a drill used for making holes in, specific for this study, the ground.

Aquifer - a water holding, subsurface layer.

Boezem - a higher laying water body that collects water pumped out of lower laying polders.

Mole drainage - unlined channels that are formed in the subsurface by pulling a cone attached to a blade through it.

Polder - an area that is protected from outer water by a embankment and that has a controlled water level.

Regenerative agriculture - a process which “describes farming and grazing practices that, among other benefits, reverse climate change by rebuilding soil organic matter and restoring degraded soil biodiversity – resulting in both carbon draw down and improving the water cycle" [Regenerative Agriculture Initiative, 2017].

Tillage - Agricultural preparation of soil by mechanical agitation of various types, such as digging, stirring, and overturning.

Contents

1 Introduction

1.1. Problem statement

The current industrial agricultural practices are not built to last. These are often large farms, growing the same crops year after year, built only for efficiency and profit while degrading soils, water and biodiversity. This agricultural intensification is also seen within the Dutch peatland food production systems [Sukkel et al., 2019]. Here, the agricultural systems deplete finite resources, make land more vulnerable to the changing climate and are monocultures [Sukkel et al., 2019, Wesselink, 2019]. To increase the loading capacity of farming parcels, ditch water levels in agricultural peatlands have been lowered for hundreds of years, with a significant intensification since the late sixties [Roncken et al., 2019]. Ditches in the western peatlands in the Netherlands have been lowered by up to 60 cm below the surface level and in Friesland as much as 150 cm below the surface level [van den Akker et al., 2010].

These lowered ditch water levels result in groundwater levels in the middle of the parcels that fall a few decimetres under the ditch level during warm, dry summers when infiltration from the ditches cannot keep up with evaporation. When the groundwater level in a peat soil is lowered, uncovered peat is exposed to oxygen and begins to oxidise. Peat oxidation is a biological decomposition process in which carbon dioxide (CO_2), methane (CH_4) and nitrous oxide (N_2O), which are initially trapped in the peat, are emitted as well as nutrients, like nitrogen and phosphorus, that stimulate eutrophication in ditches. Further, the top subsurface dries, out damaging the biodiversity, and the land subsides. Over time, as the ground level subsides, the groundwater level needs to be decreased further, creating a vicious cycle. In Figure 1.1, a diagram depicting the subsidence process is shown.

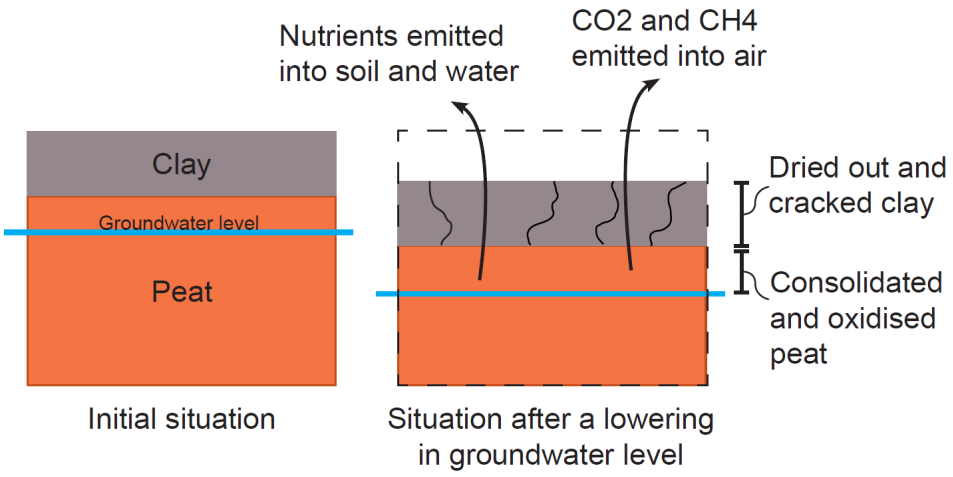

Figure 1.1: Land surface subsidence development for a clay - peat subsurface.

Provinces, water boards, peatland farmers and nature conservation organisations recognize the ongoing issue. In 2019, the Dutch Climate Act was developed following the 2015 Treaty of Paris and states that by 2030, the yearly agricultural peatland greenhouse gas (GHG) emissions need to be reduced by 1 Mton [Erkens et al., 2020]. In response to this, the Nationaal Onderzoeksprogramma Broeikasgassen Veenweiden (NOBV) re-

search program was initiated: a long-term research program that structurally monitors land subsidence and the emission of GHG from peatlands and investigates the effectiveness of measures that limit this emission. The NOBV examines five study locations across the Netherlands. However, with more than 270.000 ha of agricultural peatlands spread across North and South Holland, Utrecht, Friesland, Overijsel and Groningen [de Vries, 2011], it is difficult to make conclusions for all Dutch peatlands based on five locations. The more study locations investigated, the more representative the results are to the whole extent of the Dutch peatlands.

This study focuses on an island polder in Warmond, the Zwanburgerpolder, with a clay - peat subsurface. Half of the Zwanburgerpolder belongs to the Eenzaamheid, a biological cheese farm. By 2040, Joost van Schie, sixth generation farmer of the Eenzaamhied, hopes to have transitioned to a regenerative cheese farm. One of the key objectives Joost has set out for himself to achieve this regenerative goal is to limit the GHG emitted from the farm, i.e., limit peat oxidation and therefore land subsidence. A goal that fits well in reaching the Climate Act objective by 2030.

1.2. Research question

The research question for this study is:

How can land subsidence be limited in a clay - peat polder through the implementation of water management practices in order to reduce greenhouse gas emissions, improve (ground)water quality and stimulate biodiversity?

With the following sub-questions:

1. How does the current Zwanburgerpolder system work?
2. Which water management measures can be implemented to limit land subsidence?
3. How effective are these measures?

In this study an analysis of the current (ground)water system of the Zwanburgerpolder was done in which the focus was laid on limiting land subsidence by raising the groundwater level and thereby reducing the emission of GHG, improving (ground)water quality and stimulating biodiversity.

The results acquired within the research are an important stepping stone for the Eenzaamheid in understanding the natural system on which it is built and which water management measures are most effective in transitioning to a regenerative system with low GHG emissions. Further, the results from this study can be implemented on a larger scale by combining them with the NOBV results and other similar studies. This will allow for a better understanding of the behaviour of different peatlands and which measures are most suitable to be implement, in order to reach the national Climate Act goal by 2030.

1.3. Reading guide

In Chapter 2, a brief description of the Zwanburgerpolder is given. The shallow subsurface composition of the island is examined as well as the current farm operations of the Eenzaamheid and the biodiversity found on the Zwanburgerpolder. This is followed by an explanation the Zwanburgerpolder water level decree, a document in which water level requirements for designated surface water bodies are stated.

In Chapter 3, the literature study is presented. Here, the literature that was used to get background information for this thesis is described. This includes the subsidence process in peatlands, different measurement techniques to quantify land surface displacements and a detailed definition of regenerative agriculture and regenerative practices.

The next four chapters focus on one of four research components that link back to the research question, namely: 1) water quantity, 2) water quality, 3) GHG emissions and 4) land surface displacements. Chapter 4 deals with water quantity which is composed of the polder's water balance, the groundwater level variations and the subsurface hydraulic conductivity. The field experiments used to quantify the different elements are

explained and their results are shown. Then, the two groundwater models, iMOD and FlexPDE, used to represent the current Zwanburgerpolder system are presented.

Chapter 5 covers water quality. Here, the methodology used to find both the groundwater quality and surface water quality is explained. This is followed by the results of the experiments. Chapter 6 focuses on GHG emissions. Again, the chapter starts off explaining the methodology of the field tests. Then, using the results from the tests and literature values, a distinction between the different GHG contributors from the Eenzaamheid was made. Finally, Chapter 7 analyses land surface displacements. In this chapter, the field work methodology is firstly given and then the results are presented.

In Chapter 8, the future scenarios for the Zwanburgerpolder are looked at. Firstly, different water management measures that can be used to tackle land subsidence are described. Then, the future models are presented: the base scenario in which no changes were made to the polder compared to the current situation and the adapted scenarios in which five different water management measures were taken to limit land surface subsidence.

In Chapter 9, the results are discussed. This includes both a discussion of the relationships between groundwater level, yearly land subsidence and GHG emissions, as well as a discussion of the different future scenarios laid out in Chapter 8 and the limitations met during this study.

In the final chapter, Chapter 10, the conclusions are drawn and the efficiency of the adapted scenarios in limiting land subsidence while reducing the emission of GHGs, improving (ground)water quality and stimulating biodiversity is evaluated. Finally, recommendations are given regarding the applicability of the study results to the Zwanburgerpolder as well as to a wider, national scale and about further research that can be done at the polder to strengthen the understanding of the polder system and similar systems.

2

Site description

2.1. Research area

The Eenzaamheid is located on the Zwanburgerpolder, a peat island polder, in Warmond, in the province of South Holland. The polder has an area of 87.7 ha, out of which 9 ha (10 %) is covered by water [Vaartjes, 2020]. A little less than half of the polder, 40.7 ha, belongs to the Eenzaamheid. Apart from the Eenzaamheid, another farmer uses the western parcels for his cows to graze on and there are a few inhabitants that live on the island or on houseboats docked on the island. The Zwanburgerpolder has a winter water level of −1.81 mNAP, a summer level of −1.71 mNAP and a current average surface level of −1.33 mNAP. The boezem summer and winter water levels fluctuate between −0.61 mNAP and −0.64 mNAP respectively. An overview of the polder and the Eenzaamheid can be seen in Figure 2.1 and the transect of the north eastern part of the island, transect A-B, can be seen in Figure 2.2. What stands out in the height transect, is that there are narrow gutters in the middle of almost every parcel and the island is fairly concave.

Figure 2.1: Map of the Zwanburgerpolder, with an outline of the Eenzaamheid in the east.

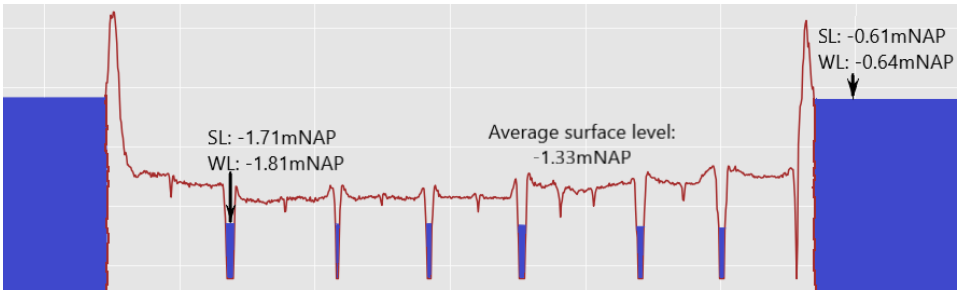

Figure 2.2: Height transect A-B (left to right) of the Zwanburgerpolder in which the summer and winter water levels can be seen [AHN, 2019].

As can bee seen in Figure 2.1, the polder inlet is located on the eastern side of the polder. This inlet is used to raise the ditch water level or flush the ditches. Generally, the polder inlet is only opened in summer periods. On the western side of the polder there is a lock, a windmill and a pumping station. The lock is used about twenty times a year by the farmer that brings his cows into the polder to graze. The windmill is operated once every week on Thursdays to lower the polder water level when there is a water surplus in the area. The pumping station further regulates the water level in the polder by discharging water into the boezem when the windmill is not operated.

The first use of the Zwanburgerpolder for agriculture dates back to 1000 AD. Back then, the island was not a polder, as it surface level was above the surrounding water level in the summer. As agriculture intensified, the peatland subsided and small hand mills and horse mills were placed around 1500 in the island to lower the polder water level. In 1632, the polder was established as the Zwanburgerpolder and one large windmill was placed in the polder to regulate the polder water level. This windmill was replaced in 1805 by the current Zwanburgermill [Slingerland, 2006]. The milling history of the Zwanburgerpolder insinuates that since about 1500, the land has subsided from about −0.61 mNAP, the boezem target water level, to −1.33 mNAP, the current average polder surface level. This is equal to 70 cm in about 500 years or 1.3 mm/year. A similar estimate is also made by SkyGeo Netherlands in the land subsidence map of the Netherlands, when the Zwanburgerpolder has a yearly subsidence of about −0.5 mm to −1.5 mm [SkyGeo, 2018].

2.2. Shallow subsurface composition

Realistically mapping out the shallow subsurface composition is an important aspect in understating the Zwanburgerpolder system. The shallow subsurface composition was reconstructed by combining both field results of eight auger samples of the top 2 m of the subsurface and data from 82 boreholes collected from DINOloket [DINOlokket, 2021]. The location and composition of the different boreholes can be seen in Figure A.1 in Appendix A. It was established that the peat subsurface layer is sandwiched between two clay layers, a top, thin clay layer and a deeper, thick clay layer. Below this, the first sand aquifer is found at a depth of −5 mNAP.

Using the DINOloket borehole data, an interpolation was made of the top 2 m of the polders subsurface. The results of this interpolation can be seen below in Figures 2.3 and 2.4, where four subsurface transects are displayed. From these figures, it can be seen that the clay to peat transition occurs between 0.5 m and 1 m below the surface level.

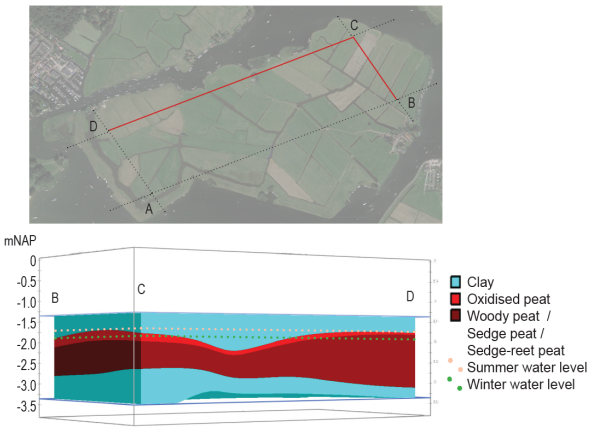

Figure 2.3: Subsurface composition from borehole interpolation of the north eastern part of the polder.

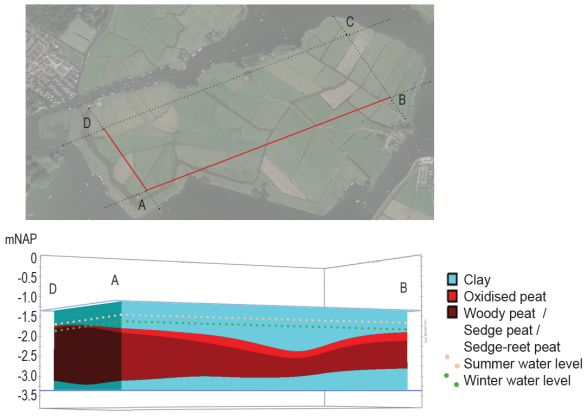

Figure 2.4: Subsurface composition from borehole interpolation of the south western part of the polder.

This was also confirmed in the eight manually executed boreholes. During the field sampling, different types of clay and peat were found, depending on the degree of decomposition of the sample. In the field, highly decomposed peat samples (oxidised peat) were identified at the top of the peat layer by their black color, lack of fibrous texture and little amounts of distinct plant remains. In contrast, the lower peat layers had a brown color, along with a fibrous texture and an odor of decay, suggesting a layer of unoxidised peat covered by groundwater. The remains of the oxidised peat only makes up a small portion of the total peat layer. In

Appendix A, the thickness of each subsurface layer can be seen. Below, a map was made that shows that distance between the summer ditch water level and the bottom of the oxidised peat layer, see Figure 2.5. Essentially, this map shows by how much the groundwater can drop before stimulating peat oxidation in the currently unoxidised peat layer.

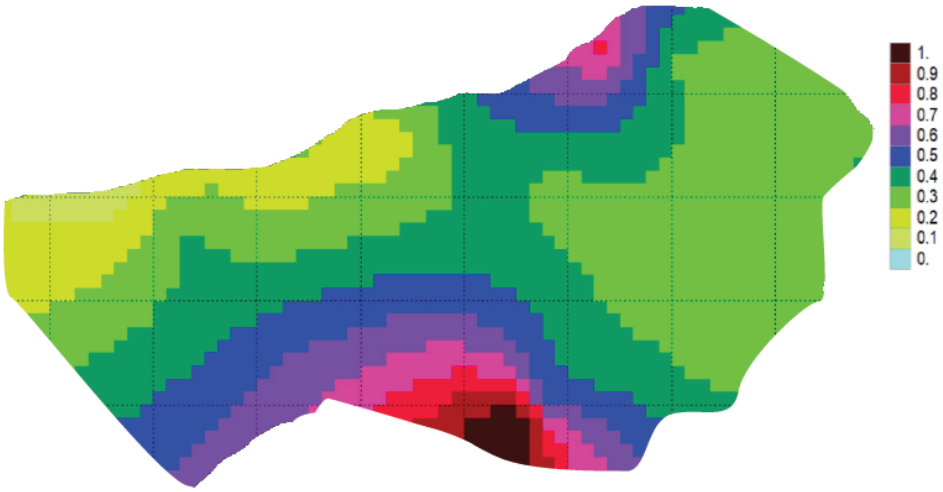

Figure 2.5: Map showing the distance between the summer ditch water level and the bottom of the oxidised peat layer, and so the acceptable groundwater drop relative to the summer ditch water level before peat oxidation is stimulated [m].

2.3. Farm operation

The Eenzaamheid has been in the van Schie family since 1849 and has been a biological cheese farm for twenty years. The farm currently has fifty dairy cows, 25 calves and 40.7 ha of land. The current farm operation can be seen in Table 2.1. This information was gathered during an interview with Joost van Schie, the sixth generation farmer at the Eenzaamheid. The table is split up into the substances imported into the island, the substances exported off from the farm and the substances collected and used/stored on the island.

Table 2.1: Overview of the farm operations done on the Eenzaamheid.

Brought in to island				Brought out from island				Stays on island			
What	How much	When	How	What	How much	When	How	What	How much	When	How
Concentrate (Dutch: *krachtvoer*)	24 t/ year	Continuous	Cows get 1.5 kg/day in the summer and 3 kg/day in the winter.	Cheese	20 t/year	Continuous	Made from about 275.000 l milk.	Ecological dredging	Top 20 cm of ditch bottom is dredged.	Every year in September	Sludge and riverbank plants removed are laid along the ditch banks.
Agricultural liming (Dutch: *bekalking*)	0.5 - 1 t/ha/application	Maintenance liming happens once every two years	The previous maintenance liming was done with quarry lime. During the last reparation liming eggshell lime was used (2 t/ ha).	Milk	90.000 l/year	Continuous	Goes to milk factory.	Extensive dredging		1 x per 2 years in the summer	The removed sludge is sprayed up to 30 m inwards from the ditch banks.
Mowed grass - Lakerpolder	22.500 kg/year	Mowing happens begin July and September	90 barrels of 250 kg mowed grass.	Mowed grass - Lakerpolder and Zwanburgerpolder	32.000 kg/year	Lakerpolder: Begin July begin September. Zwanburgerpolder: Between 10 May and 10 July first mowing, then 2 - 3 x per parcel till September.	80 barrels of 400 kg used as horse food.	Liquid manure	1200 m^3/year	End of March then 2 - 3 x per parcel after the parcels has been mowed.	Liquid manure from the stable winter store is laid in strips across the parcels. It consists of liquid manure and water.
								Solid manure	60 m^3/year	End of March	Solid manure is laid out in the meadow bird field, in the northern part of the island. Consists of solid manure and leftover food.
								Mowed grass - Zwanburgerpolder	168.75 t/year	Between 10 May and 10 July first mowing, then 2 - 3 x per parcel till September.	
								Whey	80,000 l		Liquid left over after cheese making process. Half is given to the calves and the over half is added to the manure pit.
								Cows	50		
								Calves	25		

2.4. Biodiversity

The Zwanburgerpolder has a rich biodiversity. In the northern part of the island a few parcels are constantly kept wet, making it an ideal breeding location for black-tailed godwits, lapwings, oystercatchers and redshanks. Common terns, skylarks, curlews, field fares, herons, storks, hen harriers and buzzards also appear in considerable numbers, as well as aquatic and wading birds like avocets, geese, cormorants, grebes, gadwall ducks, tufted ducks and coots. Apart from birds, the Zwanburgerpolder is also home to fish, especially carp and bream, amphibians like frogs, toads and lizards, and small mammals like hares, mice and ermine [Slingerland, 2006].

The topsoil in the Zwanburgerpolder also contains a varied biodiversity. During a study done on the topsoil biodiversity, four soil samples of 20 cm x 20 cm x 10 cm were dug out and the soil life was examined [Melman et al., 2021]. Samples 1 and 2 were collected close together on one parcel, and samples 3 and 4 were collected on a different parcel. In all four samples, earth worms and ground beetles were counted while the number of crane flies were only identified in samples 3 and 4. The quantification of the tallied insects can be seen in the Table 2.2.

Table 2.2: Tallied biodiversity in a 20 cm x 20 cm x 10 cm soil samples from the top subsurface [Melman et al., 2021].

Sample	Earthworm	Crane fly	Ground beetle
1	52	0	1
2	41	0	2
3	16	3	1
4	26	7	3

At the beginning of May and the end of August, a study was done on the soil moisture and soil penetration resistance of three transects in the Zwanburgerpolder. Across the measured transects, the soil moisture was significantly lower in August then in May and the soil penetration resistance higher [Melman et al., 2021]. To preserve such a vast biodiversity, it is important to keep the soil moisture in the topsoil high. The desiccation of the top soil reduces the availability of worms for meadow birds as the worms then remain deeper in the soil [Onrust et al., 2019] and a high soil resistance makes it hard for birds to poke their beaks into the soil [Onrust, 2017].

2.5. Water level decree

In a water level decree, the water level requirements for designated surface water bodies are stated. These water level decrees are written by the responsible waterboards. When determining the desired water levels, waterboards need to take different factors into consideration like: the land use (urban areas, agriculture, nature), the ecological quality of the area and any water system functions (shipping).

Through the Hoogheemraadschap van Rijnland waterboard (mentioned as Rijnland hereafter), the current and previous water level decrees for the Zwanburgerpolder were received. The designated summer and winter water levels of the 1995 and 2010 decrees can be seen in Table 2.3. Until recently, the water level decrees had to be revised every ten years, with the opportunity to prolong the decree by five years. This is what happened to the water level decree of 1995. It was valid until 2005 and then extended by five years, after which a new decree was made for 2010 onward. However, since recently, the province of South Holland has discarded this regulation, so the current water level decree written in 2010 will be valid until at least 2027 [Hoogheemraadschap van Rijnland, 2021].

Table 2.3: Water level decrees of the Zwanburgerpolder for 1995 - 2010 and 2010 - 2027.

	Summer water level [m NAP]	Winter water level [m NAP]
Decree 1995	−1.70	−1.80
Decree 2010	−1.71	−1.81

3
Literature study

In this chapter background knowledge that was collected prior to beginning the study is described. This includes information about the impacts of subsidence in peatlands, different methods to measure land surface displacements and finally more in depth information about what regenerative farming entails.

3.1. Subsidence in peatlands

Subsidence in peatlands happens due to: 1) shrinkage, 2) compression and 3) peat oxidation. When groundwater levels drop, the newly uncovered peat firstly shrinks (due to loss of volume and changes in moisture content) and compresses (under its own weight due to the loss of buoyant force of water), then the uncovered peat oxidises (due to the exposure of carbon in peat to oxygen) [Doornenbal and Melman, 2021]. During peat oxidation, carbon is removed from the soil, changing the texture of the peat and causing a loss in volume. Up to 70 % of the subsidence can be attributed to oxidation [Erkens et al., 2020].

Next to land subsidence, during peat oxidation, the CO_2 and CH_4 initially trapped in the peat are emitted and nutrients, like nitrogen and phosphorus, are flushed into ditches, stimulating eutrophication and reducing the water quality. Furthermore, due to a lowering groundwater level, the top subsurface layer dries out, which is unfavourable for biodiversity. A simplified diagram of this process can be seen back in Figure 1.1.

Often, in agricultural peatlands, through the lowering the surface water level, the groundwater level is lowered to improve surface loadability, leading to peat oxidation and land subsidence. Over time the surface water level will need to be lowered again, creating a vicious cycle and making reclaimed peatlands large carbon sources, when in comparison, natural, unreclaimed, swampy peatlands act as carbon sinks. Under natural conditions, large amounts of carbon are locked away in peat tissues. In 2017, about 15 % of all the peatlands across the world had been drained [International Union for Conservation of Nature, 2017, Uijl, 2010].

3.2. Land surface displacement measurement

Land surface displacement can be measured using different techniques, varying between manual and digital measurements, and terrestrial and spaceborne measurements. In the following section, three levelling instruments are briefly described (extensometer, SET and digital leveller) as well as two spaceborne techniques (GNSS and InSAR). Following this, an overview of each technique's pro's and con's is given.

Extensometer

An extensometer is a device that is used to measure changes in the length of an object and in the case of land surface displacements, extensometers measure the compaction and expansion of the subsurface. The lower end of extensometers is anchored in a stable layer and over time, the extensometer continuously measures the change between the deep reference point and the land surface elevation [Harris-Galveston Subsidence District, 2020].

SET

The surface elevation table (SET), similar to the extensometer, is a portable mechanical leveling device that measures the relative elevation change between the surface level and an anchored reference point. This method, however, is specifically used for making highly accurate and precise measurements of wetlands and shallow water environments [Lynch et al., 2015].

Digital leveller
A digital leveller relies on an electronic laser that scans a leveling rod with bar code markings. The digital leveller is placed on a stable tripod at a random location and starts off by measuring the rod placed on a stable reference point. After this, the levelling rod is moved across a predefined transect. At each new measuring location, the difference in surface level height between the reference point and the measuring point is measured [Doornenbal and Melman, 2021]. The maximum distance between the digital leveller and the levelling rod, without setting up a network, depends on the levelling instrument used, but usually goes up to 60 m. However, the further away the levelling rod is to the digital leveller, the larger the measuring error [Algarni and Ali, 1998].

GNSS
Global Navigation Satellite System (GNSS) receivers use a constellation of at least four GNSS satellites to determine the vertical and horizontal location of the receiver [EUSPA, 2021, Fokker et al., 2018]. The satellites broadcast a time code, and the GNSS receiver compares this received code to its internal clock. The time difference is then multiplied with the speed of light to get the pseudo-range measurement or the distance between the satellite and receiver. Accurate, geodetic GNSS receivers are able to track the carrier phase and can simultaneously track numerous GNSS satellite bands eliminating delays in the post processing and providing millimetre range measurements [Fokker et al., 2018].

InSAR
Interferometric Synthetic Aperture Radar (InSAR) is a measurement technique that uses radar images of the Earth's surface to detect ground deformation. Synthetic aperture radar (SAR) satellites orbit the Earth and actively transmit radar signals towards the surface [Fokker et al., 2018], meaning they are not dependent on natural waves and can track deformations in bad weather and at night. At two different time periods, a SAR satellite makes a radar image of the land surface, after which an interferogram is created of how much the surface moved during the time period between the subsequent images [Helz, 2005].

Technique comparison
In Table 3.1, the comparison of the five different measuring techniques can be seen.

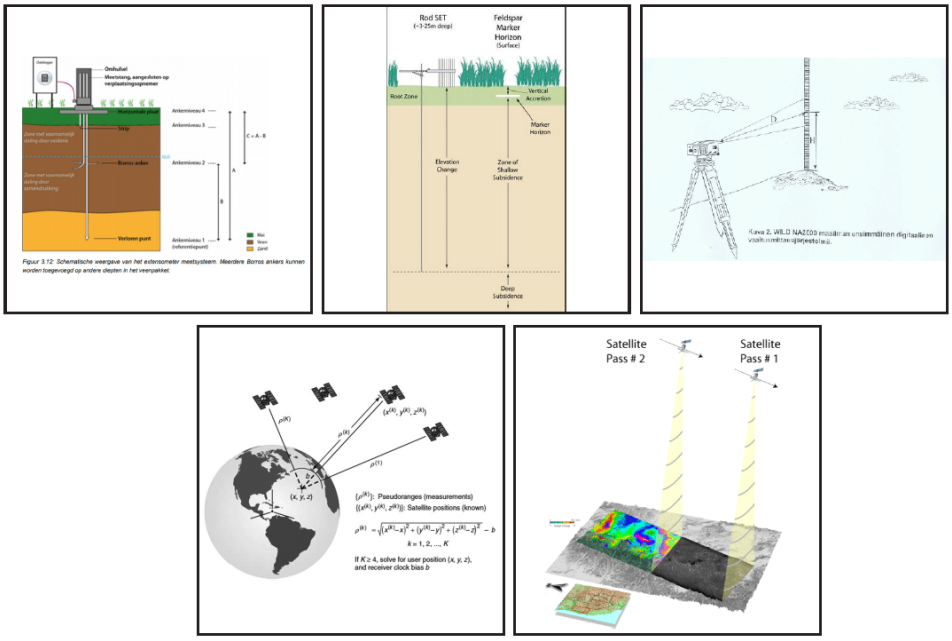

Figure 3.1: Surface elevation measuring techniques (L to R, T to B): extensometer [Asselen et al., 2020], SET [Lynch et al., 2015], Digital leveller [Takalo and Rouhiainen, 2004], GNSS [Fokker et al., 2018] and InSAR [Helz, 2005].

Table 3.1: Comparison of five discussed land surface displacement measurement techniques [Doornenbal and Melman, 2021, Fokker et al., 2018, GalileoGNSS, 2018, Galloway et al., 2000, Lynch et al., 2015].

Technique	Resolution [mm]	Spatial density [samples/survey]	Spatial scale [elements]	Advantages	Disadvantages
Extensometer	0.01 - 0.1	1 - 3	Point	High accuracy and continuous data.	Expensive, complex to install and limited coverage.
SET	0.1 - 1	1 - 3	Point	Accurate and continuous data.	Expensive, complex to install and limited coverage.
Digital leveller	0.1 - 1	10 - 100	Line - network	High accuracy.	Labour intensive and limited measuring range.
GNSS	2 - 10	10 - 100	Network	Provides accurate, reliable and quick location estimates.	Difficult to apply in densely built areas.
InSAR	2 - 10	100,000 - 10,000,000	Map pixel	High spatial coverage.	Difficult to apply in rural, vegetation covered areas.

To measure the land surface displacements in this study, it was decided to use GNSS receivers. The extensometer and SET were directly discarded, as these did not fit the financial scope of this project. InSAR data works best on hard surfaces like roofs and exposed rock and has difficulties to measure surfaces with a vegetation cover [Chen et al., 2021]. As the Zwanburgerpolder is mainly covered by grass, it was decided that InSAR data would therefore not be appropriate either.

In terms of accuracy, the digital leveling instrument is better than GNSS receivers. However, the preference still went to using GNSS receivers due to its spatial freedom. When using a digital levelling instrument, all measurements have to be done within a 60 m range from the steady reference point, limiting the measuring area to a small section of an individual parcel. However, in this study, the relationship between surface level and groundwater level will be looked at, so the surface displacements by the different boreholes is wanted, which are located further than 60 m from each other. Furthermore, based on land surface displacements results obtained by the NOBV [Erkens et al., 2020], it is expected that the peat subsurface will fluctuate several centimeters during rain events and dry periods, meaning the land surface fluctuations will be big enough to monitor with a GNSS receiver.

3.3. Regenerative agriculture

Regenerative farming describes farming practices that focus on regenerating topsoil, increasing local biodiversity and improving the water holding capacity of the soil [Regenerative Agriculture Initiative, 2017]. Regenerative farming practices result in an increased resilience against climate change, reverse human caused soil loss, strengthen the health and vitality of soil, reduce CO_2 emissions and make the soil more resistant to pests and diseases [Wageningen University and Research, 2019]. Regenerative farming practices include [California State University, 2021]:

- *Limiting tillage* : tillage breaks up soil aggregations, increasing soil erosion. When using heavy machinery, the top soil spaces become plugged, stimulating surface runoff and being unfavourable for the water holding capacity of the soil.
- *Ceasing the use of artificial and synthetic fertilizers* : by replacing artificial and synthetic fertilizers with soil amendments like compost and manure, physical properties of the soil can be enhanced, like soil texture and pH. This in turn helps restore soil fertility, increases fungal:bacteria ratios and in the long term, can lead to carbon sequestration.
- *Applying multi-species cover crops* : cover crops are crops that are specifically used for the purpose of improving soil health. They are not necessarily cash crops, but when applied to a parcel they increase soil fertility, improve the water retention capacity of the soil, manage soil erosion and stimulate a varied biodiversity.
- *Applying crop rotations* : crop rotation is the practice of growing different crops in the same parcels across different growing seasons. This reduces the crops' vulnerability to different diseases and when done correctly, limits soil erosion and enhances soil biodiversity and fertility.
- *Implementing well-managed grazing practices* : instead of following a set protocol, farmers should modify grazing patterns according to actual conditions and feedback from the environment in order to avoid overgrazing. In this practice it is also important to carefully control the livestock density according to available space.
- *Implementing well-managed water management practices* : it should be ensured that sufficient, clean water is available at all times by applying water storages, dynamic (ground)water level management and specified irrigation. This can, in turn, prevent droughts, over saturation of crops and nutrient runoff.

In this study, the focus has been laid on the water management practices that can be applied in favour of both transitioning to a regenerative farm and limiting land subsidence.

4

Water quantity

This chapter looks at understanding the different interactions between the phreatic groundwater, deeper groundwater and boezem-water. This is done by looking at the polder's water balance, groundwater level variations and the subsurface hydraulic conductivity. Using field experiments and collected time series, these different elements were quantified. After this, it was possible to make two groundwater models that represent the current Zwanburgerpolder. In this chapter, the methodologies for both the data collection and the models are presented as well as their results after which a short conclusion is given about the interactions between the different water bodies.

4.1. Methodology

4.1.1. Water balance

Yearly water balances for 2017 - 2020 of the polder were made to investigate the size of the different recharge and discharge fluxes in the polder and how these vary over time. These balances were used when making and calibrating the model of the current polder situation. The different recharge and discharge fluxes examined during this study can be seen in Figures 4.1 and 4.2. Below, the approach to how each flux was found is explained.

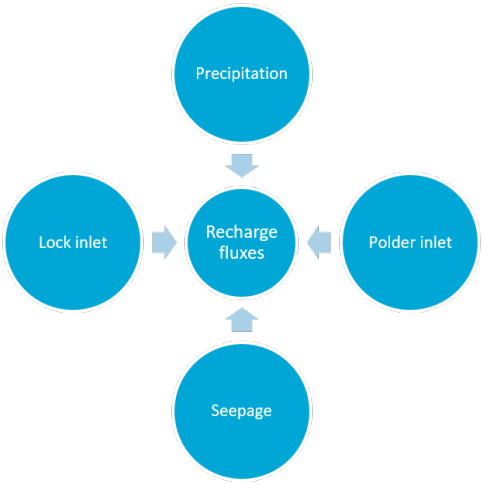

Figure 4.1: Water balance recharge fluxes.

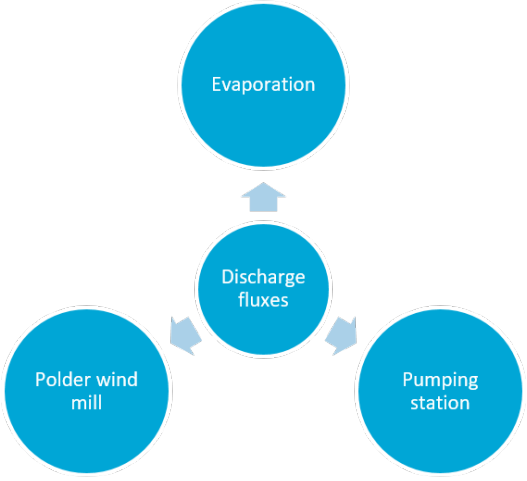

Figure 4.2: Water balance discharge fluxes.

Precipitation : For the 2021 balance, a Hobo tipping bucket rain gauge was placed in a central parcel, away from obstructing structures (buildings, trees etc.). A logger was activated to count how many times, and when, the tipping bucket tipped throughout the research period and in which the nominal value of one tip is equal to 0.2 mm of rain. For the previous balances, hourly precipitation data was collected from the nearby KNMI station at Schiphol [KNMI, 2021a].

Evaporation : For the evaporation discharge flux, daily KNMI reference crop evaporation (Makkink) data from Schiphol was collected [KNMI, 2021a].

Polder inlet : To estimate the inlet discharge, the inlet was fully opened and the time needed to fill a 60 liter bucket was measured. This was found to be 1 m^3/min. Combining the measured discharge with the duration the inlet was opened during the research period results in the total polder inlet water volume. For the previous balances, the values found in a study done by Rijnland were used [Vaartjes, 2020].

Pumping station : The pumping station is activated when the ditch water level reaches a certain threshold above the designated water level and stops once the water level falls back down bellow a certain threshold under the designated ditch water level. The pumping station run time data was retrieved from Rijnland. Using the pump capacity and pump operation duration, the amount of water pumped out of the polder was calculated.

Polder wind mill : To find the wind mill contribution, the polder wind mill operators were interviewed. The wind mill is operated every Thursday between 8:00 and 16:00, and occasionally on Saturdays as long as there is a sufficient high polder water level or in response to individual requests from the water board. With low force winds up to wind force 2, ±1.5 - 3 m/s, the mill is not able to mill any water out of the polder. At wind force 3, ±3.5 - 5.5 m/s, the polder mills a small amount of water. From wind force 5 upwards, ±8 - 10.5 m/s, the polder mill can mill between 40 m^3/min and 50 m^3/min. In this study, it was assumed that on any Thursday on which the average wind force was 5 or higher, the mill ran during the eight hour milling day, at a capacity of 40 m^3/min.

Lock inlet : The lock is predominantly used by a farmer who transports his cows to and from the island. Yearly, the lock is opened about twenty times. The opening times were multiplied by the lock area and the difference in water level on both sides of the lock to find the total volume of water entering the polder through the lock. The lock dimensions are 13.35 m by 4.37 m and the water level difference between both sides of the lock gate is 1.1 m, meaning a volume of 64 m^3 per lock turn.

Seepage : The seepage from the boezem and the first aquifer layer was estimated by examining historical pumping station discharges. In cold and dry periods, when the inlet and lock were not operated, it was assumed that all water being pumped out of the system after a dry period of one week was seepage from the boezem.

4.1.2. Groundwater behaviour

A network of twelve monitoring wells was made. This included eight shallow wells at a depth of 2 m which reached the peat subsurface layer, two intermediate wells placed at a depth of 7 m that reached the first sand aquifer and two deep wells at 15 m depth which tapped into the deep Pleistocene sand layer. The eight shallow wells were placed such that the groundwater level variation across a parcel could be monitored, see the diagram in Figure 4.3. The deeper wells were spread out across two measuring clusters. All the borehole locations can be seen in Figure 4.3. A pressure monitor was installed in each monitoring well and recorded the hourly groundwater variation between the 16th of April till the 23rd of September.

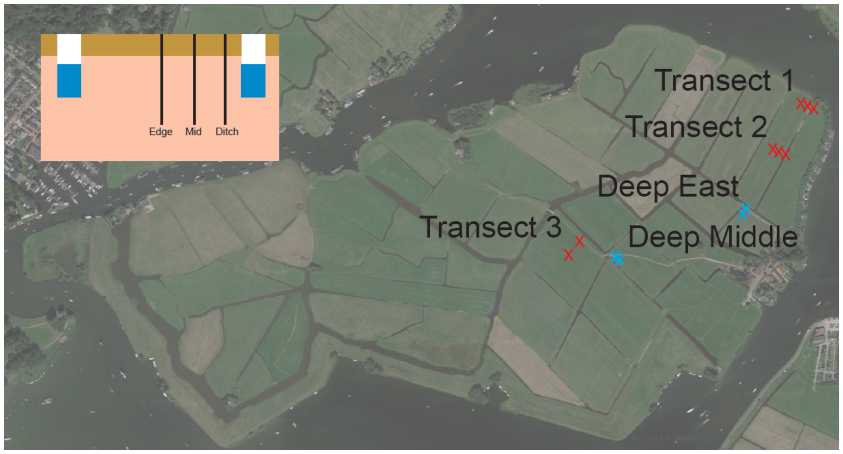

Figure 4.3: Locations of the installed boreholes. Red X are the shallow boreholes and the blue X are the intermediate and deep boreholes.

An important parameter linking surface water and groundwater interactions is the saturated hydraulic conductivity. This was measured in the field for the peat layer by numerous pumping tests. For each test, a 10 cm wide and 2.5 m deep borehole was made. This depth ensured that the full length of the peat layer was captured. As the subsurface in the first 2 m is made up of peat and clay, the borehole was able to support itself without the walls caving in, so no filter tube needed to be installed. However, a short 40 cm PVC pipe was placed in the top layer of the hole to block off the top clay layer that could contain burrow holes, cracks and fissures.

The two types of pumping tests considered for this study were: an auger test and an inverse auger test. For both tests, a pressure monitor, measuring the groundwater level every five seconds, needs to be installed into the holes before starting the tests. For the auger test, the groundwater level is lowered by pumping out the water. After the pump is turned off, the rate at which the groundwater rises is measured by the pressure monitor. For the inverse auger test, the hole is filled up until the surface level with water, after which the pressure monitor measures the lowering rate of the water level. Unfortunately, the field pump failed to lower the groundwater in the borehole enough, so only the inverse auger test was done in this study.

To find the hydraulic conductivity of the peat layer from the inverse auger test results, the van Hoorn formula was used [van Hoorn, 1979]:

$$K = 1.15r \frac{\log_{10}\left(h_0 + \frac{r}{2}\right) - \log_{10}\left(h_t + \frac{r}{2}\right)}{t - t_0} \tag{4.1}$$

In which the parameters are: hydraulic conductivity K [cm/d], borehole radius r [cm], water level at starting time relative to the bottom of the borehole h_0 [cm], water level at time t relative to the bottom of the borehole h_t [cm], starting time t_0 [s], time t [s].

The van Hoorn formula is derived from Darcy's Law in which it is assumed that the hydraulic gradient is 1 [van Hoorn, 1979] and that the surfaces over which water infiltrates into the soil are the straight borehole walls and the flat circular bottom [Ojha et al., 2017].

4.1.3. Groundwater models

Two groundwater models were made to represent the groundwater level and flows of the Zwanburgerpolder: one in iMOD and one in FlexPDE. The iMOD model was used to get a visual representation of the groundwater level variations across the island and to see the groundwater response to precipitation and evaporation. The FlexPDE model was used to get a clear overview of the phreatic groundwater level drop between two ditches in the summer and to compare the efficiency of different measures to raise the groundwater level. Below, the theory behind both models is explained as well as the input parameters used to represent the current groundwater situation of the Zwanburgerpolder. Further, in Section 4.2.3, the results of the current Zwanburgerpolder models are shown. The models for the future scenarios will be presented in Chapter 8.

iMOD model

iMOD is a graphical user interface version of MODFLOW made by Deltares in which groundwater flows and subsurface compositions can be modelled. The Actueel Hoogtebestand Nederland (AHN) 3 was used as a basis for the land surface level and DINOloket data as well as GEOTOP data was used to build up the subsurface composition of the model. The used hydraulic conductivities for the different subsoil types were based on literature values, the results from the inverse auger tests and an iterative process in which the hydraulic conductivities were adjusted in the model until the modelled groundwater level matched with the measured groundwater level.

Precipitation and evaporation time series collected from the KNMI up until the end of the study period (September 2021) were entered into the model to 'start it off'. A trade off had to be made between model efficiency and model accuracy. The longer the inputted time series, the better the representation of reality, but also the longer the model run time. It was decided to use a time frame of three years, so inputting data from October 1st 2018 till September 30th 2021. For more information regarding iMOD and the parameters applied to the model, see Appendix B.

FlexPDE model
FlexPDE is a finite element model builder and solver. For this study, the program was used to model the groundwater head across a 2D parcel transect between two ditches. The 2D transect was chosen to represent the parcel in which Transect 1 and 2 are found, so with a parcel width of 50 m. The model boundary includes the top clay and peat layers of the subsurface and goes down to −5 mNAP, up to the interface of the first aquifer. Using the pressure heads found from the measured pressure monitor time series, the boundary of each subsurface layer was defined and can be seen in Figure 4.4. Further, the used hydraulic conductivity values can also be seen in the figure.

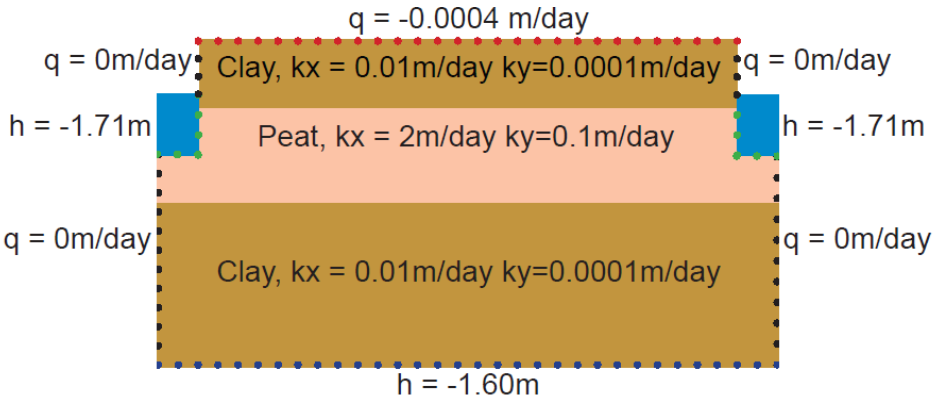

Figure 4.4: Pressure head and specific discharge boundary conditions used in the FlexPDE model as well as the used hydraulic conductivities.

In contrast to iMOD, FlexPDE is a steady state model meaning it is time independent. Therefore, instead of using daily values like the iMOD input values, an average value was used in this model. Namely, the average precipitation surplus across the study period (summer precipitation − summer evaporation). The daily surplus between the 1st of April and the 30th of September was found to be −0.4 mm/day [KNMI, 2021b].

4.2. Results

4.2.1. Water balance

In Table 4.1, the water balances for the past four years can be seen. The balance errors give an indication of the high uncertainty in the values. Across the past years, the water decree has not changed, meaning there should not be a difference in the groundwater level between the beginning of the year and the end of the year, or in other words, the groundwater storage should be relatively constant over the years. This means that the observed differences in the yearly water balances give an indication of the uncertainty of the different balance terms and not of a groundwater storage shortage or surplus. The seepage and polder mill values are the values with the largest uncertainties as these values are based off of other climate values like wind (polder mill) and, lack of, precipitation (seepage) which also have their own uncertainties.

When adding the balance errors to the respective seepage values, all the values come near to about 1100 mm. As stated above, the water decree has not changed in the previous years, meaning that the yearly seepage values should be approximately the same each year. In 2017, adding the balance error to the seepage value results in a seepage of about 800 mm, 300 mm smaller than the other years. A possibility is that the polder wind mill was operated more frequently than the windy Thursdays in 2017. This inconsistency highlights once more the uncertainties associated with the different flux terms, in this case the polder wind mill term.

Table 4.1: Yearly water balances for the past four years.

Year	Precipitation [mm]	Polder inlet [mm]	Lock inlet [mm]	Seepage [mm]	Evaporation [mm]	Pumping station [mm]	Polder wind mill [mm]	Balance error [mm]
2017	936	110	1	485	602	858	383	−311
2018	559	110	1	705	680	713	364	−382
2019	861	110	1	600	646	1077	306	−458
2020	870	110	1	1054	666	1110	345	−85

The water balance for the research study period, April 2021 till September 2021 can be seen below in Table 4.2. During the whole period, the polder inlet was kept closed. For the seepage values, the 1100 mm/year was divided over the 182 day period between April and September. In this balance, there is a negative balance error. Unlike the errors in Table 4.1, this negative error was expected, as it suggests that during the study period, there is a lowering in ground water level.

Table 4.2: Water balance between the 1st of April 2021 till the 30th of September 2021.

Period	Precipitation [mm]	Polder inlet [mm]	Lock inlet [mm]	Seepage [mm]	Evaporation [mm]	Pumping station [mm]	Polder wind mill [mm]	Balance error [mm]
Apr - Sep 2021	417	0	1	548	483	372	134	−22

4.2.2. Groundwater behaviour

The hourly pressure monitor data collected from the twelve pressure monitors can be seen in Figures C.1 till C.6 in Appendix C. In Figures C.1, C.2 and C.3, the response of the phreatic groundwater to precipitation can be seen. Here, the twelve shallow pressure monitors are plotted per transect as well as the daily precipitation. In Figures C.4, C.5 and C.6, the relationship between the phreatic groundwater level and the deeper, aquifer pressure heads can be seen. Here, each shallow pressure monitoring time series is plotted on a graph with the associated deeper pressure head time series. Below in Figures 4.5 and 4.6, the response of the phreatic groundwater level to precipitation and the relationship between the phreatic groundwater level and the deeper aquifers respectively for Transect 3 are highlighted.

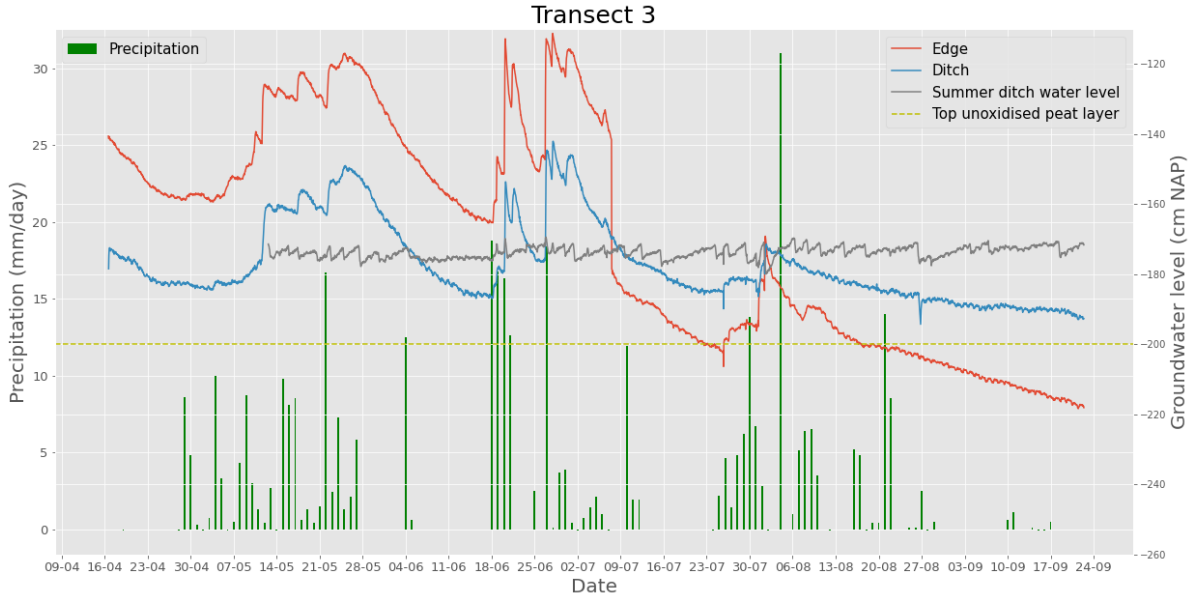

Figure 4.5: Pressure monitor data for the boreholes along Transect 3 between the 16th of April and the 23rd of September

When looking at Figure 4.5 or Figures C.1 to C.3, a distinct response to precipitation can be seen in all eight shallow monitoring wells. The groundwater level peaks are reached after a day / period with significant rain. For the intermediate and deep wells, Figure 4.6 or Figures C.4 to C.6, it is clear that there is no relation between groundwater pressure heads and precipitation. Instead, these groundwater bodies are influenced by surrounding water bodies.

From the beginning of July on wards, the shallow phreatic water level seems to respond less substantially to precipitation than in the previous time phase. This can be explained by the higher summer temperatures stimulating evaporation and reducing the soil moisture content below field capacity. At this point, the water in the top soil is held so tightly by the soil matrix that no water drains down into the deeper depths and no water can be absorbed by plant roots [Kirkham, 2005].

In Transect 1 and Transect 3, the winter groundwater bulge can be identified between April and July: the groundwater level at the edge of the parcels is higher than by the ditch. By August, this groundwater bulge starts to transform into a groundwater dip. By September, the phreatic groundwater levels at the edge of the measurement rows drop much lower than the groundwater levels closer to the ditches.

Between the end of April and the end of May, the heads in the deep sand layers are lower than the phreatic groundwater level in the peat layer. This suggests, that in this period, the phreatic groundwater seeps into the lower aquifer. However, from the beginning of June on wards, following a warmer and drier period, the phreatic groundwater level falls under the pressure head in the first aquifer (intermediate borehole), suggesting deep groundwater starts percolating upwards and influences the phreatic groundwater level.

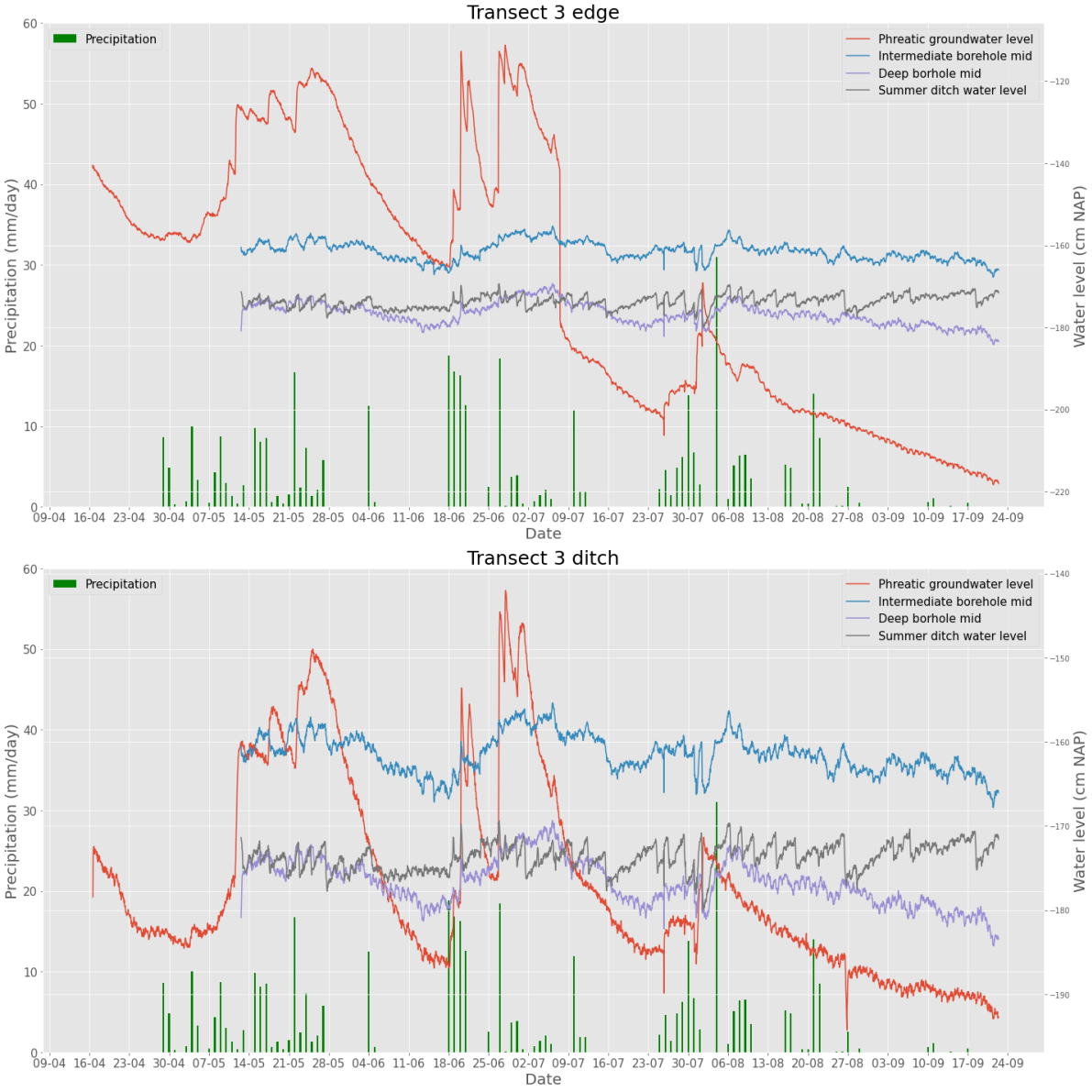

Figure 4.6: Pressure monitor data for the boreholes along Transect 3 as well as the deep borehole pressure monitor data between the 16th of April and the 23rd of September.

The interaction between the phreatic groundwater level and the deeper aquifers can be seen when zooming in to a shorter time period, see Figure 4.7. When looking at the different pressure heads, it can be seen that the fluctuations are all very similar in magnitude and occurrence, especially the phreatic groundwater level and the intermediate borehole results. When looking closely at the figure, it can be seen that it is the phreatic

groundwater level follows the first aquifer fluctuations, confirming the influence of the groundwater in the first aquifer on the phreatic groundwater level in the summer period.

The summer of 2021 was quite a wet one, especially in compassion to the previous three summers in the Netherlands. During the April till September period, the measured phreatic groundwater levels almost never dropped down below the top of the unoxidised peat layer, which is beneficial against peat oxidation. Only in transect three, located in the widest parcel, did the phreatic water level in the middle of the parcel drop down into the unoxidised peat level.

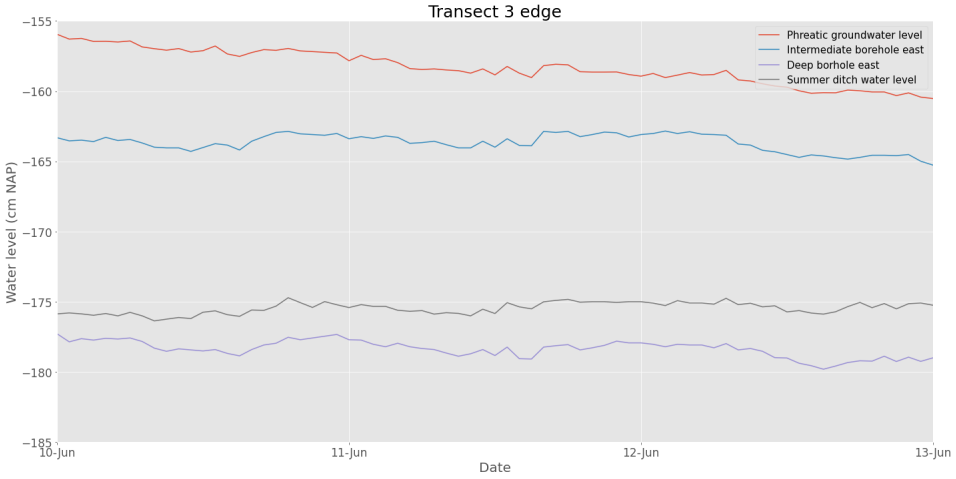

Figure 4.7: Three day zoom in of the pressure monitor data across the edge transect 3 in which the phreatic groundwater level relationship with the aquifer pressure head can be seen.

Using the results from the inverse auger test and van Hoorn's formula seen in Equation 4.1, the following hydraulic conductivity values were found:

Table 4.3: Inverse auger pumping test results.

Hole, Trial	t [s]	r [cm]	H_0 [cm]	H_t [cm]	K [m/d]
1,1	185	5	175	155	1.40
1,2	145	5	175	145	2.70
2,1	2980	5	180	176	0.02
3,1	45	5	175	160	4.20
3,2	40	5	175	136	13.4

As can be seen in Table 4.3, there is a considerable variation in the hydraulic conductivity values found in the field. These variations can be explained by cracks and fissures in the underground, but also by the heterogeneity of peat layers in itself. This is influenced by the degree of peat decomposition and the organic content of the peat [Päivänen, 1973]. Additionally, the first inverse auger tests for each hole may have added pressure along the borehole wall, flushing out some of the sediments and creating new corridors. The pumping test results show the importance of keeping soil heterogeneity in mind, especially when modelling the subsurface.

4.2.3. Groundwater models

iMOD

A snapshot of the model of the 1st of June can be seen in Figure 4.8 in which the pressure head across the island for the current situation can be seen. A quick drop in head can be seen around the sides of the polder, as the groundwater head is significantly lower compared to the surrounding boezem surface water. The winter groundwater bulge can still be seen, which matches the collected pressure monitor data. The modelled phreatic groundwater level at the edge of Transect 1 reaches −1.60 mNAP, which is comparable to the obtained pressure monitor data for that point.

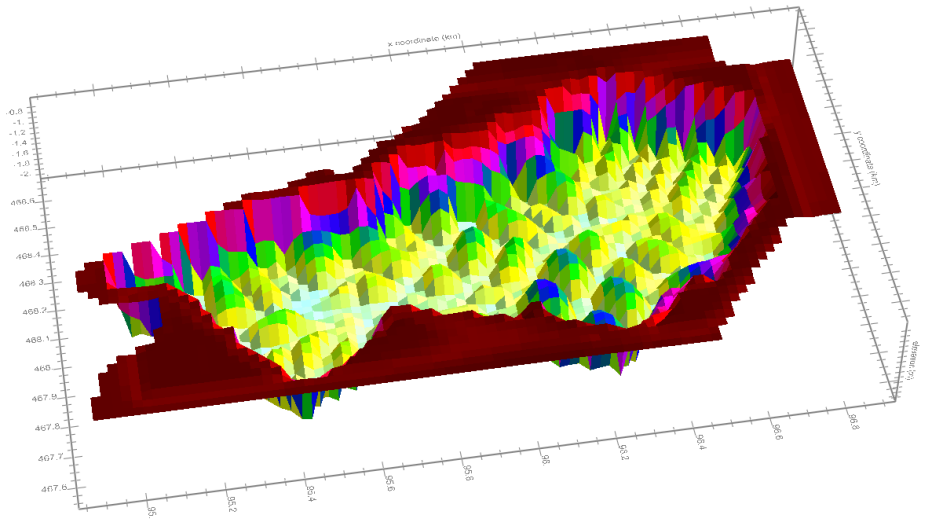

Figure 4.8: Head variations in the iMOD model relative to NAP across the polder in the top clay layer for the 1st of June.

In Figure 4.9, a snapshot later in the summer on the 29th of September can be seen. Here, the winter groundwater bulge is not visible anymore and the groundwater levels between the ditches drop down below the summer ditch water level. The lowest groundwater level in the middle of Transect 1 is about −1.80 mNAP, once again coinciding with the pressure monitor data retrieved in the field.

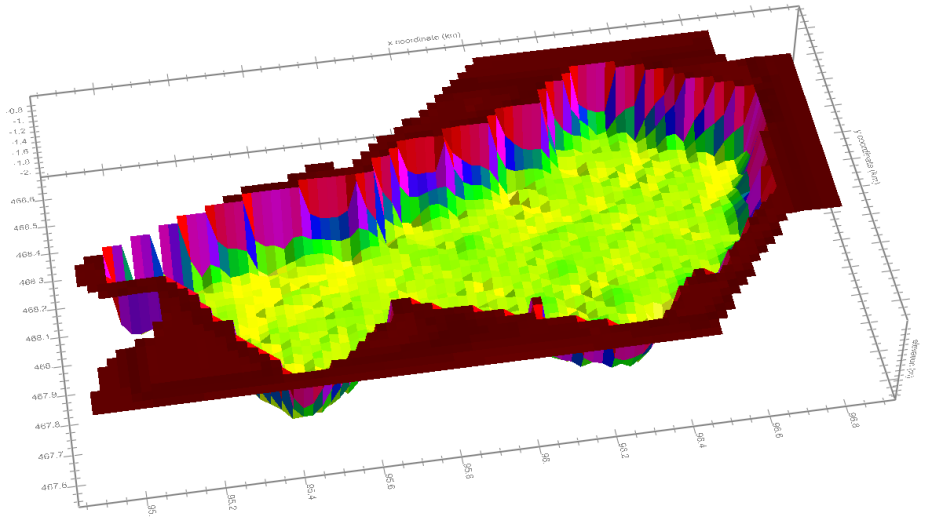

Figure 4.9: Head variations in the iMOD model relative to NAP across the polder in the top clay layer for the 29th of September.

In Figure 4.10, the modelled phreatic groundwater levels across the edge of Transect 1 can be seen for the study period. The modelled results of the phreatic groundwater peaks react much stronger to rain than the peaks monitored in the field. This can be explained to the absence of a top unsaturated zone in the model. In reality, this zone serves as a buffer delaying the influence of precipitation and evaporation on the phreatic groundwater level. In the iMOD model, all precipitation and evaporation directly influences the phreatic groundwater level, explaining the strong peaks.

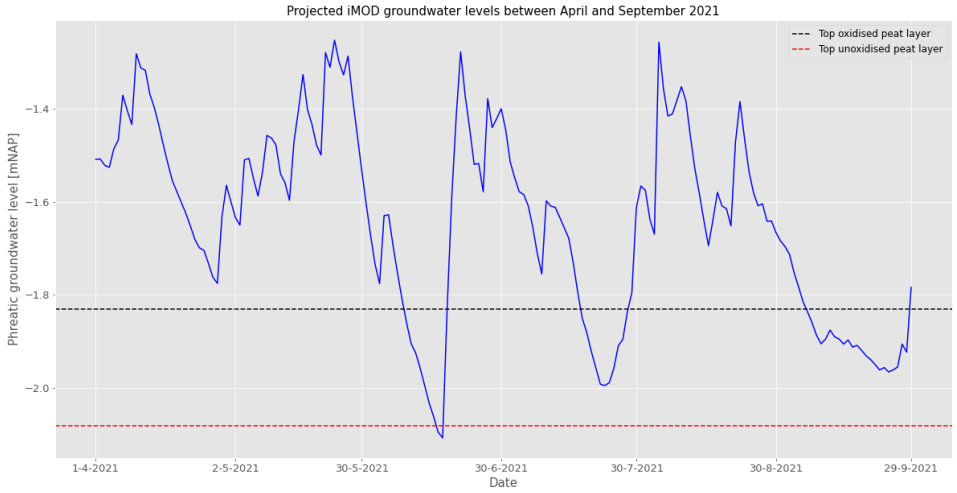

Figure 4.10: Time dependent head variations in the iMOD model at the edge of Transect 1 between the 1st of April and the 29th of September.

FlexPDE

The groundwater head across the FlexPDE model region can be seen in Figure 4.11. As stated before, the input precipitation surplus term is the average precipitation value minus the average evaporation value across the study period. With this input, the lowest groundwater level reached in the middle of the parcel is at about −1.89 mNAP. This fits well with the order of magnitude found for the phreatic groundwater levels at the edge of Transects 1 and 2.

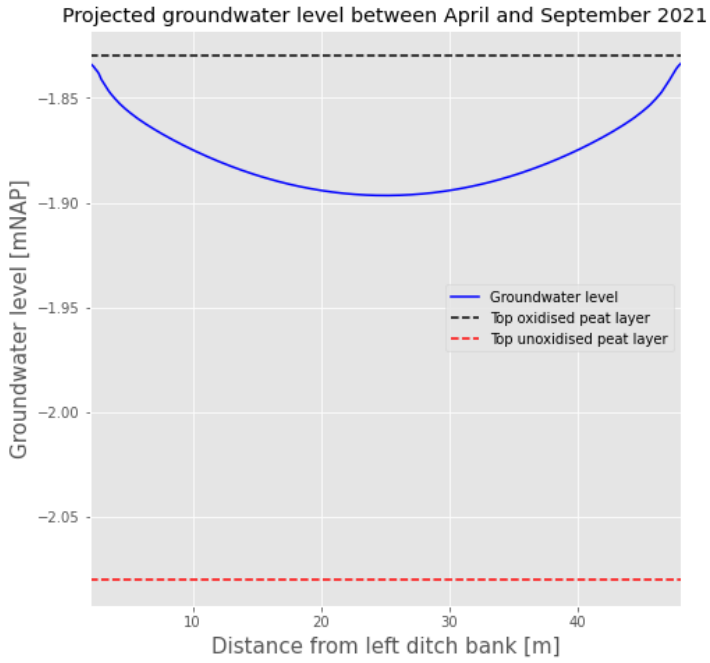

Figure 4.11: Phreatic groundwater variation between two ditches modelled in the FlexPDE model.

4.3. Conclusions

From the results found in this chapter the following can be concluded about the interactions between the phreatic groundwater, the deeper groundwater and the boezem water:

- As seen in the water balance from Table 4.1, an important recharge flux for the Zwanburgerpolder is seepage. This is both seepage originating from the first aquifer as from embankment seepage.

- During wetter periods, when the unsaturated soil is at field capacity, the phreatic groundwater level reacts more strongly to precipitation. Here, rain water immediately infiltrates into deeper layers. In drier periods, like end of June on wards, the phreatic groundwater level is less reactive to precipitation, as a portion of the rain water is kept in the top, unsaturated root zone, therefore not reaching the phreatic groundwater [Kirkham, 2005].
- As seen in the inverse auger test results from Table 4.3, there is a large heterogeneity in the hydraulic conductivity values across the peat layer. In the models, a single hydraulic conductivity value was chosen for all the peat layers. This means that on certain locations there is a slight under or overestimation of the hydraulic conductivity.

5
Water quality

Monitoring the ground and surface water quality gives insightful information about the presence of water contaminants. To achieve this, it is important to identify and understand the variations in quality. When comparing a collected sample to other samples within the same study area, or with samples collected at different time frames, water quality variations will emerge making it possible to identify the contamination source(s). In this study, both the spatial and temporal variations of the groundwater and surface water quality are investigated. The gathered results are used to answer the following questions:

- How does the water system work?
- Can the effect of peat oxidation be seen?
- Can the effect of the agricultural land use be seen?

5.1. Methodology

5.1.1. Groundwater

For the groundwater analysation, groundwater samples were collected from each borehole and analysed in the lab. The large spread in borehole locations lead to results showing the spatial variations in water quality across the island and more importantly across the different subsurface depths.

Before gathering the samples, each borehole was purged, meaning that the stagnant water in the borehole was pumped out. This was done to ensure that the collected samples were representative of the surrounding groundwater. After purging the boreholes, groundwater samples were collected. In the field, the pH, electrical conductivity (EC), temperature, redox potential and dissolved oxygen (DO) of each sample was measured. This was done using three different multimeters, as seen in Figure 5.1.

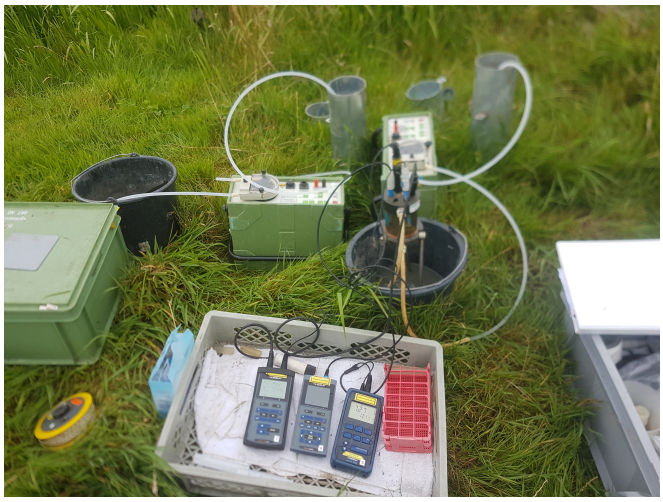

Figure 5.1: Groundwater sampling setup in two deep boreholes. The pump can be seen as well as the three multimeters used to measure pH, EC, temperature, redox potential and DO.

After the field sampling was done, the collected water samples were passed through 0.45 μm membrane filter to remove the majority of the suspended particles unintentionally pumped out from the subsurface. The samples were split into two containers; a 5 ml container which was diluted by a 1:10 dilution factor and a 30 ml container which was not diluted. The 5 ml samples were analysed using Inductively Coupled Plasma - Optical Emission Spectrometery (ICP-OES), a technique in which the composition of elements in samples is determined. The 30 ml samples were analysed using Ion Chromatography (IC). This is a method that separates and measures ions in water samples.

5.1.2. Surface water

To evaluate the surface water quality, three different processes were used: 1) surface water sampling and lab analysation, 2) ditch routing and 3) historical water quality evaluation. The first two processes gave an indication of the spatial water quality variations across the island and the third process gave an indication of the temporal variations.

For the surface water sampling, seven samples were taken from the following locations. See also the green crosses in Figure 5.2:

- 1 sample at the polder inlet and outlet and 1 in the middle of the polder (3 samples total)
- 1 sample at each monitoring cluster (2 samples total)
- 1 sample at the possible leaking manure pit (1 sample total)
- 1 sample of the boezem water (1 sample total)

Figure 5.2: Surface water sampling locations (green X's) done in this study and the Rijnland historical surface water sampling locations (red O's).

For each location, two samples were collected: an unfiltered sample and a filtered sample. As with the groundwater samples, the samples were analysed through ICP-OES and IC in which the ICP-OES samples were diluted by a 1:10 dilution factor in the field. Once again, the pH, EC, temperature, redox potential and DO were measured in the field for the unfiltered samples using multimeters.

For the ditch routing, a so-called drone boat was used. This is a remote controlled boat, under which several sensors are hanged, which navigates through the ditches and continuously measures water quality parameters. The sensors attached to the boat measured the DO, EC, pH and temperature of the ditches. All parameters were automatically corrected for temperature.

The final process was evaluating historical surface water quality data collected from Rijnland. The available data consisted of nitrate nitrogen, total phosphorus, and chloride concentrations, spanning between 1976 till

2021 for the four locations marked by the red circles in Figure 5.2. Throughout the measurement period, the samples were sporadically collected.

To see the seasonal variation in water quality, the collected data was plotted per month for the most recent sample collection spanning between March 2020 and July 2021. Plotting all the collected data across the forty year collection period would have given a distorted idea of the seasonal water quality variations, as different unknown, factors could have impacted the water quality in the past. The total Rijnland water quality time series from 1976 till 2021 can be seen in Appendix D.

In order to compare the results of these parameters to the one obtained during the surface water sampling, the nitrate nitrogen values were converted to nitrate and phosphorus values to phosphate using the following conversion factors [Hach, 2013]:

$$NO_3\text{-}N \xrightarrow{\times 4.427} NO_{3-} \qquad P \xrightarrow{\times 3.067} PO_4^{3-}$$

5.2. Results

5.2.1. Groundwater

The results from the groundwater field tests, ICP-OES analysis and IC analysis can be seen in Table 5.1. Both phosphate and chloride concentrations are higher in the four deep boreholes than in the shallow boreholes. Further, the nitrate concentration is slightly higher in the shallow boreholes.

Table 5.1: Field test results, ICP-OES analyses and IC analyses for the collected groundwater sampels.

Parameter		1	2	3	4	5	6	7	8	East intermediate	East deep	Mid intermediate	Mid deep
pH	[-]	6.99	6.85	6.12	7.16	6.89	7.02	6.95	7.15	7.5	7.27	7.27	7.33
EC	[μs/cm]	1648	1504	1734	1771	1254	1364	1507	1765	1064	1662	1492	1752
Temperature	[°C]	14.9	15.2	16.7	15.8	15.9	16.1	15.6	14.8	12.4	12.1	12.4	11.9
Redox	[mV]	-292	-294	0	-288	-150	-210	-275	-255	-297	-280	-329	-241
Oxygen	[mg/l]	0.9	3.26	0.86	1.2	3.14	1.4	1.49	1.67	0.01	0.02	0.01	0.00
Chloride	[mg/l]	190	136	107	114	69	67	129	182	142	247	201	263
Phosphate	[mg/l]	5.56	5.92	0.98	5.90	1.40	1.67	5.08	4.75	8.90	10.96	15.55	11.48
Nitrate	[mg/l]	0.41	0.33	0.25	0.20	<MDL	0.34	<MDL	0.19	0.19	<MDL	<MDL	0.19
Iron	[mg/l]	0.04	0.08	6.34	0.05	1.95	0.05	0.11	0.19	0.01	0.15	0.00	0.17
Bromide	[mg/l]	1.00	1.14	1.47	1.53	1.27	1.53	0.98	1.37	0.52	1.08	0.84	1.05

5.2.2. Surface water

During the surface water sampling, both filtered and unfiltered samples were analysed in the lab. For most elements, the extra filtration step did not greatly affect the results, except for iron. In the unfiltered samples, the iron concentration was in some cases almost twice as high, see Table 5.2. However, the iron values found were all very small, so the absolute difference between the values are in the same order of magnitude as the absolute difference between the other elements.

Table 5.2: Variation in iron concentration between the filtered samples and unfiltered samples.

Location	Filtered sample iron [mg/l]	Unfiltered sample iron [mg/l]
East measure	0.18	0.20
Inlet	0.41	0.22
Manure pit	0.09	0.12
Boezem	0.01	0.02
Mid bridge	0.08	0.14
Mid measure	0.14	0.20
Windmill	0.03	0.05

In Table 5.3, the rest of the water quality results from the surface water sampling can be seen. As the values between the unfiltered and filtered samples did not vary that much, only the filtered samples are shown in the table, so that they can be compared to the groundwater samples, which are also all filtered. What

stand out is the difference between the boezem water quality and the polder samples. The boezem has a low phosphate concentration and high nitrate concentration, while, the polder samples have a high phosphate concentration and low nitrate concentration. This suggests that the polder surface water is strongly influenced by internal agricultural and chemical processes and the quality of groundwater seepage from the first aquifer, and not so much by the boezem water or boezem seepage.

Table 5.3: Field test results, ICP-OES analyses and IC analyses for the collected surface water samples from the 23rd of June and the 22nd of September.

Parameter		East measure		Inlet		Manure pit		Boezem		Mid bridge		Mid measure		Windmill	
		June	Sep	June	Sep	June	Sep	June	Sep	June	Sep	June	Sep	June	Sep
pH	[-]		7.79		7.18		7.82		8.08		8.01		8.27		8.12
EC	[μS/cm]		1066		1170		1175		829		1170		1089		961
Temperature	[°C]		16.5		17.6		17.1		19.6		18.3		18.4		19.1
Redox	[mV]		-165		-258		-39		140		87		1		122
Oxygen	[mg/l]		3.48		0.55		4.55		8.39		7.70		9.10		8.40
Chloride	[mg/l]	136	139	128	150	137	157	143	116	132	166	131	156	137	131
Phosphate	[mg/l]	4.09	8.72	7.89	10.57	3.57	15.31	0.30	0.66	2.80	9.21	4.27	9.60	1.38	3.04
Nitrate	[mg/l]	0.49	<MDL	0.28	<MDL	0.51	0.63	4.91	4.39	0.37	<MDL	<MDL	0.19	0.34	0.77
Iron	[mg/l]	0.05	0.18	0.057	0.22	0.03	0.44	0.022	0.07	0.055	0.45	0.055	0.42	0.027	0.24
Calcium	[mg/l]	71.93	88.99	91.02	91.21	74.21	77.59	82.29	64.60	70.56	69.52	73.85	58.46	79.72	68.71
Sodium	[mg/l]	89.84	91.70	87.86	103.94	94.38	113.77	81.03	70.45	94.02	122.44	98.65	120.73	94.55	88.77

In Figures 5.3 till 5.6, the ditch routing results can be seen. In Figure 5.3, the variation in temperature can be explained by the time of day the measurements were taken. The measurements by the farm (in the East of the island) were done early in the morning, while the measurements in the West of the polder were done in the afternoon on a very warm day.

When looking at the DO figure, a significant difference can be seen between the area closer to the farm and along the main water way. This can be explained by a higher ammonia content and organic matter content in the ditches, originating from cow manure. Ammonia wants to oxidise to nitrate (nitrification) and in doing so, takes out oxygen from the water. Additionally, organic matter originating from the manure is broken down by microbial decomposers which consume oxygen [Wheeling University, 2004].

The pH of the ditches is determined by rain water, biological processes like the blooming of algae or cyanobacteria and chemical processes like ammonia nitrification. Across the polder, a lower pH is seen by the farm, which can be explained by a higher ammonia concentration caused by the manure pit or urine runoff from the parcels where cows graze [EPA, 2002].

Finally, in Figure 5.6, a similar pattern is seen in the EC distribution as in the other figures. However, it was expected that the agricultural processes would increase the EC of water, while in Figure 5.6, the EC in proximity to the farms is lower than the EC further away from the farm. A possible explanation could be that the inlet was opened, letting boezem water with a low EC enter the polder.

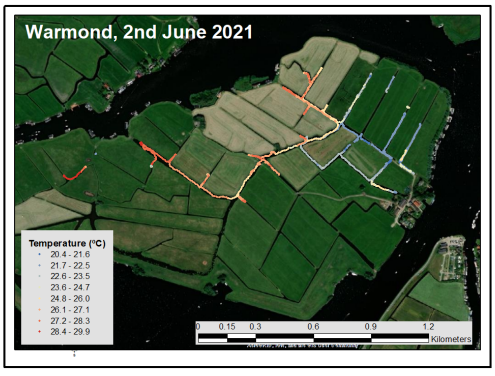

Figure 5.3: Ditch routing: temperature results.

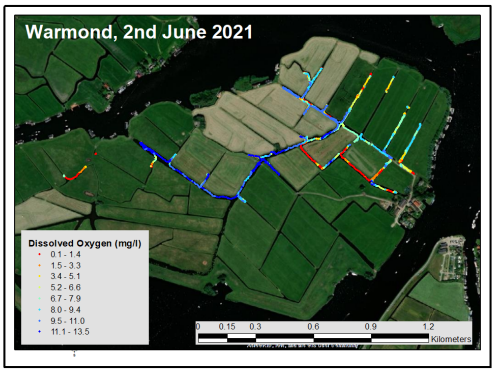

Figure 5.4: Ditch routing: DO results.

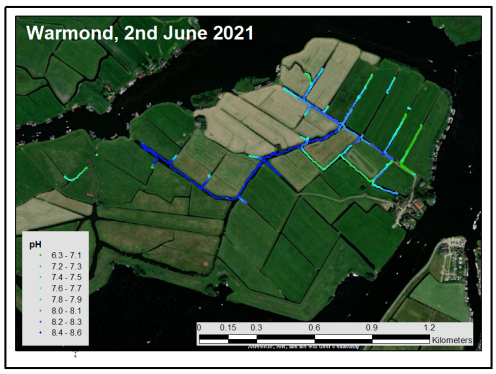

Figure 5.5: Ditch routing: pH results.

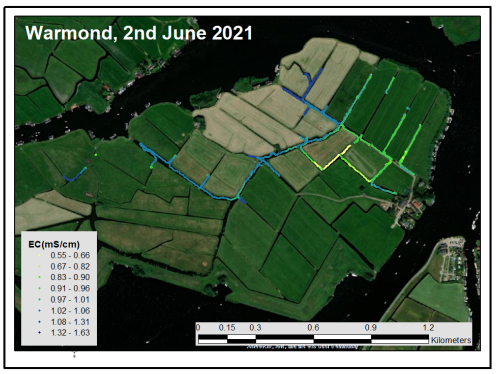

Figure 5.6: Ditch routing: EC results.

The historical Rijnland data for nitrate (as NO_{3}-), phosphate (as PO_4^{3-}) and chloride (as CL^-) plotted per month can be seen below in Figures 5.7, 5.9 and 5.10 respectively. The monthly nitrate concentrations in Figure 5.7 show a clear seasonal pattern. There is a higher concentration in the winter months (October - March) than in the summer months (April - September). This indicates a strong relationship between the ditch nitrate concentrations and peat oxidation. In the summer, when the groundwater level lowers, the newly uncovered peat oxidises, emitting nutrients, like nitrogen and phosphorus, into the subsurface. These nutrients are trapped in the soil during the summer. During the winter period, when there is the groundwater bulge across a parcel, these nutrients are flushed into the ditches. A simple diagram of this mechanism can be seen in Figure 5.8.

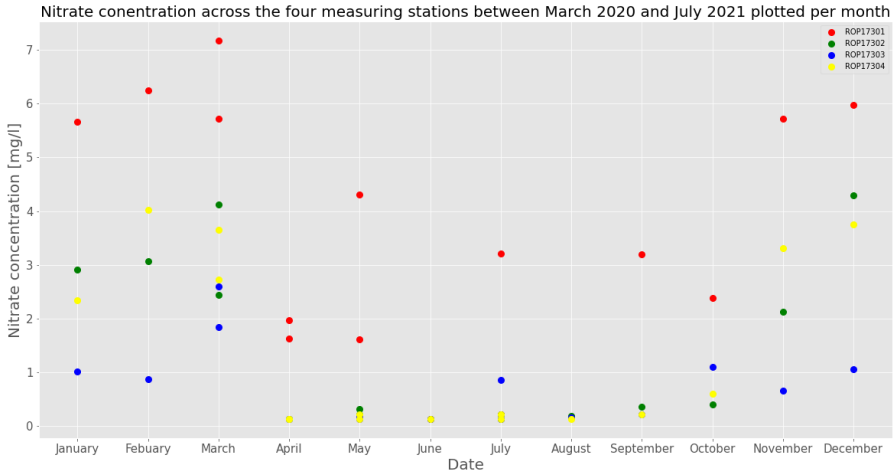

Figure 5.7: Monthly variations in nitrate concentrations across the four Rijnland sample locations.

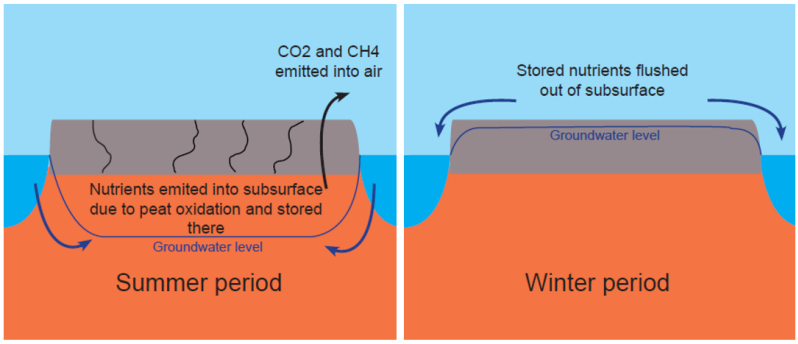

Figure 5.8: Diagram showing the seasonal pattern seen in the nitrate ditch concentration.

This seasonal pattern is however not reproduced in the monthly phosphate, see Figure 5.9, where the opposite trend is seen. This suggests that the phosphate concentration in the ditches is less influenced by peat oxidation, but rather by other biological processes stimulated by higher temperatures. Raised temperatures triggers the release of phosphate in ditch sludge [RIVM, 2020].

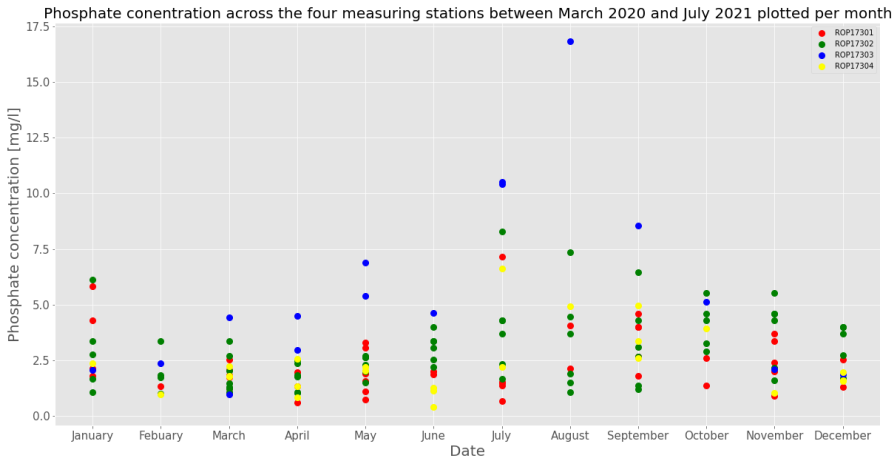

Figure 5.9: Monthly variations in phosphate concentrations across the four Rijnland sample locations.

Then when looking at the chloride concentrations, a similar seasonal pattern can be seen as with the yearly phosphate concentrations where the highest chloride concentrations are reached in the summer. A possible explanation for is the influence of the upwards seepage from the first aquifer during the summer.

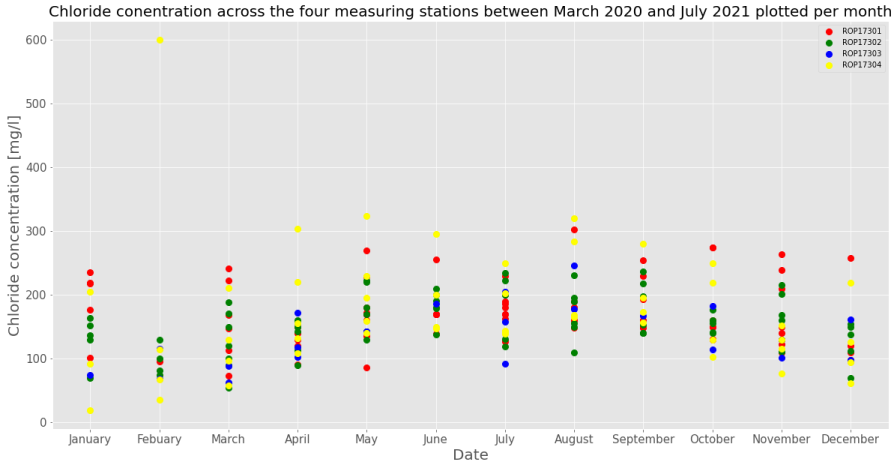

Figure 5.10: Monthly variations in chloride concentrations across the four Rijnland sample locations.

When comparing the water quality results from the surface water sampling and the historical Rijnland data, the nitrate, chloride and phosphate concentrations around August and September are within similar ranges.

5.3. Conclusions

In the table below, the water quality parameters for different water components are summarized. The values for the boezem water, ditch water, top aquifer groundwater and deep groundwater were collected from the results in Section 5.2. The values for precipitation and the Kaderrichtlijn Water (KRW) goals were added from literature values. The Kaderrichtlijn Water is a policy in which European ground and surface water quality goals are stated. Using the values from Table 5.4, as well as the other results from Section 5.2, water quality conclusions for the Zwanburgerpolder were made by answering the questions posed at the beginning of the chapter.

Table 5.4: Water quality variations for water from different components. 1 van Dijk [2008], 2 Water [2013], 3 van der Swaluw et al. [2010], 4 STOWA [2012].

Parameter		Rain water	Boezem water	Ditch water	Phreatic groundwater	First aquifer groundwater	Deep groundwater	KRW goal[4]
pH	[-]	5.60 - 6.40[1]	8.08	7.18 - 8.27	6.12 - 7.16	7.27 - 7.50	7.27 - 7.33	5.50 - 8.00
EC	[uS/cm]	10 - 150[2]	829	829 - 1175	1254 - 1771	1064 - 1492	1662 - 1752	-
Oxygen	[mg/l]	10.00[1]	4.55	0.55 - 9.10	0.10 - 3.26	0.01	0.00	3.46 - 11.85
Chloride	[mg/l]	4 - 5[3]	116 - 143	128 - 166	67 - 190	142 - 201	247 - 263	300
Phosphate	[mg/l]	0.00 - 0.01[3]	0.30 - 0.66	1.38 - 15.31	0.98 - 5.92	8.90 - 15.55	10.96 - 11.48	0.67
Nitrate	[mg/l]	2.50 - 2.61[3]	4.39 - 4.91	0.28 - 0.77	0.19 - 0.41	0.00 - 0.19	0.00 - 0.19	10.62
Iron	[mg/l]	0.01 - 0.02[3]	0.02-0.07	0.03 - 0.45	0.04 - 6.34	0.00 - 0.01	0.15 - 0.17	-

How does the water system work?

When comparing the surface water sampling results from Table 5.4, it can be concluded that the boezem water quality has little impact on the water quality of the ditches in the polder. The nitrate concentration in the boezem is much higher than in the ditches, and inversely, the phosphate concentration in the boezem is much lower. This insinuates that the water quality values in the ditches are largely dependent on processes happening within the polder like biological / chemical processes and agricultural impacts.

Interestingly, the phosphate concentration in all the water bodies is extremely high, compared to the KRW goal. In the ditch water and phreatic groundwater, it would be expected that the concentration would be slightly higher due to the release of phosphate during peat oxidation. However, the phosphate concentration is also extremely high in the deeper groundwater. This suggests that the phosphate contamination within the polder is not provoked by peat oxidation, but rather by a high phosphate concentration in the first aquifer. Within the ditches, the highest phosphate concentration of 15.31 mg/l was sampled by the manure pit, also suggesting that cow manure is an important cause of the high phosphate concentrations.

The chloride/bromide (Cl/Br) ratio says something about the origin of groundwater in which a Cl/Br ratio of 288 suggests groundwater originating from sea water [Aquilina et al., 2015]. In Figure 5.11, the Cl/Br ratios for the different water bodies have been plotted, along with the sea water ratio of 288.

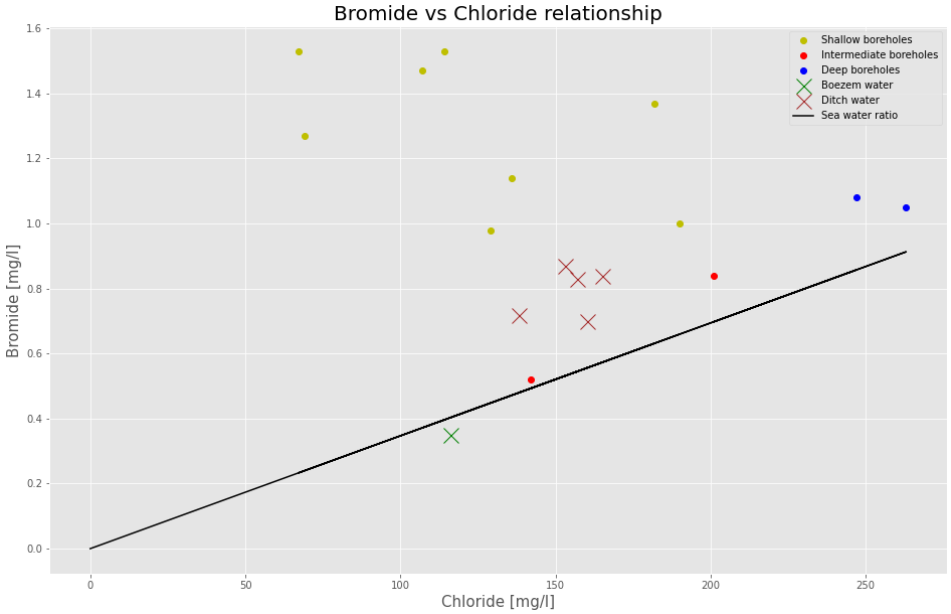

Figure 5.11: Bromide - chloride relationship of the Zwanburgerpolder samples in relation to the sea water ratio.

Ideally, more water samples would have been taken to validate the relationship, but with the points seen in Figure 5.11, there seems to be a difference between the Cl/Br ratios of the deep groundwater samples and the shallow groundwater samples. Implying the deep groundwater originates from sea water, while the phreatic groundwater is influenced by other things like precipitation and manure.

Can the effect of peat oxidation be seen?
The effect of peat oxidation can be seen in the nitrate concentrations from Table 5.4. The nitrate concentration of the ditches and the phreatic groundwater level is significantly different than the deeper groundwater. During peat oxidation, nitrogen is released which mineralises to ammonium and then further oxidises to nitrate. The ditch water and phreatic groundwater are the water bodies in contact with the nutrients released during peat oxidation. Due to the oxidation of ammonium, the dissolved oxygen left in the ditches is reduced. The oxygen content measured in certain locations was lower than the KRW goal. By discouraging peat oxidation, less ammonium will be released into the water, resulting in higher dissolved oxygen contents in the ditches.

Can the effect of the land use be seen in the water quality results?
Yes, when looking at the results from Chapter 5.2, it can be concluded that the effect of agricultural land use can be seen back in the water quality results. First of all, the highest phosphate concentration in the surface water was measured by the manure pit. Secondly, the looking at Figures 5.3 to 5.6, distinct color variations are seen between the ditches closer to the farm and the grazing parcels and the ditches further away from the farm.

6

GHG emissions

When looking at the GHG emissions emitted from the polder, a distinction was made between short-term and long-term emissions. The top vegetation layer contributes to short-term GHG emissions, both as a GHG contributor and as a GHG stock. These fluxes are caused by soil organic matter decomposition, photosynthesis and soil respiration. The long-term emissions within the polder can be linked to one of the following three groups: peat oxidation, dairy farming and pumping station operation, see Figure 6.1. The three major GHGs emitted from dairy farms on peatlands are: carbon dioxide (CO_2), methane (CH_4) and nitrous oxide (N_2O). In this study, the short-term emissions are not taken into account in the total island emissions. When looking at the GHG emissions across long periods, it is assumed that the short-term soil respiration and decomposition balances out with the CO_2 absorption from photosynthesis [Erkens et al., 2020]. In this chapter, the different contributors from Figure 6.1 are quantified and conclusions are made about the most critical GHG emitter.

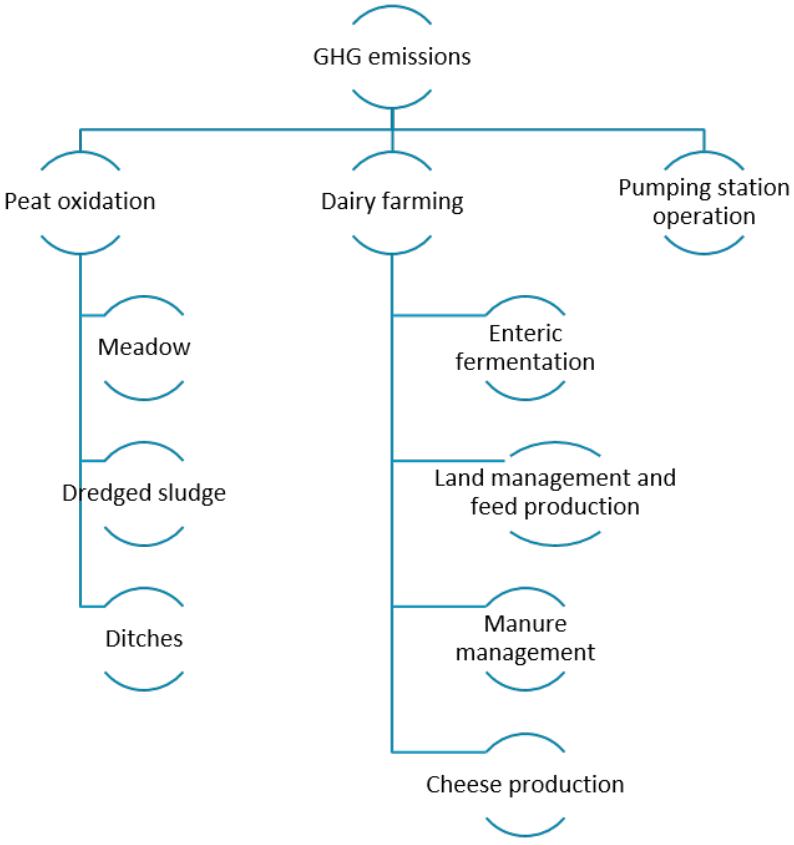

Figure 6.1: The considered CO_2, CH_4 and N_2O emission contributors within the Zwanburgerpolder.

6.1. Methodology

For the peat oxidation component of the GHG emissions, the contribution from the meadow, sludge and ditches was quantified through field experiments and literature values. For the field experiments, six flux

chambers were installed across the island to measure the emitted CO_2 and CH_4 gasses. The six flux chambers consisted of:

- 1x short flux chamber in the top clay layer,
- 1x intermediate flux chamber resting on the clay / peat interface,
- 1x deep flux chamber in the peat layer,
- 1x borehole on the edge of Transect 2, anchored in the peat layer 2 m below the surface level,
- 1x shallow flux chamber resting on the surface and
- 1x floating flux chamber in one of the ditches.

Figure 6.2: From left to right: the three flux chambers placed in different subsurface layers, the MGGA connected to one of the flux chambers and the floating flux chamber.

To install the flux chambers, the soil between the surface level and the layer of interest was removed and the flux chambers were pushed into the holes. The sides around the flux chambers were then filled up with the removed clay to make the flux chambers airtight.

At the end of the summer, October 7th, a micro-portable greenhouse has analyzer (MGGA) was taken into the field. This is an instrument that instantaneously, and continuously, measures emitted CO_2 and CH_4 gasses. Different caps could be fitted onto the MGGA through a rubber hose to then clamp onto the different flux chambers. Once the caps were attached to the chambers, the MGGA was turned on and monitored all the gas emissions in the chambers during a four minute period.

The MGGA results only give a momentary impression of the GHG emissions in the field, meaning it is not possible to estimate the total yearly GHG emissions from these results. Therefore, the field results were only used to get an idea of the different emission ratios between the meadow, dredged sludge and ditches. For the total yearly GHG emissions, literature values were found. Kwakernaak estimated that the total yearly GHG emissions produced by peatlands is equal to 30 t CO_2 per hectare [Kwakernaak et al., 2010]. In this study, it was assumed that this value included the emissions from the meadow, dredged sludge and ditches. Using the emission ratios found through the field experiments and the yearly total emission from literature, the yearly emissions for the three peatland contributors were quantified.

The GHG emissions produced by the dairy farming were gathered from literature values from the Food and Agriculture Organization of the United Nations [Food and of the United Nations, 2019] and a previous study done on GHG emissions from the Eenzaamheid [Moens, 2020]. For the pumping station contribution, the yearly station energy consumption was estimated through literature found for the average consumption of a small polder pumping station with a capacity of 10 m^3/min [Clevering et al., 2009], similar to the pumping station in the Zwanburgerpolder. This energy consumption was then converted to a GHG emission by multiplying the energy consumption by the emission factor of 0.37 kg CO_2 per kWh [CBS, 2019].

6.2. Results

The MGGA results from the 7th of October can be seen below in Figure 6.3. In the top figure the concentrations in the top clay layer are shown. For both CO_2 and CH_4, the emissions over time are quite stable. This suggests that there are no processes with in the clay layer that influence the GHG emissions.

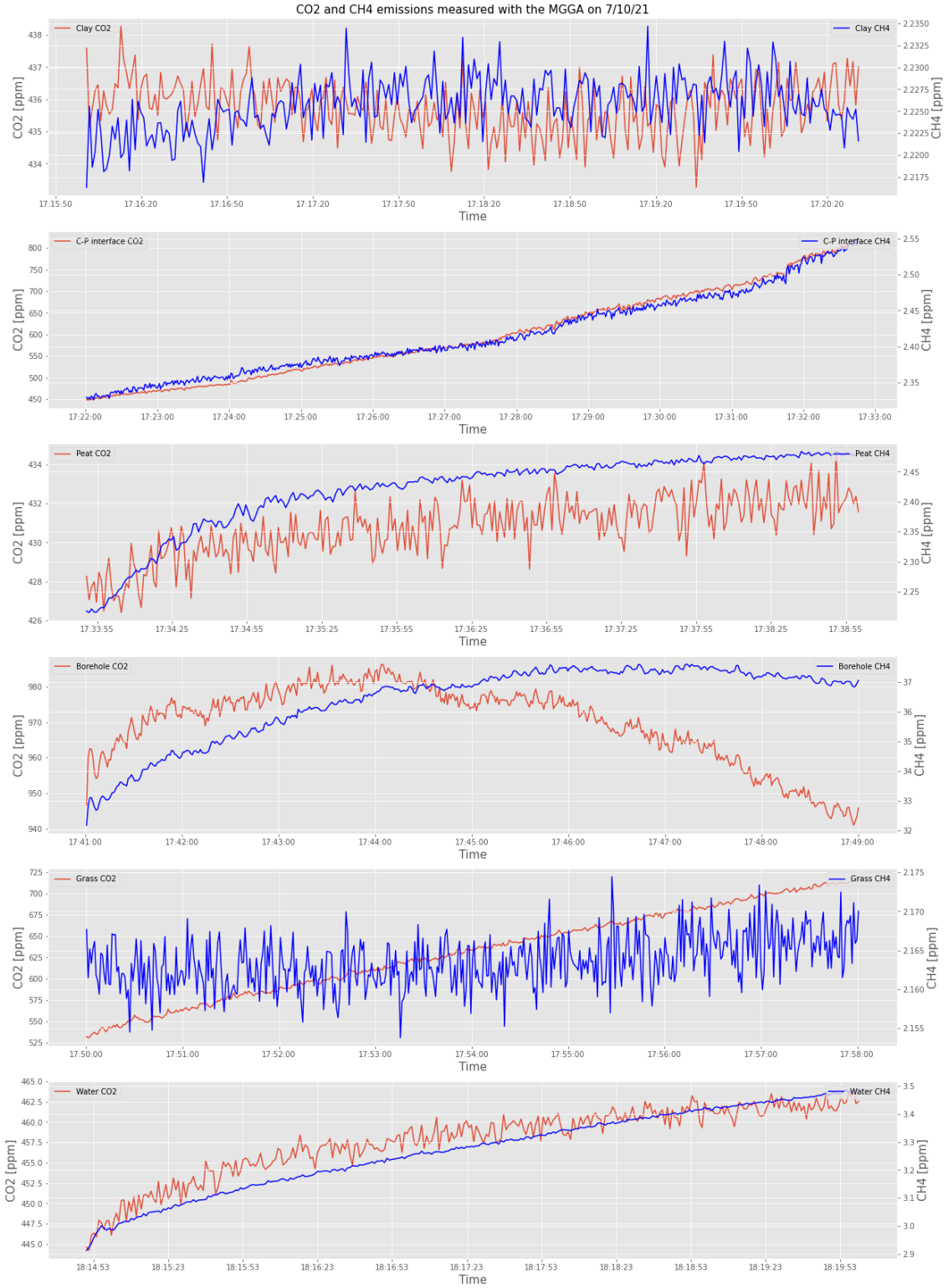

Figure 6.3: CO_2 and CH_4 emissions in ppm for the different flux chambers. From top to bottom: clay layer, clay-peat interface, peat layer, borehole at the edge of Transect 2, top vegetation layer and water.

A very different pattern is seen at the clay - peat interface. Here there is a steep increase in the measured CO_2 and CH_4 concentrations. The top part of the peat layer is the part that is most vulnerable to peat oxidation when the groundwater level drops. In the third plot, the measured concentrations deeper in the peat layer, both the CO_2 and CH_4 concentrations are significantly lower. At this depth, the peat is still below the water table and so not exposed to oxidation.

The most extreme concentrations were measured in the borehole, which can be seen in the fourth graph. Here the CO_2 concentrations almost reached 1000 ppm and the CH_4 concentrations were a factor ten larger than all other measurements. This can be explained by the preparation of the experiment. Expect for the borehole, all flux chambers were left open before the MGGA was connected, meaning that the measured concentrations were the instantaneous GHG emissions. In contrast to the other flux chambers, the borehole had been capped for a significant period of time before connecting the MGGA. The measured concentrations therefore show the CO_2 and CH_4 build up over time and not the instantaneous emissions.

The flux chamber in the top vegetation layer also produces interesting results. In this chamber, increase CO_2 emissions were measured while the CH_4 emissions stayed relatively constant over time. The increase in CO_2 emissions can be explained by peat oxidation happening in the lower peat layers, however it would be expected that the CH_4 concentration would then also increase over time. It is unclear why this pattern is identified in the vegetation layer.

The final floating flux chamber shows a slow increase in both CO_2 and CH_4 emissions. These emissions are determined by the water quality, the sludge quality at the bottom of the ditches and the runoff quality from the neighbouring parcels.

To compare the values quantitatively, the ppm values were converted to a mg/m^2/hour rate. The conversion steps are further explained in Appendix E and are proportional to the slopes seen in Figure 6.3, the volume of air in each flux chamber, the surface area of the flux chambers and the volume of 1 mol of ideal gas. The conversions can be seen in Table 6.1.

Table 6.1: GHG emissions for each flux chamber converted from ppm to a rate in mg/m^2/h and then to CO_2 equivalent.

Flux chamber	CO_2 flux [mg/m^2/h]	CH_4 flux [mg/m^2/h]	CO_2 e flux [mg/m^2/h]
Clay	0	0	0
Clay - peat interface	996	0	1002
Peat	66	1	80
Borehole	162	12	445
Grass	830	0	830
Water	77	1	89

Interesting is to compare the clay - peat interface emissions to the top vegetation emissions. The CO_2 emissions in the vegetation layer are slightly lower than in the clay - peat interface. This suggests that the top clay layer limits the amount of CO_2 and CH_4 released through peat oxidation. This most likely happens due to oxygen that is not able to get through the clay layer and stimulate peat oxidation.

As stated in Section 6.1, the MGGA results were used to quantify the emission ratios between the meadow, dredged sludge and ditches. From the results in Table 6.1, the results from the grass flux chamber were chosen as representative for the meadow contribution and those from the water flux chamber for the ditches contribution. For the dredged sludge contribution, the clay - peat results were taken as representative value. This flux chamber is the one that best represents the emissions caused when peat comes in direct contact with air, which is what happens when dredged sludge is laid along the sides of the ditches. In Table 6.2, the areas of the different components within the Eenzaamheid are listed along with their calculated ratios for the total yearly GHG contributions. It was assumed that the area on which the dredged sludge is laid is equal to the ditch area.

Table 6.2: GHG emission ratios between the three peat oxidation components: meadow, dredged sludge and ditches.

Contributor	Area [ha]	CO2 e flux [mg/m^2/hour]	CO_2 e flux [t/hour]	CO_2 e flux [%]
Meadow	40.47	830	0.336	89
Dredged sludge	4.50	1002	0.037	10
Ditches	4.50	89	0.004	1

Linking the total yearly peat oxidation emission of 30 t CO_2e / ha, or 1214 t CO_2e per year for the Eenzaamheid, to the ratios seen in Table 6.2, the yearly emission values for the meadow, dredged sludge and ditches become: 1081 t CO_2e, 120 t CO_2e and 13 t CO_2e respectively.

Using literature values collected from Food and of the United Nations [2019], Moens [2020] and Clevering et al. [2009], Table 6.3 was made, in which the total yearly emissions produced by the Eenzaamheid can be seen. All values in the table have been translated to CO_2 equivalent. In Appendix F, the calculations used to find these values as well as the CH_4 and N_2O to CO_2 equivalent conversion factors are listed.

Table 6.3: Total CO_2 equivalent emissions produced within the Eenzaamheid.

Emitter	**Process**	**kg CH_4/year/cow**	**kg N_2O/year/cow**	**kg CO_2/year/cow**	**t CO_2e/year/cow**
Cows	Enteric fermentation	80.90	-	-	1.86
Land management and feed production	Mowing, liming, feed production and importing	-	27.66	12.31	8.20
Manure management	Spreading	6.64	6.22	-	1.99
				kWh per year	**t CO_2/year**
Dairy production	Energy consumption			30000.00	11.10
					t CO_2e/year/ha
Peat	Oxidation				30.00
					Total t CO_2e/year
					1827.93

Knowing that there are fifty dairy cows, excluding calves, at the Eenzaamheid and 40.47 ha of land, the total yearly CO_2 equivalent emission from the Eenzaamheid adds up to 1828 t CO_2e. In comparison to the dairy farm emissions, the pumping station emissions are minimal. For a small polder pumping station like the one in the Zwanburgerpolder, a yearly emission of 3.7 t CO_2 was found. The percentage of the total emissions for each component listed in Figure 6.1 is plotted in the pie chart in Figure 6.4.

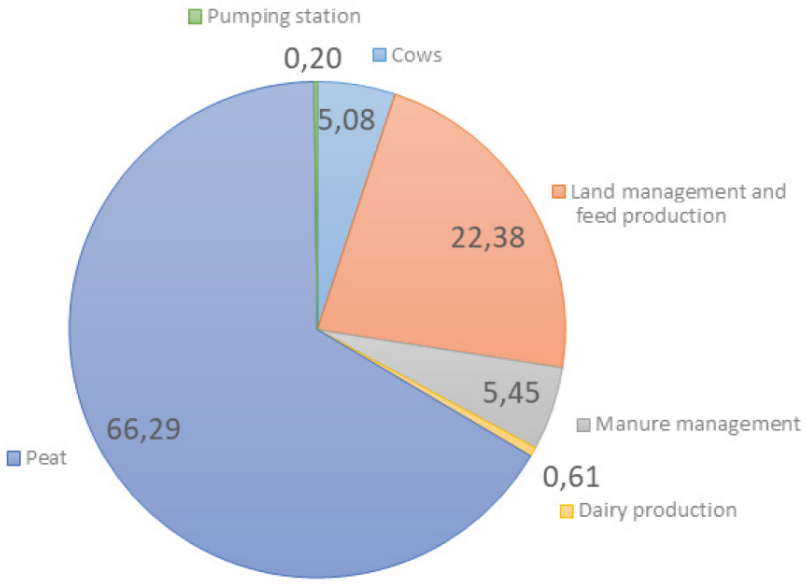

Figure 6.4: Percentage of total CO_2 equivalent emissions of the Eenzaamheid.

6.3. Conclusions

From the MGGA results, it was found that the top clay layer has a positive influence on the amount of CO_2 and CH_4 emitted from the peatland. The clay layer serves as a sort of impermeable layer through which oxygen can not easily pass, hindering peat oxidation. The oxygen that does get through the layer most likely travels through cracks in the clay layer that are formed when the clay dies out. This theory however stills need to be verified through additional tests.

In Figure 6.4, it was seen that peat oxidation contributes to more than sixty percent of the total GHG emissions. Within this component, almost all of the emissions originate from peat oxidation in the meadow, as seen in Table 6.2. This highlights the necessity to mitigate the peat oxidation GHG emissions from the meadow and confirms that tackling land subsidence through raising the groundwater level is an effective step towards the Eenzaamheid lowering its emissions and reaching a regenerative goal.

A certain uncertainty marge must must be kept in mind when evaluating the values from Figure 6.4. The 30 t CO_2e/ha/year emissions originating from peat oxidation in peatlands that was taken from literature represents an average emission for all Dutch peatlands. In Friesland, groundwater drainage, and so GHG emissions, is significantly higher than in the west of the Netherlands and in the Zwanburgerpolder [Kwakernaak et al., 2010]. Furthermore, this value gives a representation of yearly emissions for both peatlands without a top clay layer as peatlands with a top clay layer. So the 30 t CO_2e/ha/year used to determine the total GHG emissions from the Eenzaamheid is a slight overestimation.

7

Land surface displacements

In this chapter, the land surface displacements between April and September are analysed. The yearly average land subsidence of the Zwanburgerpolder is estimated to be between −0.5 mm and −1.5 mm [SkyGeo, 2018], however, the short term behaviour of the subsurface displacement is not yet well-known. To get a better grasp of these short term effects, the land surface displacements results obtained in this chapter are compared to the monitored groundwater levels from Chapter 4 and a distinction is made between the subsurface shrink and swell of the different subsurface layers.

7.1. Methodology

To measure the land surface displacements across the study period, periodical and continuous measurements were done. For the continuous measurements, three GNSS stations were installed across the island: one fixed to a stable point in the middle of the polder and one sensor in each of the two measurement clusters: one by the boreholes to the east of the island and one by the boreholes in the middle of the island. The assumed to be stable station in the middle of the island was attached to a wooden pole on the bridge in the middle of the polder that is founded on sheet pile walls anchored in the deep subsurface.

Each station recorded the X, Y, and Z coordinate of the GNSS receiver every 30 seconds between the 29th of July till the 1st of September. The period should have lasted till the end of September but unfortunately, due to technical issues, the three GNSS stations stopped monitoring the land surface levels from the 1st of September on wards. The stations consist of a GNSS receiver installed on the top of a pole, a cabinet in which the logger and eight batteries are housed and a solar panel that charges the batteries. In Figure 7.1, the GNSS stations can be seen. The pole on which the receiver was installed was inserted 30 cm into the ground, meaning that the monitored data points represented the displacement within the top clay layer, or any shrink and swell occurring in the deeper layers.

The results for the mobile GNSS stations were obtained as the difference in meters between the X, Y and Z coordinates of the stable reference station and the two stations in the parcels. As the GNSS receivers were not displaced throughout the monitoring period, the results of the X and Y coordinates were unvarying. The results for the changing Z coordinates were plotted against time. The initial time series included a lot of outliers and instrument noise. The outliers were removed by going through an iterative process. To start off, all points further than one standard deviation away from the time series mean were removed. Then, with the left over points, the new mean was calculated and again, all points further than one standard deviation away from the new mean were removed.

To find the subsurface movement pattern underneath the instrument noise, moving averages across different time periods were plotted. Ideally, the moving average time period should be slightly smaller than the time it takes for the subsurface to move after an extensive wet or dry period. A too small time period will still display instrument noise, masking the displacement pattern, and a too long time period will overlook the subsurface movement pattern. n the end, two different moving averages were plotted: a six hour moving average to identify a daily pattern in land surface displacement, and a five day moving average to identify a relationship with the phreatic groundwater level. The moving averages are centered, meaning that they are calculated using both data points preceding the time step in question and succeeding it.

Figure 7.1: Left and center: GNSS station used to measure land surface displacements. The GNSS receiver can be seen on the top of the pole, inserted 30 cm into the ground. In the cabinet, the logger and batteries are stored and the solar panel recharges the batteries. Right: Manual GNSS measurements with the Trimble R8.

For the periodical measurements, a GNSS receiver was used to manually measure land surface level at three moments: the 22nd of June, the 23rd of September and the 7th of October. This was done so that a distinction could be made between subsurface shrink and swell happening in the top clay layer and in the deeper peat layer. The GNSS receiver was attached to a 2 m long pole with a pointy tip on the end. The pole was carefully placed on the measurement surface and, when the pole was held level, the GNSS receiver was instructed to connect to the GNSS satellites and save it's estimated X, Y and Z coordinate.

These manual measurements were done on all the twelve boreholes as well as eight metallic poles that were inserted 40 cm into the subsurface, next to the eight shallow boreholes. The measured borehole results were used to look at the peat behaviour and the metallic pole results for the clay behaviour. Aside from the boreholes and the poles, three other locations were measured with the GNSS receiver: the ditch edge by the Eastern deep boreholes, the ditch edge by the deep boreholes in the middle of the polder and the bridge in the middle of the polder. From all these measurement points, it was assumed that the two 15 m deep boreholes and the bridge in the middle of the polder would be stable, unmoving points that could be used as reference points during the three measurements.

On the 23rd of June a Leica GS14 rover was used with Real-Time-Kinematic processing. On the 22nd of September and the 7th of October, a Trimble R8 rover was used with post processing, increasing the accuracy of the results.

7.2. Results

In the figures below, the land surface displacements monitored by the GNSS stations can be seen. In Figures 7.2 and 7.3, a weekly time period is looked at with a six hour moving average period to identify daily patterns. In Figures 7.4 and 7.5, a longer, monthly time period is looked at, with a 24 hour moving average period to see the longer term relationship with the phreatic groundwater level. In all figures, the plotted groundwater levels are collected from the borehole nearest to the GNSS stations (Transect 2 edge for the eastern station and Transect 3 ditch for the middle station, see Figure 4.3) and the outliers have been removed as explained in the methodology section above.

In Figures 7.2 and 7.3, a clear daily pattern can be seen. There is an increase in the land surface level between about midnight till noon, after which the level starts to drop. A possible explanation for this short-term fluctuation is the expansion and contraction of the wooden pole to which the stable sensor was attached to. During the day, with the sun hitting it, the sheet pile expanded. Then in the evenings, the sheet pile returns to its normal length. The smallest fluctuation recorded on the 22nd of August happened on a cloudy day with only 0.7 hours of sun [KNMI, 2021b].

When looking at Figure 7.4, a strong correlation can be seen between the phreatic groundwater level fluctuations and the land surface level fluctuations. However, when then looking at Figure 7.5, this correlation is not at all observable. An explanation for this, is that in the eastern parcel, the GNSS station and the nearest borehole are located right next to each other, while for the middle GNSS station, the nearest borehole is about

30 m away, obscuring the relationship between groundwater level and land surface level. During the month of August in the eastern parcel, the groundwater level varied with up to 30 cm while the land surface level only varies with about 5 mm.

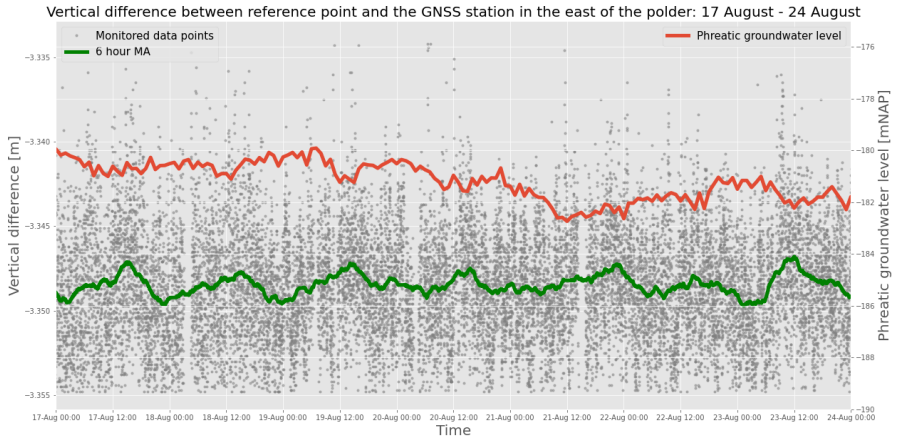

Figure 7.2: Vertical difference between the reference GNSS station and the eastern GNSS station across a weekly time period with the six hour moving average plotted.

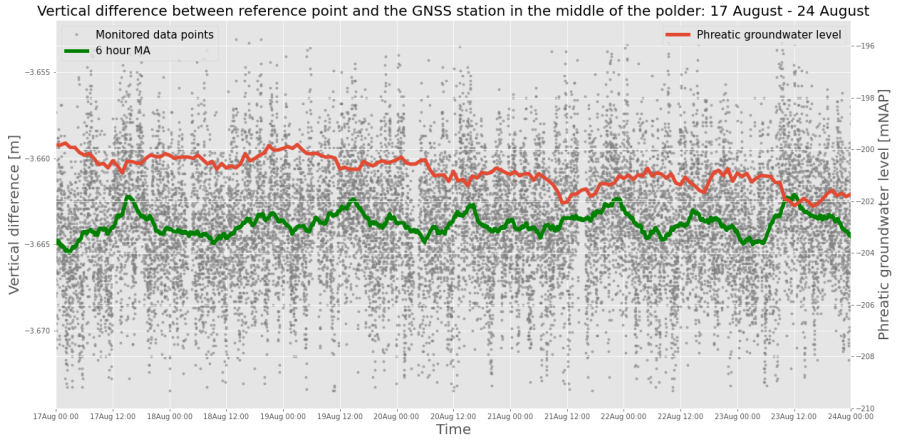

Figure 7.3: Vertical difference between the reference GNSS station and the middle GNSS station across a weekly time period with the six hour moving average plotted.

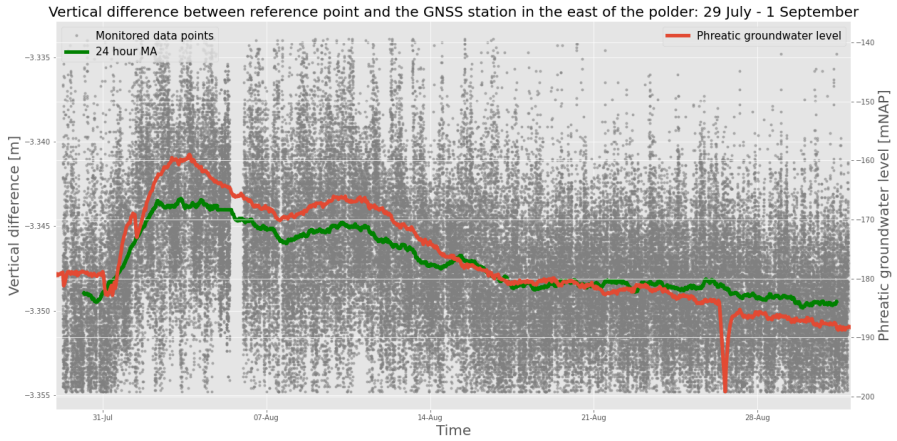

Figure 7.4: Vertical difference between the reference GNSS station and the eastern GNSS station across a monthly time period with the 24 hour moving average plotted.

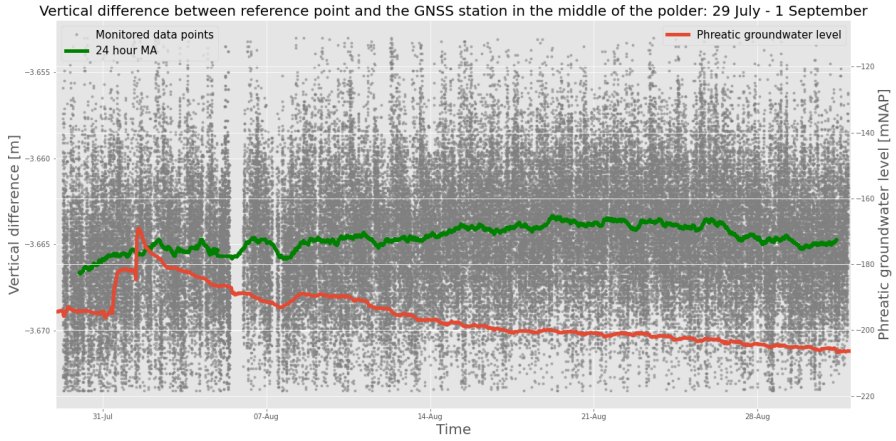

Figure 7.5: Vertical difference between the reference GNSS station and the middle GNSS station across a monthly time period with the 24 hour moving average plotted.

The results of the manual land surface measurements can be seen in Table 7.1. In the figures above, it can be seen that the largest land surface displacement across August was about 5 mm. Therefore, the measurements with standard deviations larger than 5 - 6 mm indicate that the measurements are not precise enough to correctly say something about the land surface displacement that took place across the study period. Unfortunately, these standard deviations occur quite a lot throughout the measurements, especially on the 23rd of June when no post-processing was done. The locations that were expected to be stable points, like the two deep boreholes, show large and unrealistic land surface displacements across the measurements.

Table 7.1: Land surface measurements for the 22nd of June, 23rd of September and 7th of October and the land surface level difference between two consecutive measurements.

Measurement location	H 23 Jun [mNAP]	STD [mm]	H 22 Sep [mNAP]	STD [mm]	H 7 Oct [mNAP]	STD [mm]	Dif Sep-Jun [cm]	Dif Oct-Sep [cm]
East undeep	-1.07	20	-1.28	27	-0.99	6	-21.17	29.24
East deep	-0.97	10	-1.24	5	-0.89	4	-26.29	34.69
Transect 2 edge	-1.16	10	-1.10	6	-1.10	3	6.57	0.30
Transect 2 edge pole	-0.65	10	-0.58	5	-0.59	4	6.35	-0.30
Transect 2 mid	-1.04	20	-0.97	6	-0.97	4	7.50	-0.28
Transect 2 mid pole	-0.53	10	-0.46	6	-0.45	4	6.87	1.15
Transect 2 ditch	-1.09	10	-1.02	5	-1.05	5	7.10	-2.66
Transect 2 ditch pole	-0.60	10	-0.53	5	-0.54	3	6.78	-0.25
Transect 1 edge	-1.04	10	-0.96	4	-0.97	4	7.50	-0.68
Transect 1 edge pole	-0.51	10	-0.46	5	-0.47	4	5.52	-1.01
Transect 1 mid	-1.05	10	-0.10	5	-0.97	4	5.25	2.64
Transect 1 mid pole	-0.54	10	-0.49	5	-0.45	4	4.56	4.04
Transect 1 ditch	-1.04	30	-1.03	6	-1.01	4	1.21	1.96
Transect 1 ditch pole	-0.52	50	-0.58	5	-0.48	4	-5.43	10.05
Ditch by deep boreholes	-1.27	20	-1.23	5	-1.19	4	4.05	3.93
Mid undeep	-0.82	10	-0.75	4	-0.75	4	6.87	0.37
Mid deep	-0.81	30	-0.76	4	-0.75	8	4.36	1.27
Mid ditch by mid deep	-1.10	10	-1.03	5	-1.05	4	7.66	-2.65
Transect 3 ditch	-1.07	50	-1.04	4	-1.01	4	2.52	2.44
Transect 3 ditch pole	-0.69	35	-0.56	4	-0.55	5	13.05	1.05
Transect 3 edge	-0.84	10	-0.79	5	-0.69	5	5.13	9.75
Transect 3 edge pole	-0.71	20	-0.69	6	-0.60	5	1.48	9.18
Bridge middle polder	-0.36	10	-0.15	8	-0.27	4	20.7	-11.95

7.3. Conclusions

Initially, based on land surface data from the NOBV report from 2020 [Erkens et al., 2020], it was expected that the land surface level would vary in the order of magnitude of centimeters. For the subsurface in the Zwanburgerpolder, this is not the case. Small daily fluctuations of about 2 mm were recorded and when looking at a longer monthly, time span, slightly larger fluctuations of about 7 mm were recorded. For the GNSS station in the east of the polder, these long-term land surface measurements had a high correlation with the phreatic groundwater level. In which a 7 mm drop in land surface level occurred for a 30 cm drop in phreatic groundwater level.

The daily fluctuations in the land surface level are most likely caused by the thermal expansion of the wooden pole on which the stable sensor is attached. Then, when looking at a longer, monthly time span a clear rela-

tionship can be seen between the land surface level and the phreatic groundwater level.

When looking back at Table 7.1, relatively large differences can be seen within the manually collected data for the individual locations. As the land surface displacements were smaller than expected, the inaccuracies of the manual GNSS receiver results unfortunately overshadowed the land surface displacements. In hindsight, using a more accurate digital leveller would have been more appropriate to measure the short-term land surface displacements of the Zwanburgerpolder. Due to these inaccuracies, it is not possible to make any conclusions regarding the different degree of land surface displacements between the top clay layer and the deeper peat layer in this study.

8

Future scenarios

In this chapter, the models depicting future Zwanburgerpolder scenarios are presented in which land surface subsidence was limited due to the incorporation of water management practices. Two types of scenarios were made:

1. A base scenario, in which no changes were made to the polder compared to the current situation.
2. Adapted scenarios, in which different measures were implemented to limit land surface subsidence.

The base scenario was made in order to better compare the performance of the adapted scenarios. All scenarios were made using the projected climate scenario for 2065 and were modelled in both iMOD and FlexPDE. The iMOD models give a visual indication of the phreatic groundwater level variations across a summer period and across the island. The FlexPDE models were used to quantitatively compare the lowest groundwater levels between the base scenario and the adapted scenarios.

8.1. Water management measures against land subsidence

When tackling land subsidence, three types of methods can be thought of: 1) decreasing water losses from peatlands, 2) increasing water supplies to peatlands and/or 3) enlarging water storages in peatlands. The water management measures associated to these three methods and examined in this study are listed below. A sketch of their expected influence on the groundwater level can be seen in Figure 8.1.

- Adding ditches,
- Installing horizontal drains,
- Temporarily inundating parcels,
- Installing vertical drains and
- Raising the summer ditch water level.

8.2. Future scenario models

The KNMI climate scenarios (referred to as the KNMI'14 scenario's) were used as the input parameters in the future models. These climate scenarios were developed in 2014 and give a representation of both the changes in average weather and the changes in climate extremes for 2050 and 2085. To make these projections, the KNMI used the worldwide IPCC forecasts and translated them to Netherlands specific scenarios [KNMI, 2015].

The KNMI'14 scenarios consist of four boundary scenarios within which climate change in the Netherlands is likely to take place. Each scenario is an individual combination of two factors: the possible global temperature rise ('Moderate' and 'Warm') and the possible change in airflow pattern ('Low value' and 'High value'). For each of the four scenarios, specific conversion factors are applied to the daily reference time series of 1981 till 2010 in order to create the daily 2050 till 2079 and 2085 till 2114 projections [KNMI, 2015].

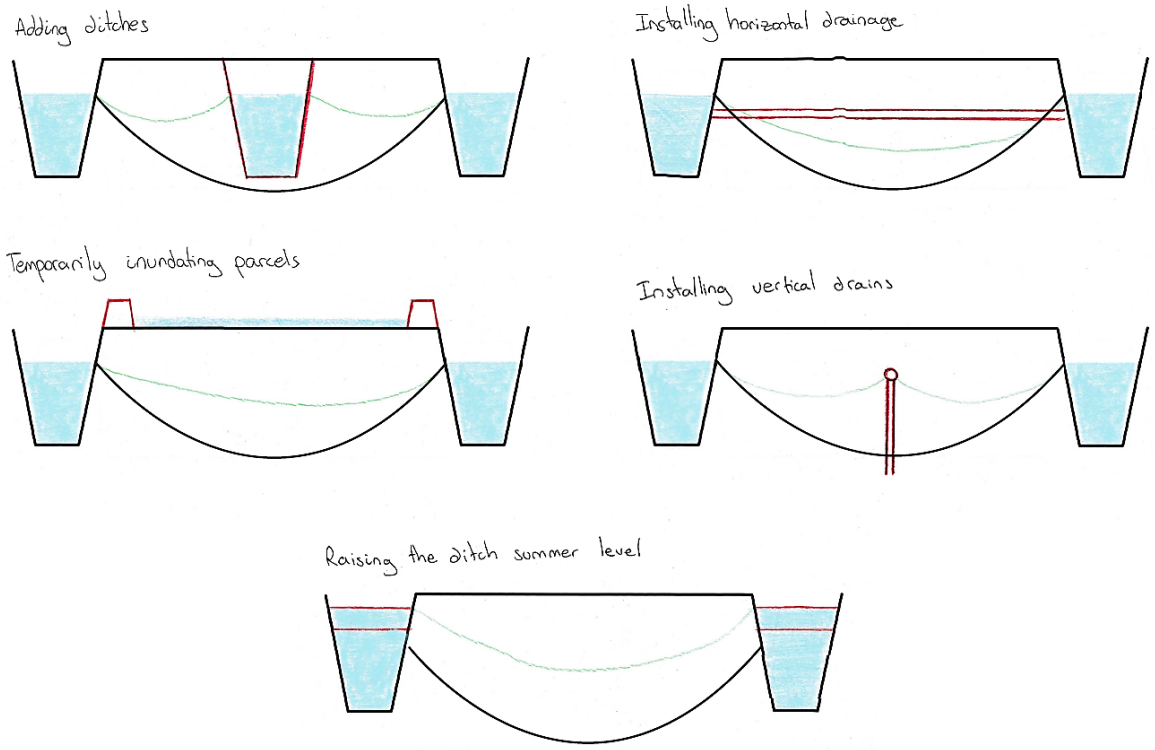

Figure 8.1: Sketch of water management measures examined in this study. The application of the measures are shown in red, and the expected impact on the groundwater levels are shown in green.

The future Zwanburgerpolder models were modelled using the "worst case" KNMI scenario: the scenario with a warm global temperature rise and a high change in airflow pattern (the W_H scenario). This scenario is projected to lead to a 10 % increase in yearly evaporation in 2085 compared to the 2010 evaporation. Further, this scenario projects the largest increase in precipitation, with there being a 7 % yearly increase, in which the winters become a lot wetter (increase of 30 %) and the summers much drier (decrease of 23 %). The seasonal changes in precipitation and evaporation can be seen in Figures 8.2 and 8.3 respectively.

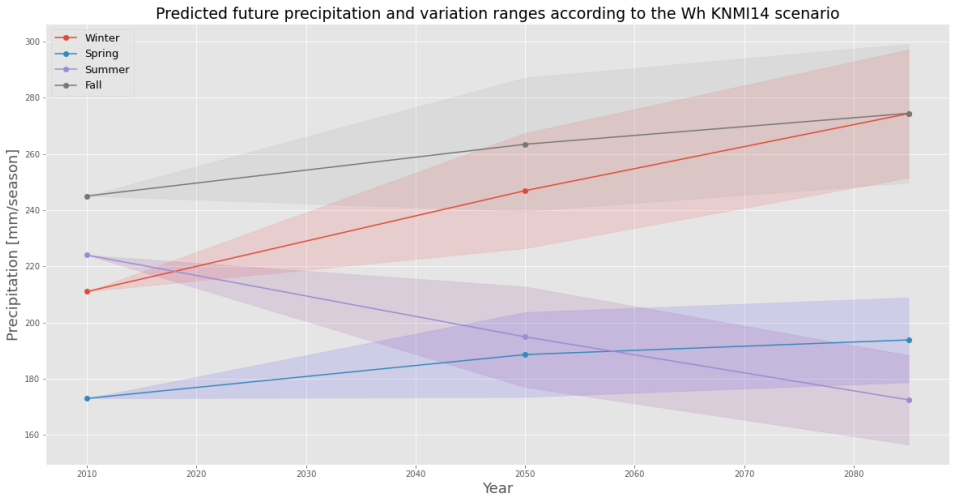

Figure 8.2: Projected future seasonal precipitation and possible variation ranges according to the W_H KNMI'14 scenario.

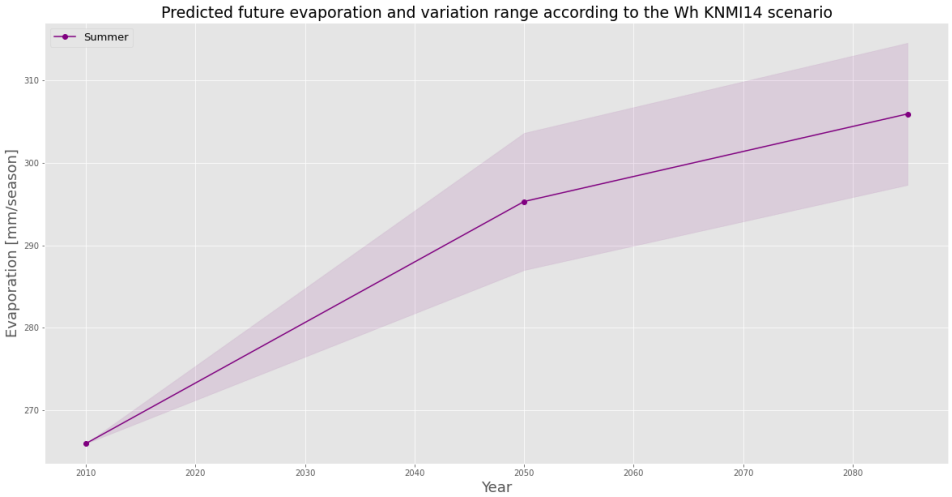

Figure 8.3: Projected future seasonal potential evaporation and possible variation range according to the W_H KNMI'14 scenario.

The use of conversion factors on the daily reference time series results in a slight underestimation of the severity of climate change in future summer periods. In the current KNMI'14 scenarios each rainy day between 1981 and 2010 is converted into a rainy day in the future. However, it is expected that dry spells will last longer in the future [Bresser, 2005, Geijzendorffer et al., 2011]. These longer dry spells will play a critical role on lowering the groundwater level.

To best rectify this shortcoming, the average consecutive dry summer days for the 29 reference years were compared, see Figure 8.4. In this comparison, it was assumed that a dry day was any day which received less than 5 mm of water. From this figure, it can be seen that 1996 was the year with, on average, the longest dry summer periods, in which the individual longest consecutive dry summer period lasted 88 days. Based on this graph, it was decided to use the 1st of October 1993 till the 30th of September 1996 as the reference period for the input parameters of the future iMOD models.

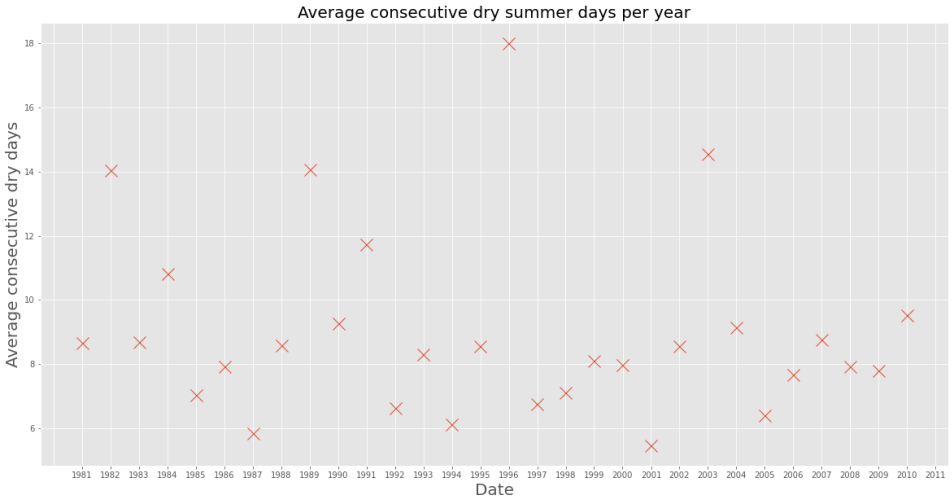

Figure 8.4: Average consecutive dry summer days across the 29 reference years.

Applying the KNMI conversion factors to 1993 till 1996 results in the climate forecast for 2062 till 2065 and 2097 till 2100. As can be seen back in Figures 8.2 and 8.3, the longer the forecast period, the greater the possible variation range and parameter uncertainty. Therefore, it was chosen to use the 2062 to 2065 projections in the future iMOD models, for a smaller parameter uncertainty. As done with the FlexPDE model of the current Zwanburgerpolder situation, the recharge input parameter was taken as the average daily precipitation surplus across the April 2065 till September 2065 period, which was found to be -1.5 mm/day.

8.2.1. Base scenario

In Figures 8.5 and 8.6, the modelled base scenario for the Zwanburgerpolder can be seen. Compared to the groundwater level between the beginning of April and end of September in 2021, the water level in the base scenario is significantly lower. Here, the lowest water level reaches −2.35 mNAP, which is 20 cm lower than the lowest point in 2021. When comparing the groundwater levels obtained in the FlexPDE model, the lowest groundwater level is about 50 cm lower than in 2021.

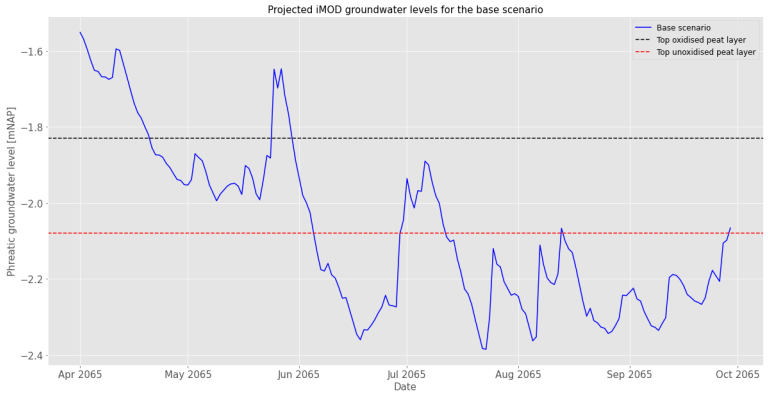

Figure 8.5: iMOD model results for the 2065 base scenario, in which the 2063 till 2065 precipitation and evaporation KNMI projections were used as input data.

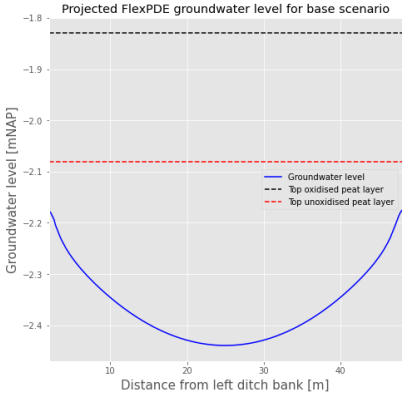

Figure 8.6: FlexPDE model results for the 2065 base scenario with a precipitation surplus of −1.5 mm/day.

8.2.2. Adapted scenarios

Below, the five applied water management measures are briefly described and the model results are presented. The model parameter inputs used for the different measures can be found in Appendix B.

Adding ditches

In the first scenario, extra ditches were added in the middle of the parcels. The additional ditches were given the same characteristics as the current dimensions of the smaller side ditches, so a width of 5 m, a depth of 0.4 m and a summer water level of −1.71 mNAP.

Installing horizontal drains

In this future scenario, horizontal drains were added to the shallow subsurface, perpendicular to the ditches. When the phreatic groundwater level drops below −1.71 mNAP, ditch water infiltrates into the subsurface through the drains.

Temporarily inundating parcels

In this scenario, the parcels were temporarily inundated during a three day period. To work efficiently, the parcels need to be inundated at the beginning of the summer period, before the lowest groundwater levels are reached. In the modelled scenario, the parcels were inundated between the 10^{th} and the 13^{th} of June. In practice, a small embankment would need to be built around the parcels, after which, the parcels can be inundated by siphoning boezem water into the polder through a large hose. Further, a rotation system needs to be applied, in which parcels are inundated consecutively so that grazing land is still available.

Installing vertical drains

Here, the high groundwater head from the first aquifer was used to replenish the phreatic groundwater. Vertical drains anchored into the aquifer were added to transport water up to the shallow subsurface. From there, the collected water infiltrates into the parcel through a horizontal drain placed parallel to the ditches, in the middle of the parcel. A brief illustration of a similar construction can be seen in Figure 8.7.

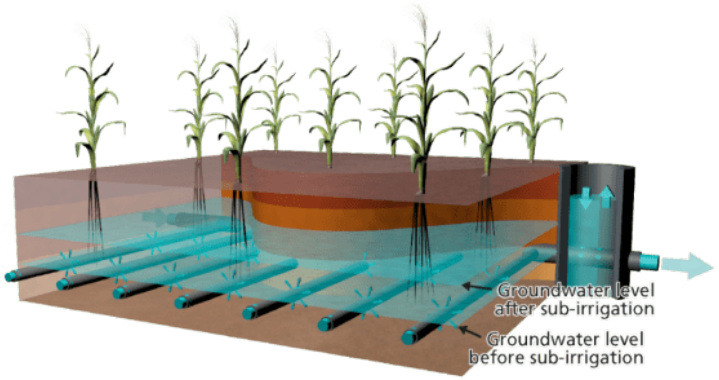

Figure 8.7: Vertical drains illustration. In this study, the vertical drain is connected to the first aquifer from which water is transported up and then across the parcel through a horizontal drain placed in the middle of the parcel, parallel to the ditches [Narain-Ford et al., 2020].

Raising the summer ditch water level

For the raised water level scenario, the summer ditch water level was raised by 20 cm, becoming −1.51 mNAP. This scenario still leaves a 20 cm difference between the ditch water level and the parcel land surface level.

In Figure 8.8, the 2065 groundwater level variations between April and September produced in iMOD for the five adapted scenarios can be seen in contrast to the base scenario and in Figure 8.10, the time independent, FlexPDE results are shown. It can be seen that the groundwater levels obtained with all five measures are higher than the base scenario during the critical summer months. Though, despite the measures abilities of raising the groundwater, the phreatic groundwater levels in each scenario still briefly fall under the top of the currently unoxidised peat layer.

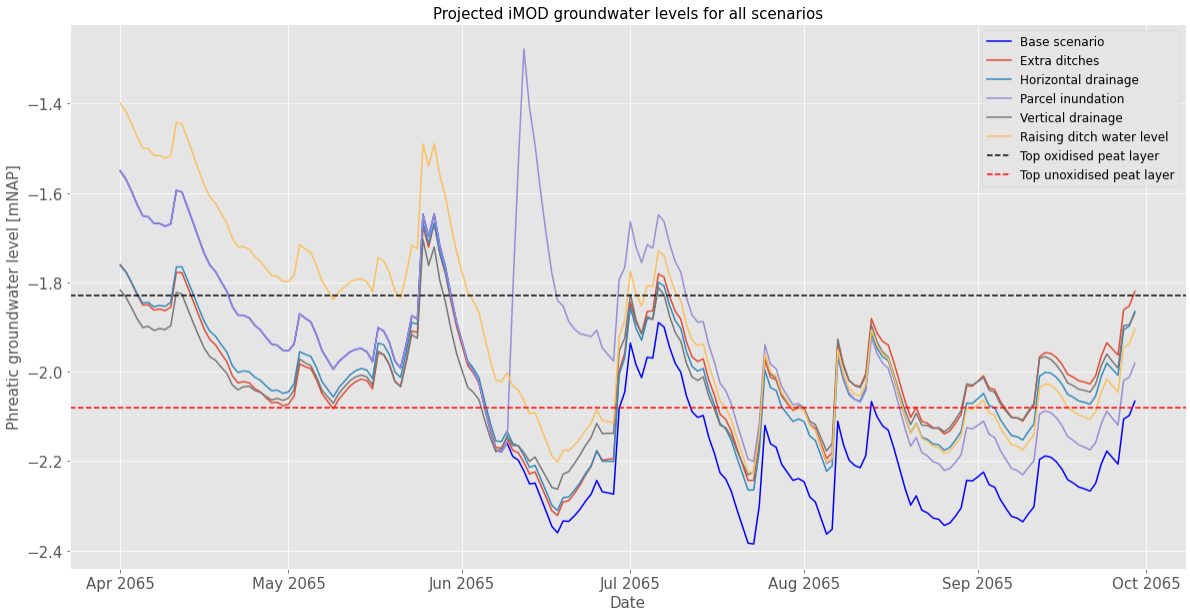

Figure 8.8: iMOD results for the phreatic groundwater level projections in 2065 for the five adapted scenarios compared to the future base scenario.

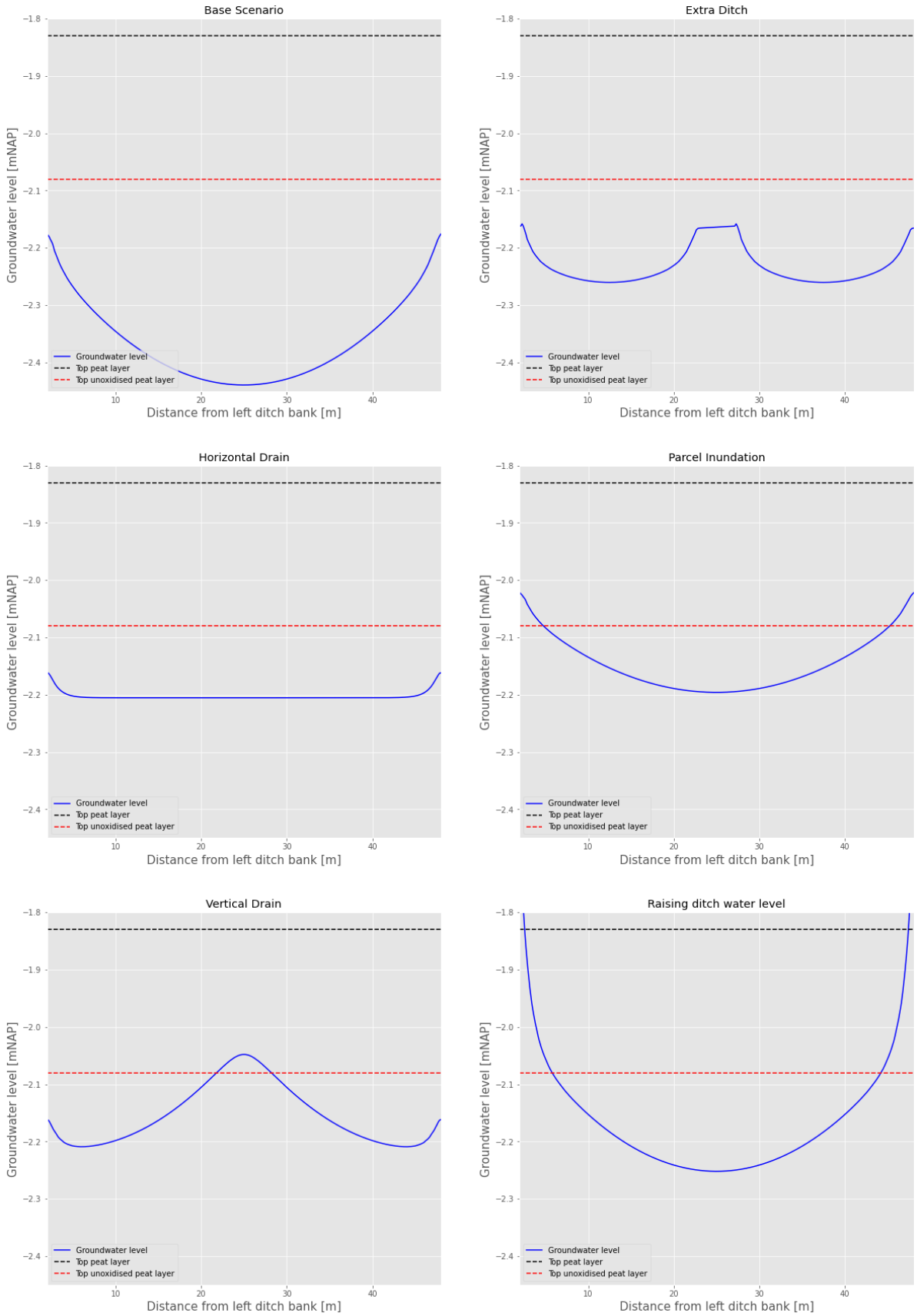

Figure 8.9: FlexPDE results for the phreatic groundwater levels in 2065 for the five adapted scenarios compared to the future base scenario.

8.2.3. Critical areas

Applying measures across the entire 40.7 ha of land belonging to the Eenzaamheid is a huge, financial and operational task. Due to the slightly varying subsurface composition across the island and the varying parcel widths, the lowest, critical groundwater levels are not reached in every parcel. Using the iMOD base scenario, the critical ares in the Eenzaamheid's parcels were identified, where the lowest summer groundwater levels were reached.

Two patterns could be identified for critical areas. Firstly, critical parcels tend to be the larger parcels, where the lowest groundwater levels are reached right in the middle of the parcels. Secondly, the edge of the parcels further away from the main ditch channel tend to be more critical than the areas closer to it. The most critical areas can be seen in Figure 8.10.

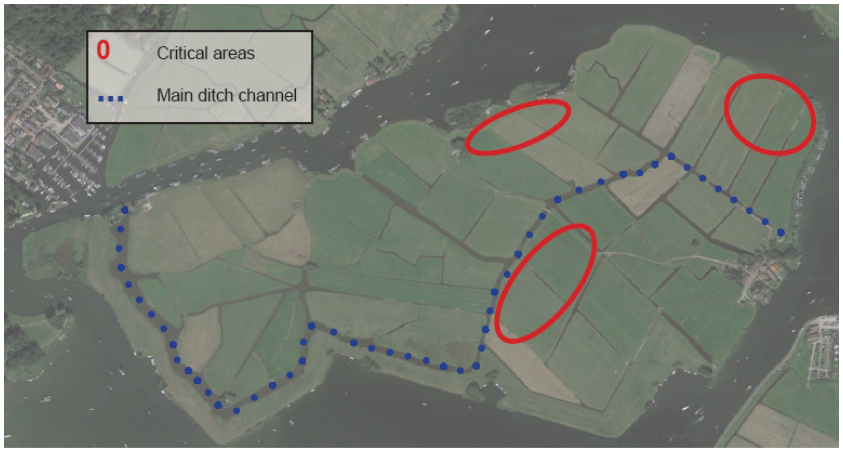

Figure 8.10: Critical areas of the Eenzaamheid identified in iMOD model where the lowest groundwater levels are reached.

9
Discussion

In this chapter, the relationship between the lowest groundwater level and GHG emissions are firstly quantified using empirical formulas defined by van den Akker. Then, the advantages and disadvantages of the five measures presented in Chapter 8 are discussed. Finally, some study limitations are given.

9.1. Lowest groundwater level and GHG emission relation

For a peatland with a clay top layer larger than 40 cm, the empirical relation between land subsidence [mm/year] and the lowest groundwater level (LGL) [m below surface level] is equal to [van den Akker et al., 2007]:

$$\text{Subsidence} = 23.54 \times \text{LGL} - 10.47 \tag{9.1}$$

In an other van den Akker formula, the GHG emissions are related to the freeboard values; the difference between the summer ditch water level and the surface level. For all future management measures, except for raising the summer ditch level, the freeboard values remain unchanged, meaning no impact on GHG emissions would be noted from implementing the water management measures. It was therefore decided to use the land subsidence value from equation 9.1 and put in van den Akker's empirical formula that links yearly land subsidence [mm/year] to freeboard value [m], which is [van den Akker et al., 2007]:

$$\text{Freeboard value} = \frac{\text{Subsidence} + 9.79}{15.455} \tag{9.2}$$

Then, the van den Akker formula that links GHG emissions, as t/ha/year CO_2e, to freeboard values [m] for peatlands with a top clay layer is [van den Akker et al., 2007]:

$$CO_2\text{e} = 2.30 \times \text{Freeboard value} + 1.99 \tag{9.3}$$

Applying the equations above to the base scenario where the LGL dropped down to −2.44 mNAP results in a yearly land subsidence of about 16 mm/year (equation 9.1). So, in the scenario where no water management measures are implemented to the Eenzaamheid parcels, the yearly GHG emitted in 2065 would be 4.85 CO_2e t/ha/year.

9.2. Advantages and disadvantages of measures

As seen in Chapter 8, all five measures increase the modelled 2065 groundwater levels when compared to the base scenario and in doing so they all limit land subsidence, restrict peat oxidation and therefore lower the amount of CO_2, CH_4, phosphorus and nitrogen released into the atmosphere and water. The higher groundwater levels also have a positive effect on the meadow birds, as worms will be less deep in the ground and therefore easier to catch [STOWA, 2021]. Individual advantages and disadvantages are discussed below.

Adding ditches

Adding ditches in the middle of the parcels is an expensive option. Large machinery would be needed to excavate the top 5 m of the subsurface and distribute it across the surrounding land. This option is a permanent measure, that leaves little flexibility in the future, during wet summers.

Further, extra ditches will mean that there will be more ditches to be dredged later on, which will be unfavourable towards GHG emissions. However, when looking back at the emission ratios in Chapter 6.2, it was found that the meadow emissions ratio was much larger than the dredged sludge ratio. Therefore, it is

expected that overall, the reduced meadow emissions from limited peat oxidation will outweigh the extra emissions coming from the extra dredged sludge.

Installing horizontal drains
Horizontal drains can be implemented with casings or as mole drains. In the latter, a cone attached to an arm is pulled through the subsurface with the help of a tractor. Therefore, no pipes are added to the subsurface, making the process economically attractive compared to installing drains with casings. However, mole drains are much more susceptible to blockages [Dekker, 1999] and therefore need frequent maintenance.

Installing horizontal drains is a permanent option that works in both the summer and in the winter. In the summer water is infiltrated into the subsurface and in the winter it is drained from the subsurface. For both the drains with casings as the mole drains, the installation process would be considerably difficult. Further, using horizontal drains with casings does not fit into the Eenzaamheid's regenerative idea, as man made elements would need to be added to the subsurface. Mole drain on the other hand, would fit better, as the horizontal holes would not be filled with any unnatural elements.

Temporarily inundating parcels
Temporarily inundating parcels is quite economically attractive when compared to the other measures. Further, it is one of the few measures with high flexibility. During a wet summer, it can simply be chosen to skip parcel inundation or to only inundate the critical parcels. However, it must be kept in mind that parcels that are temporarily inundated, cannot be used for grazing for a while, making it unfavourable for agricultural use.

In Chapter 4, it was found that the boezem water nitrate concentration was ten times higher than the concentrations in the polder. Therefore, using the boezem water to inundate the parcels could cause an increase in nitrate concentration within the polder, stimulating eutrophication and negatively influencing aquatic animals. Further, inundating parcels will drown the smaller mammals that borrow in the shallow subsurface.

Installing vertical drains
Similar to horizontal drains, installing vertical drains is an expensive and challenging process. With the vertical drains going down to a depth of -5 mNAP, the maintenance process will also be demanding and the costs will be high. The installation of the drains and water storage tank is a permanent process that can not easily be altered, if the need to do so would arise. This could happen for instance if for some reason the water body that is connected to the first aquifer would experience a change, significantly altering the water pressure head in the layer.

When using the vertical drains, the water quality of the deep groundwater will also influence the phreatic groundwater quality. The phosphate and chloride concentrations in the ditches and phreatic groundwater will likely increase. When looking back at Table 5.4, the chloride concentration in the first aquifer is lower than the KRW goal of 300 mg/l, so it is not expected that the adjusted ditch chloride concentration will exceed this goal if vertical drains were installed, causing water quality concerns. However, the increased phosphate concentration will be problematic for the water quality. Now, it is already much higher than the KRW goal and a further increase in phosphate concentration means a larger stimulation of euthrophication and a further lowering of the dissolved oxygen content in the ditches.

Raising the ditch water level
Raising the ditch water level is a financially good option. It can be implemented by installing an adjustable culvert by the bridge in the middle of the polder, at the boundary of the Eenzaamheid's territory. This way, the other island stakeholders (the other farmer, the waterboard, the millers and the handful of island inhabitants) would not need to be impacted by raising the water level in the whole polder.

Raising the summer ditch level is a method that provides high flexibility in the future. During wet summers, the ditch water level simply does not have to be raised. Raising the ditch water level needs to be done with some care. Having a water level that is too high can cause the ditch banks to crumble, having a negative impact on its habitat potential [STOWA, 2021]. With one adjustable culvert at the boundary of the Eenzaamheid, raising the water level will however impact the whole territory. To adjust individual ditches, culverts would have to be added to each ditch channel, increasing the installation costs.

Using the van den Akker formulas as well as the advantages and disadvantages mentioned above, Table 9.1 was made. In the table, a quantitative comparison is first done for each future scenario in which the limited land subsidence and saved CO_2e emissions compared to the base scenario are given. Then a qualitative comparison is done on how well the measures meet specific criteria.

Table 9.1: Comparison of the five different measures for the 2065 projection. For the evaluation of the criteria the following scale was used: 0: negative impact, 1: limited impact, 2: positive impact

Measure	Lowest groundwater level [mNAP]	Limited land subsidence [mm]	CO_2e saved [CO_2e t]
Adding ditches	−2.26	4.24	25.66
Installing cased horizontal drains	−2.21	5.41	32.79
Installing horizontal mole drains	−2.21	5.41	32.79
Inundating parcels	−2.19	5.81	35.21
Installing vertical drains	−2.20	5.65	34.21
Raising the ditch water level	−2.25	4.47	27.09

Measure	Influence on water quality	Influence on biodiversity	Financial feasibility	Needed maintenance	Installation feasibility	Flexibility	Use of regenerative techniques
Adding ditches	2	2	0	1	0	0	2
Installing cased horizontal drains	2	2	0	1	0	0	0
Installing horizontal mole drains	2	2	1	0	0	0	2
Inundating parcels	1	0	1	1	1	2	2
Installing vertical drains	1	2	0	1	0	0	0
Raising the ditch water level	2	1	2	2	1	1	2

Each measure manages to raise the groundwater level by about 20 cm compared to the base scenario and when looking at the amount of CO_2e saved, each measure results in a similar order of magnitude. Therefore, the most appropriate technique can be chosen dependent on the qualitative comparison of each technique.

For Joost van Schie, with the goal of becoming a regenerative farm, there is a strong preference to apply regenerative techniques, or techniques that do not add man made materials into the subsurface, eliminating the cased horizontal drain and the vertical drain. Temporarily inundating the parcels is the measure that, quantitatively, works best. However, as mentioned above, this measure brings along a main downside: causing a reduction in grazing land.

As seen back in Section 8.2.3, some parcels within the Eenzaamheid are more critical than others. For this reason, the preference goes out to measures that can be applied locally. This way, the groundwater level, water quality and GHG emission can be monitored on a smaller scale to see their actual effects before applying the measure to the whole Eenzaamheid.

Keeping all the advantages and disadvantages mentioned in this chapter, the advice for the Eenzaamheid is to start by applying local measures in the critical parcels and to apply a combination of the methods mentioned above. Temporarily inundating parcels scores well on all the criteria in Table 9.1, but is unfavourable for grazing. Therefore, the advice is to combine this with adding ditches. As mentioned in Chapter 2.1, each parcel already has a shallow gutter running down the middle. Enlarging these gutters and inundating them during the summer would allow the rest of the parcel to be used for grazing, while the groundwater level is recharged in the middle of the parcel, where the lowest groundwater level occurs. This measure would result in less maintenance as when adding an extra ditch, as no yearly dredging would be needed. The enlarging of the gutter can be done by pulling an embankment bucket (*taludbak*) through the parcel. The gutters can be inundating by siphoning water from the boezem and as this measure does not disrupt grazing, the gutters can be inundated during a longer time period than the three days used in the parcel inundation model.

This recommended scenario was modelled in FlexPDE. With the average summer precipitation recharge of −1.5 mm/day in 2065, the lowest groundwater level reached was −2.25 mNAP, see Figure 9.1, which is com-

parable to the five other modelled scenarios. In Figures 9.2 and 9.3, a transect and a top view of the measure can be seen.

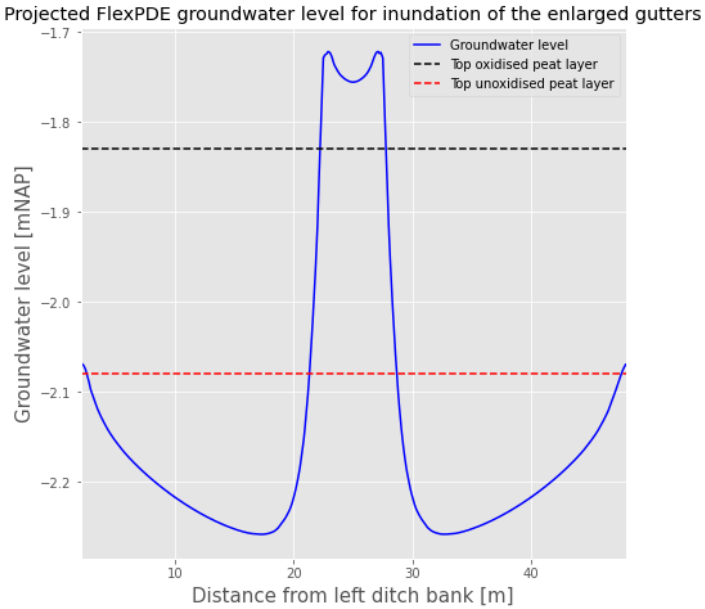

Figure 9.1: Projected FlexPDE groundwater level for the scenario in which the enlarged gutters are inundated.

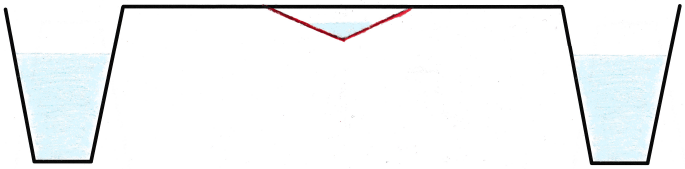

Figure 9.2: Transect of the scenario in which the enlarged gutters are inundated.

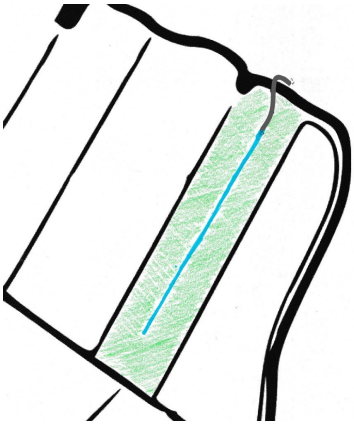

Figure 9.3: Top view view of the scenario in which the enlarged gutters are inundated.

9.3. Study limitations

Throughout this study, certain limitations were noted. Below, these limitations are split up per theme and further discussed.

Parameter uncertainty

The first limitation encountered in this study was parameter uncertainty. When making the yearly water balances in chapter 4.2.1, this especially applied to the evaporation, seepage and polder wind mill values. The KNMI evaporation used in the balance fluxes is estimated through Makkink's reference crop evaporation formula. This is a formula that estimates the potential evaporation of shortly mowed grass that has no shortage of water. In reality, during dry periods when there are water shortages, the actual evaporation is lower than the potential evaporation, making the evaporation values used in Chapter 4 a slight overestimation of reality. The seepage and polder wind mill values also have a high degree of uncertainty. As briefly mentioned in

Chapter 4.2.1, these values are based on other collected time series such as, lack of, precipitation, the pumping station operating hours (both used for the seepage flux), wind and the mill operating hours (both used for the polder mill flux).

Further, in the water quantity chapter, only a few inverse auger pumping tests were performed to calculate the peat hydraulic conductivity. As mentioned in Chapter 4.1.2, the auger pumping test was not carried out due to limitations in field equipment and time constraints. Ideally, both tests would have been carried out a dozen times. This would have given a clearer indication of which values were outliers and of the degree of soil heterogeneity in the Zwanburgerpolder. Lastly, when looking at the future scenarios, the projected time series used, contain significant uncertainties. The longer the projected period, the larger the variation range as was seen in Figures 8.2 and 8.3.

The water balances fluxes, results from the inverse auger pumping tests and the KNMI'14 climate projection were used as basis for the input parameters of the iMOD and FlexPDE models. These uncertainties mean that the final model outputs also have a certain error range. To minimize the error range, a model sensitivity and uncertainty analysis could have been done [Loucks, 2005]. A sensitivity analysis shows how sensitive the model output is to the individual parameters and an uncertainty analysis tries to describe the total set of possible outcomes with their occurrence probabilities. Doing these analyses would have shown for which influential parameters, with high uncertainties, it would be worthwhile to try to reduce the parameter uncertainty. These analyses were not done in this study due to time constraints.

iMOD ability to represent reality
The current iMOD model represents reality quite well. The timing and order of magnitude of the most significant modelled groundwater level peaks coincide with that of the measured groundwater levels. However, the modelled groundwater level reacts much stronger to precipitation. This is because of the lack of a top unsaturated zone in the model. This zone serves as a buffer. During a dry period, this zone holds on to water, delaying the influence of a rain shower on the phreatic groundwater. Conversely, after a wet period, water is firstly evaporated from the top unsaturated zone, before the phreatic groundwater level evaporates. In reality, this smooths out the rate of change in the groundwater level, which currently does not happen in the iMOD model. The parameter uncertainty limitation discussed above also has an influence on the models ability to represent reality. A model will always remain a simplification of the real world.

Field experiments time constraint
The time period set out for this study was experienced as a limitation during the field experiments. To better understand the groundwater level behaviour and the interactions between the different water bodies, at least a one year data set is required. With this, it is possible to see if the groundwater head in the first aquifer is constant throughout the year and whether it is indeed appropriate to use to raise the phreatic groundwater level.

Also, with a longer research period, it would have been possible to see the seasonal pattern in the land surface displacements. Within the measured time span, a relationship was seen between the land surface level and the phreatic groundwater level. However, having a longer, yearly time series, it would have been possible to identify yearly patterns in land displacement and better understand the land displacement behaviour.

Wet summer
The summer of 2021 was a relatively wet summer, especially when compared to the 2018 and 2019 summers. The phreatic groundwater level remained above the unoxidised peat level during the majority of the study period. Due to this, it was not possible to evaluate to what extent a largely lowered groundwater level may impact GHG emissions, land subsidence and water quality.

10

Conclusions and recommendations

The main goal of this study was to investigate how land subsidence can be limited in a clay - peat polder through the implementation of water management practices in order to reduce GHG emissions, improve (ground)water quality and stimulate biodiversity. To be able to answer this question, three sub-questions were defined. Below, the sub-questions are firstly looked at, after which the main research question is answered. Then in Section 10.2 a number of recommendations are given. Firstly, recommendations regarding the Eenzaamheid are given and secondly, recommendations regarding the applicability of the study results on a larger scale are given. Lastly, recommendations for further research opportunities are proposed.

10.1. Conclusions

How does the current Zwanburgerpolder system work?
As seen in the results from Chapter 4, it can be concluded that the phreatic groundwater level in the Zwanburgerpolder is strongly characterised by the precipitation surplus, especially during wetter periods when rain water immediately infiltrates through the saturated root zone. In drier periods, like end of June onward in this study, the phreatic groundwater level is less reactive to precipitation, because a portion of the rain water is kept in the top, unsaturated root zone, therefore not reaching the phreatic groundwater.

Further, in the summer, the groundwater level drops due to increased evaporation, creating a groundwater dip that falls below the ditch water level and the pressure head in the first aquifer. Due to the pressure head differences, ditch water infiltrates into the shallow subsurface and deeper groundwater seeps up from the first aquifer, but to a limited extent, as this cannot overturn the summer groundwater dip. In contrast, during the winter season, the groundwater level rises above the ditch level and the pressure head in the first aquifer. In winter, the groundwater flows from the subsurface into the ditches. The transition from a winter bulge to a summer dip is a slow process. During the wet summer of 2021, the summer dip was only reached around the beginning of August in the Zwanburgerpolder subsurface.

In Chapter 5, it was seen that the surface water quality is strongly impacted by the seepage of phreatic groundwater into the ditches. In the winter, when the winter bulge seeps into the ditches, the nutrients released during peat oxidation are flushed into the ditches. Peat oxidation happens in the summer, when the groundwater drops down below the oxidised peat layer and the newly uncovered, unoxidised, peat layer starts to oxidise. In this process CO_2, Ch_4, nitrogen and phosphorus are released into the subsurface and atmosphere.

When looking at the water quality of the surrounding boezem water, it can be concluded that the boezem quality does not significantly affect the ditch water quality or the phreatic groundwater quality. These are mostly dependent on biological and chemical process that happen within the polder, like peat oxidation, nitrification of ammonia/ammonium and runoff from agricultural land use. The phreatic groundwater quality is also determined by to the quality of the first aquifer. In the summer, when there is seepage from this layer into the shallow subsurface, water with a very high phosphate concentration infiltrates upwards.

The largest cause of GHG emissions in the Zwanburgerpolder is from peat oxidation. When looking at the total CO_2 equivalent emissions released from the Eenzaamheid shown in Chapter 6, 66 % comes from peat oxidation. With an area of 40.47 ha, the meadow is the largest contributor compared to the dredged sludge and ditches, making up 89 % of the peat oxidation emissions. The dredged sludge makes up 10 % of the emissions and lastly the ditches only accounts for 1 % of the total emissions. During the MGGA analysis, it was

found that the top clay layer that covers the Zwanburgerpolder subsurface serves as a partially impermeable layer through which oxygen cannot easily pass, hindering the peat oxidation in the meadow.

From Chapter 7, it can be concluded that the land surface level is strongly correlated to the phreatic groundwater level. During the month of August a 7 mm drop in land surface level occurred for a 30 cm drop in phreatic groundwater level.

Which water management measures can be implemented to limit land subsidence?
Peatland subsidence can be limited through water management measures by 1) decreasing water losses, 2) increasing the water supply and 3) enlarging the water storages. Based on these three approaches, the following five techniques were elaborated in Chapter 8 in order to limit future land subsidence in the Zwanburgerpolder:

- Adding ditches,
- Installing horizontal drains,
- Temporarily inundating parcels,
- Installing vertical drains and
- Raising the summer ditch water level.

How effective are these measures?
In Chapter 9, the efficiency of the different measures was evaluated. This was done quantitatively, through the use of the van den Akker formulas and qualitatively by scoring the measures against several criteria. All five measures significantly raised the groundwater level when compared to the base scenario and therefore all limited land subsidence compared to the base scenario. The measure that limited land subsidence the most for the 2065 scenario was temporarily inundating the parcels. When scoring the measures qualitatively, raising the ditch water level and temporarily inundating the parcels performed the best.

How can land subsidence be limited in a clay - peat polder through the implementation of water management practices in order to reduce greenhouse gas emissions, improve (ground)water quality and stimulate biodiversity?
In this study, land subsidence was limited through raising the groundwater level in order to limit peat oxidation. For all five measures analysed in Chapter 8, the critical, summer groundwater levels still dropped to some extent below the top of the unoxidised peat layer. However, the measures all performed better than the base scenario.

For the Zwanburgerpolder, limiting peat oxidation means that the GHG emissions from the meadows will be reduced. Further, there would be an improvement in the surface water quality through a lowering of the nitrate concentration in the ditches. In addition, as mentioned in Chapter 2.4, maintaining a higher groundwater level in the summer is beneficial for the meadow birds that breed on the island, as it results in an increased availability of worms in the top soil and lowers the soil resistance, making it possible for the birds to poke their beaks into the soil.

10.2. Recommendations

10.2.1. Recommendations for the Eenzaamheid

For the Eenzaamheid, where regenerative practices and agricultural capacity take center stage, the recommendation for limiting land subsidence is to combine and adjust two measures presented in Chapter 8 and initially apply them locally in the most critical parcels. With the two to be combined measures being: temporarily inundating parcels and adding ditches.

Temporarily inundating parcels scores well on all the criteria in Table 9.1, but is agriculturally unfavourable, as parcels cannot be used for grazing during a significant amount of time. However, as mentioned in Chapter 2.1, each parcel already has a shallow gutter running down the middle. Enlarging these gutters and inundating them during the summer would make it possible to use the rest of the parcel for grazing, while the

groundwater level is recharged through the middle of the parcel. This measure would result in less maintenance as when adding an extra ditch, as no yearly dredging would be needed. The enlarging of the gutter can be done by pulling an embankment bucket (Dutch: *taludbak*) through the parcel. The gutters can be inundated by siphoning water from the boezem and they can be inundated during a longer period of time than the three days used in the modelled scenario, as grazing can still occur along side the gutters.

The recommendation to start off by only applying the measures in the most critical parcels is given in order to use it as a testing ground to check the possibly negative effects of the measures besides the desired positive effects of limiting land subsidence, reducing GHG emissions and improving the (ground)water quality.

10.2.2. Recommendations for a wider applicability

Within the Netherlands, there are more than 270,000 ha of agricultural peatlands [de Vries, 2011]. The results discussed in this report provide an interesting addition to peatland subsidence studies, like the NOBV, and were obtained through field experiments done on a much smaller budget than the current NOBV measurement setups. The recommendation towards the NOBV and other peatland subsidence studies is therefore to apply a large network of lower cost measurement setups, instead of a few costly ones, in order to get an extensive representation of the behaviour of different Dutch peatlands, which will help towards achieving the national Climate Act goal by 2030.

Further, the water management measures examined in Chapter 8 and discussed in Chapter 9, give an indication of the different methods' efficiency, advantages and disadvantages. However, as different locations have their own set of criteria and boundary conditions, the recommendation for other stakeholders who consider implementing new measures, is to thoroughly think about the individual advantages and disadvantages applying measures has on the peatland in question.

10.2.3. Recommendations for further research

Below, recommendations are given on processes and topics that need further investigation in order to better understand the processes occurring in the Zwanburgerpolder:

- *Longer fieldwork monitoring* : The first recommendation is to monitor the different field experiments across a longer time period. In this study, the groundwater level, water quality, land surface displacement and GHG emissions were only monitored across the summer period. Monitoring for at least a year will make it possible to see seasonal differences and identify long-term patterns.

- *Oxygen passing through the clay layer* : The second recommendation is to further study the top clay layer. In this report, it was seen that the clay layer lowered the GHG emission compared to the measurement setup that was not covered by clay. However, knowledge on how the oxygen passes through the clay layer is missing.

  A possible method to see what happens in the clay layer is to dig out a 1 m x 1 m x 0.5 m piece of the subsurface at the end of the summer period. By doing so, it will be possible to see what has happened within the layer during the summer. Any cracks formed due to the clay drying out can be measured and an estimate can be made about how much oxygen can enter into the lower peat layer and how.

- *Future impact of applying measures* : The long-term water quality and GHG emission effects of the different measures are currently not well known. For example, the STOWA 2021 report summarizing possible effects raising water levels can have on biodiversity states that the raising of the water level could possibly create attractive habitats for cattle parasites and pathogens and that there is currently not enough knowledge on what raising the water level does to the botanical composition of the grass [STOWA, 2021].

  Further research into the possible (long-term) effects of raising groundwater levels or installing new measures is necessary before implementing the measures to avoid any future unexpected complications, especially when installing costly and permanent measures.

- *Practical and financial feasibility* : The final recommendation is to further work out the practical steps needed to implement the different measures and to accurately estimate their financial costs.

Bibliography

AHN. Actueel hoogtebestand nederland 3, 2019. Retrieved from https://ahn.arcgisonline.nl/ahnviewer/ on the 2021-08-09.

D. A. Algarni and A. E. Ali. Heighting and distance accuracy with electronic digital levels. *Journal of King Saud University - Engineering Sciences*, 10(2):229–239, 1998. doi: 10.1016/s1018-3639(18)30698-6.

L. Aquilina, V. Vergnaud-Ayraud, A. Armandine Les Landes, H. Pauwels, P. Davy, E. Pételet-Giraud, T. Labasque, C. Roques, E. Chatton, O. Bour, S. Ben Maamar, A. Dufresne, M. Khaska, C. Le Gal La Salle, and F. Barbecot. Impact of climate changes during the last 5 million years on groundwater in basement aquifers. 5(1), sep 2015. doi: 10.1038/srep14132.

S. van Asselen, G. Erkens, and F. de Graaf. Monitoring shallow subsidence in cultivated peatlands. *Proceedings of the International Association of Hydrological Sciences*, 382:189–194, apr 2020. doi: 10.5194/piahs-382-189-2020.

A.H.M. Bresser. *Effecten van klimaatverandering in Nederland*. Milieu en Natuur Planbureau, Bilthoven, 2005. ISBN 906960132X.

California State University. Regenerative agriculture practices that improve soil health, 2021. Retrieved from https://www.csuchico.edu/regenerativeagriculture/ra101-section/index.shtml on the 2021-06-01.

CBS. Rendementen en CO_2-emissie van elektriciteitsproductie in Nederland, update 2019. 2019. Retrieved from https://www.cbs.nl/nl-nl/achtergrond/2021/08/rendementen-en-co2-emissie-van-elektriciteitsproductie-in-nederland-update-2019 on the 2021-13-10.

Y. Chen, Q. Sun, and J. Hu. Quantitatively estimating of InSAR decorrelation based on landsat-derived NDVI. *Remote Sensing*, 13(13):2440, jun 2021. doi: 10.3390/rs13132440.

P.G.M. Clevering, J. Kamermans, and J. Horstman. Inventarisatie energieverbruik waterwerken. 2009. Grontmij.

F. de Vries. Biodiversiteit werkt voor verduurzaming van veenweidegebieden. *Programma Biodiversiteit*, 2011.

L.W. Dekker. Moldrainage in klei- en veengronden: waterafvoer door prefenete stroming via kunstmatige scheuren en gangen. *Strommingen*, 1999.

DINOlokket. Bodem- en grondonderzoek, 2021. Retrieved from https://www.dinoloket.nl/ondergrondgegevens on the 2021-08-09.

P. Doornenbal and R. Melman. Expert session: Fiber optics as land subsidence measurement technique. PowerPoint Presentation, 2021. Deltares.

EPA. Nitrification. *Office of groundwater and drinking water*, 2002.

G. Erkens, S. van Asselen, S. Hommes, R. Melman, H. van Meerten, and H. van Essen. Nationaal onderzoeksprogramma broeikasgassen veenweiden (NOBV)jaarrapportage 2019-2020. 2020.

EUSPA. What is GNSS?, 2021. Retrieved from https://www.euspa.europa.eu/european-space/eu-space-programme/what-gnss on the 2021-09-27.

P.A. Fokker, F.J. van Leijen, B.O., H. van der Marel, and R.F. Hanssen. Subsidence in the dutch wadden sea. *Netherlands Journal of Geosciences*, 97(3):129–181, sep 2018. doi: 10.1017/njg.2018.9.

Food and Agriculture Organization of the United Nations. Climate change and the global dairy cattle sector. 2019.

GalileoGNSS. The path to high gnss accuracy, 2018. Retrieved from https://galileognss.eu/the-path-to-high-gnss-accuracy/ on the 2021-09-27.

D. L. Galloway, D. R. Jones, and S.E. Ingebritsen. Measuring land subsidence from space, 2000.

I. Geijzendorffer, R. Scmidt, R. Engelbertink, T. Hermands, B. Schaap, J. Verhagen, and G. Blom-Zandstra. *Gevolgen van klimaatextremen voor de Nederlandse landbouw*. Alterra Wageningen, 2011.

Hach. *Water Analysis Guide*, 2013.

Harris-Galveston Subsidence District. Measuring subsidence, 2020. Retrieved from https://hgsubsidence.org/science-research/measuring-subsidence/ on the 2021-09-27.

R.L. Helz. Monitoring ground deformation from space, 2005.

Hoogheemraadschap van Rijnland. Gegevens waterkwantiteit Zwanburgerpolder, 2021. Email contact from Marinus Bogaard to Laura Nougues: 2021-04-05.

International Union for Conservation of Nature. Peatlands and climate change. November 2017. Retrieved from https://www.iucn.org/sites/dev/files/peatlands_and_climate_change_issues_brief_final.pdf on the 2021-09-07.

M.B. Kirkham. Field capacity, wilting point, available water, and the non-limiting water range. In *Principles of Soil and Plant Water Relations*, pages 101–115. Elsevier, 2005. doi: 10.1016/b978-012409751-3/50008-6.

KNMI. KNMI'14-klimaatscenario's voor Nederland; leidraad voor professionals in klimaatadaptatie. 2015.

KNMI. Maand en jaarsommen van de neerslag 0 - 24 utc (0.1 millimeter). 2021a. Retrieved from https://cdn.knmi.nl/knmi/map/page/klimatologie/gegevens/maandgegevens/mndgeg_240_rh24.txt on the 2021-08-09.

KNMI. Dagwaarden van weerstations. 2021b. Retrieved from https://www.daggegevens.knmi.nl/klimatologie/daggegevens on the 2021-11-06.

C. Kwakernaak, J.J.H. van den Akker, E.M. Veenendaal, J. van Huissteden, and P. Kroon. Mogelijkheden voor mitigatie en adaptatie veenweiden en klimaat. *Bodem*, 2010.

D. Loucks. *Water resources systems planning and management : an introduction to methods, models and applications*. UNESCO, Paris, 2005. ISBN 9231039989.

J.C. Lynch, P. Hensel, and D.R. Cahoon. The surface elevation table and marker horizon technique: A protocol for monitoring wetland elevation dynamics. *Natural Resource Report*, 2015.

D. Melman, N. Jonker, and J. van de Salm. Veldbezoek zwanburgerpolder 6 mei en 27 augustus 2021: biodiversiteit, bodemvocht en bodemweerstand. 2021.

D. Moens. Carbon farming techniques potentially appliable to boerderij de eeenzaamheid. *Climate Fund Managers*, 2020.

D.A. Morris and A.I. Johnson. Summary of hydrologic and physical properties of rock and soil materials, as analyzed by the hydrologic laboratory of the u.s. geological survey, 1948-60. Technical report, 1967.

D. M. Narain-Ford, R. P. Bartholomeus, S. C. Dekker, and A. P. van Wezel. *Natural Purification Through Soils: Risks and Opportunities of Sewage Effluent Reuse in Sub-surface Irrigation*, pages 85–117. Springer International Publishing, Cham, 2020. ISBN 978-3-030-67852-4. doi: 10.1007/398_2020_49. URL `https://doi.org/10.1007/398_2020_49`.

R.P. Ojha, C.L. Verma, D.M. Denis, C.S. Singh, and M. Kumar. Modification of inverse auger hole method for saturated hydraulic conductivity measurement. *Journal of Soil and Water Conservation*, 16(1):47, 2017. doi: 10.5958/2455-7145.2017.00011.x.

J. Onrust. Earth, worms and birds. *Conservation Ecology Group, Groningen Institute for Evolutionary Life Sciences*, 2017.

J. Onrust, E. Wymenga, T. Piersma, and H. Olff. Earthworm activity and availability for meadow birds is restricted in intensively managed grasslands. *Journal of Applied Ecology*, 56(6):1333–1342, mar 2019. doi: 10.1111/1365-2664.13356.

M. Pleijter and J.J.H. van den Akker. Onderwaterdrains in het veenweidegebied: toelichting op de methode en meetinrichting. *Alterra-rapport*, 2007.

J. Päivänen. Hydraulic conductivity and water retention in peat soils. 0(129), 1973. doi: 10.14214/aff.7563.

Regenerative Agriculture Initiative. What is regenerative agriculture?, 2017. Retrieved from https://regenerationinternational.org/2017/02/24/what-is-regenerative-agriculture/ on the 2021-06-01.

RIVM. Factoren van invloed op fosfoor en stikstof, 2020. Retrieved from https://www.rivm.nl/landelijk-meetnet-effecten-mestbeleid/resultaten/factoren-van-invloed on the 2021-10-31.

P. Roncken, S. Slabbers, and H. Veenenbos. *Een nieuwe aanpak voor de veenweiden van het Groene Hart : Naar optimale combinaties van bodem, water en landgebruik*. Wageningen : Blauwdruk, 2019.

SkyGeo. Bodemdalingskaart, 2018. Retrieved from https://www.atlasleefomgeving.nl/kaarten?config=3ef897de-127f-471a-959b-93b7597de188gm-b=1544180834512%2Ctrue%2C1%3B1553094282854%2Ctrue%2C0.8%3Bgm-x=150000gm-y=455000gm-z=3 on the 2021-10-09.

G. Slingerland. Geschiedenis en toekomst van de zwanburgerpolder. 2006.

STOWA. Omschrijving mep en maatlatten voor sloten en kanalen voor de kaderrichtlijn water 2015-2021. 2012.

STOWA. Biodiversiteit, bodem- en waterkwaliteit: een inventarisatie van de haalbaarheid van maatregelen in het veenweidegebied. 2021.

W. Sukkel, F.Cuperus, and D. van Apeldoorn. Biodiversiteit op de akker door gewasdiversiteit. *De Levende Natuur*, 2019.

M. Takalo and P. Rouhiainen. Development of a system calibration comparator for digital levels in finland. *Finnish Geodetic Institute*, 2004.

A.P. Uijl. *Flushing meadows : the influence of management alternatives on the greenhouse gas balance of fen meadow areas*. S.l, 2010. ISBN 9789085857181.

M. Vaartjes. Nulsituatie Zwanburgerpolder, 2020. Hoogheemraadschap van Rijnland.

J.J.H. van den Akker, J. Beuving, R.F.A. Hendriks, and R.J. Wolleswinkel. Maaivelddaling, afbraak en CO_2-emissie van Nederlandse veenweidegebieden. *Leidraad Bodembeshcerming*, 2007.

J.J.H. van den Akker, R.F.A. Hendriks, I.E. Hoving, and M.Pleijter. Toepassen van onderwaterdrains in veenweidegebieden: effecten op maaivelddaling, broeikasgasemissies en het water. *Landschap*, 2010.

E. van der Swaluw, J.H. Verboom, J.P.J. Berkhout, A.P. Stolk, and R. Hoogerbrugge. A comparison of the old and new wet-only samplers of the dutch national precipitation chemistry monitoringnetwork. *RIVM*, 2010.

H. van Dijk. Waterkwaliteit 2: Natuur en chemie, 2008. Lecture presentation, Water Management TU Delft.

J.W. van Hoorn. Determining hydraulic conductivity with the inversed auger hole and infiltrometer methods. *Agricultural University Wageningen*, 1979.

P.T.M. Vermeulen, F.J. Roelofsen, J. Hunnink, G.M.C.M. Janssen, B. Romera Verastegui, J. van Engelen, and M. Russcher. imod user manual, 2021. Published by Deltares.

Wageningen University and Research. Natuurinclusieve landbouw, 2019. Retrieved from https://v3.jamdots.nl/view/30079/Natuur-Inclusieve-Landbouw on the 2021-06-01.

Delft Blue Water. Oppervlaktewaterproductie. 2013.

M. Wesselink. The netherlands: breaking maize monoculture. 2019. Retrieved from: https://www.diverimpacts.net/case-studies/case-study-1-nl.html on th 2021-09-27.

Wheeling University. Water quality assessment: Chemical: Dissolved oxygen and biochemical oxygen demand, 2004. Retrieved from http://www.cotf.edu/ete/modules/waterq3/WQassess3f.html on the 2021-08-09.

A

Zwanburgerpolder shallow subsurface composition

Figure A.1 shows the 82 boreholes collected from DINOloket that were used to reconstruct the shallow subsurface composition of the Zwanburgerpolder. Using the DINOloket borehole data, an interpolation was made of the top 2 m of the subsurface. The results of these interpolations can be seen in Figures A.2 and A.3. From the interpolations, maps showing the thickness of the top three subsurface layers were made, see Figures A.4, A.5 and A.6.

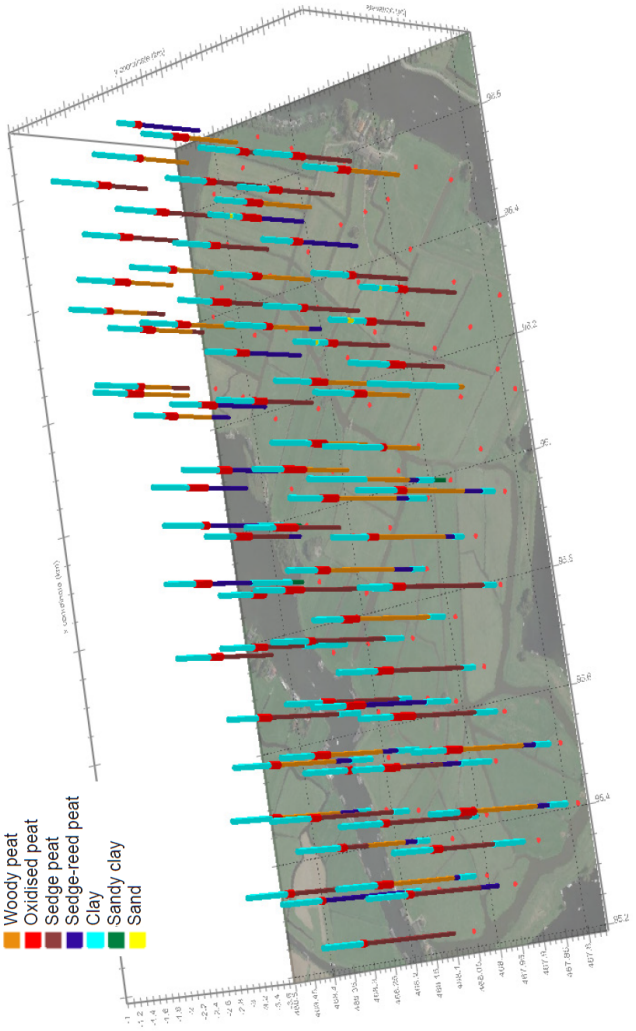

Figure A.1: Borehole subsurface composition data [DINOlokket, 2021].

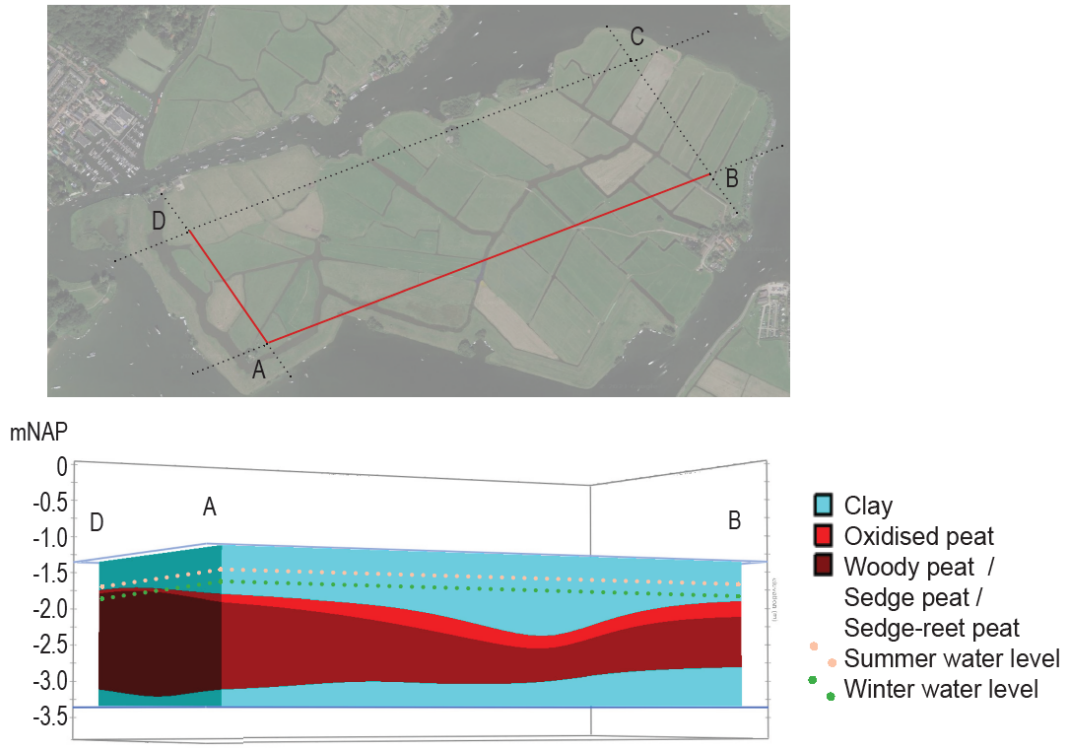

Figure A.2: Subsurface composition of the South West

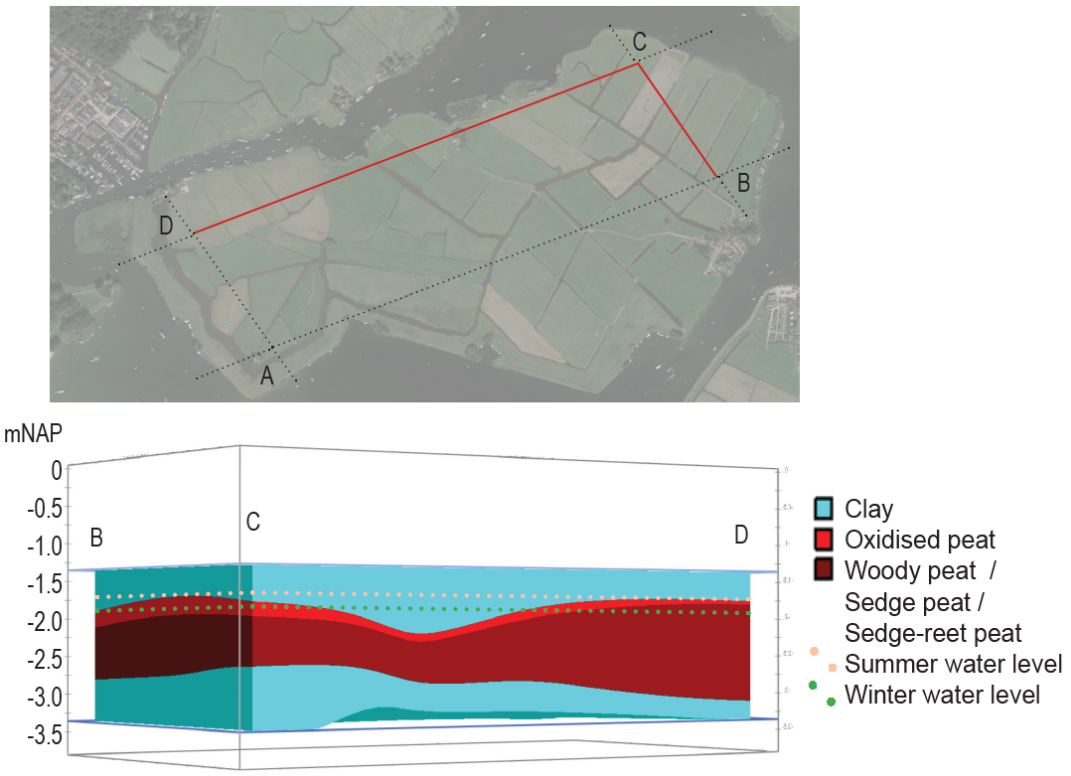

Figure A.3: Subsurface composition of the North East

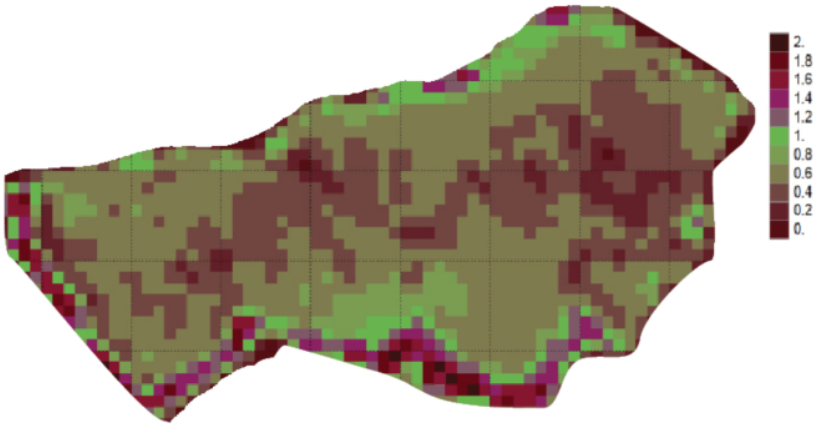

Figure A.4: Thickness top clay layer across polder, in meters.

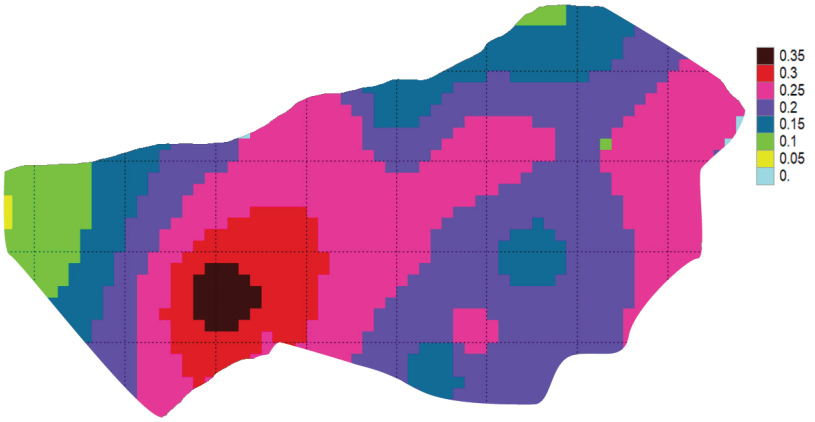

Figure A.5: Thickness oxidised peat layer across polder, in meters.

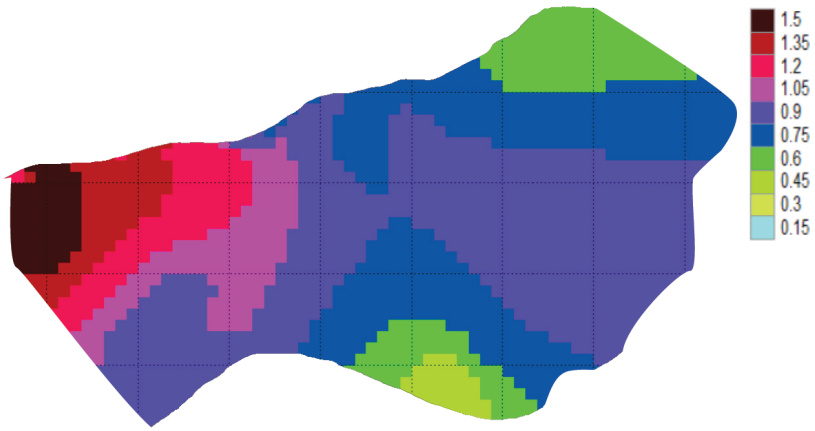

Figure A.6: Thickness unoxidised peat layer across polder, in meters.

B

iMOD

B.1. What is iMOD?

iMOD is a graphical user interface version of MODFLOW made by Deltares. An important difference between iMOD and other modeling packages is that when using iMOD it is possible to add layers together with different resolutions and sizes. The data does not have to be clipped beforehand or pre-processed to a specific model grid resolution. iMOD performs any necessary up and down scaling to the wanted model grid resolution.

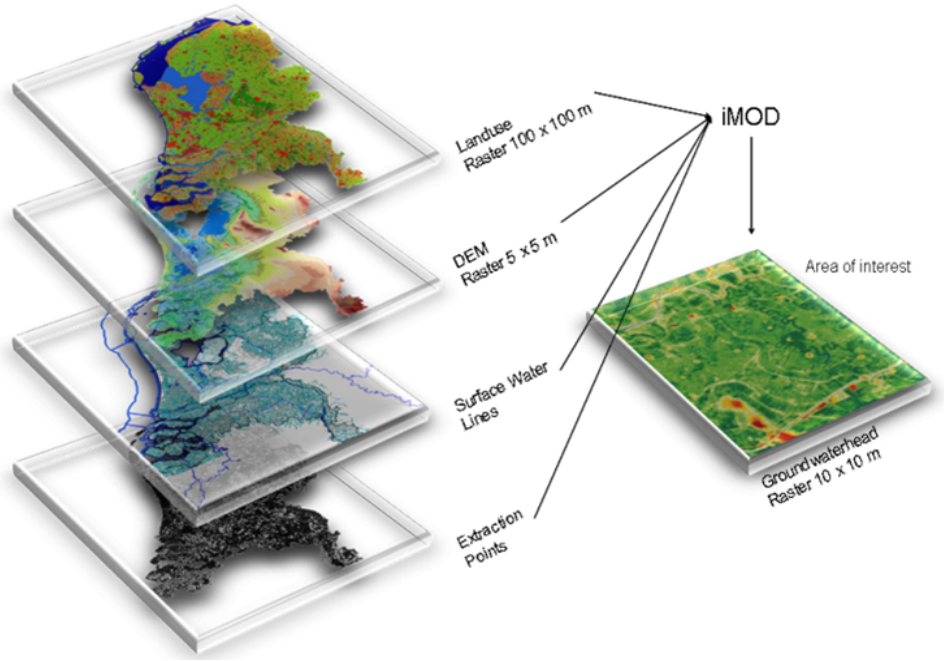

Figure B.1: iMOD layer approach [Vermeulen et al., 2021]

Within iMOD it is possible to visualize data in both 2D and 3D. This includes data like borehole data, groundwater streamlines, groundwater heads and much more. This makes iMOD an attractive tool when working with different stakeholders, as the results can all be clearly presented.

B.2. Current Zwanburgerpolder model set up

In the sections below, the input parameters used to make the iMOD model for the current situation of the Zwanburgerpolder are described.

Subsurface composition

To start off, subsurface data was collected from GeoTop, a 3D voxel model of the top 50 m of the subsurface composition of the Netherlands. GeoTop cells are 100 m x 100 m horizontally and half a meter vertically. For the Zwanburgerpolder model, this data was used to map out the deeper subsurface, between 2 m below the

surface level to 15 m. At a depth of 15 m, the deep Pleistocene sand layer is reached. The GeoTop subsurface composition can be seen in Figure B.2.

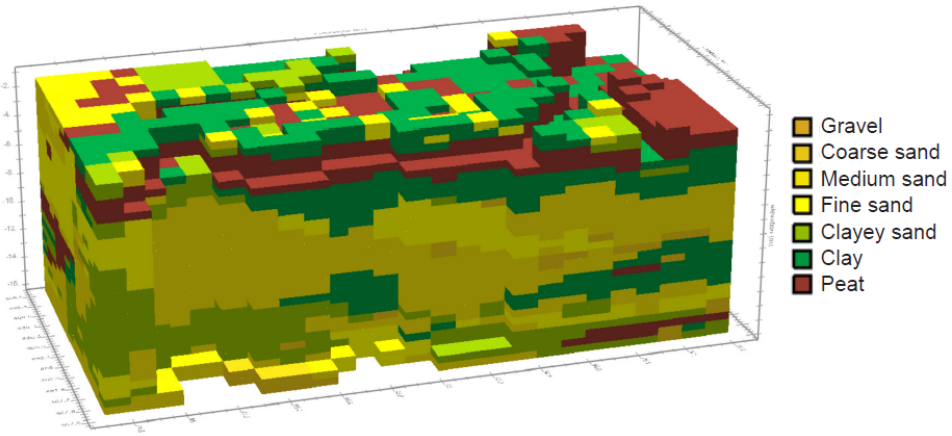

Figure B.2: Subsurface composition gathered from GeoTop data

Next to the large 100 m x 100 m cells collected from GeoTop, borehole data from 82 shallow boreholes across the island was collected from DINOlokket. This data was used to map out the top 2 m of the subsurface as with such a high spatial distribution, it was possible to represent the shallow subsurface more accurately compared to using GeoTop data. The borehole logs for the Zwanburgerpolder can be seen below in Figure A.1. The different borehole lithologies were interpolated to create the subsurface composition across the whole polder. The borehole interpolation layer can be seen in Figures A.3 and A.2.

Added parameters
In Table B.1, the different iMOD parameters used to set up the model can be found. The table also shows whether these parameters are layer based or model based, season based or constant, and which value they were given. The input parameters for each different lithology can be seen in Table B.2, the seasonal parameters in Table B.3 and the model boundary can be seen in Figure B.3. The summer period is defined as April 1st until September 30th and the winter period from October 1st until March 31st. For the model of the current Zwanburgerpolder situation, climate data (precipitation and evaporation) from October 1st 2019 till September 30th 2021 collected from the KNMI was used [KNMI, 2021b].

As explained in Chapter 4.1.3, the used hydraulic conductivities for the peat and clay layers are based off of the results from the inverse auger tests and an iterative process in which the hydraulic conductivities were changed into the model until the modelled groundwater level matched with the measured groundwater level. All other values were based off literature values.

For layer 8, the model layer at the top of the first sandy aquifer, the model boundary was set to -1 making it a layer with a constant head. From the pressure monitoring data, it was seen that across the study period, the aquifer had approximately a constant head of -1.6 m NAP.

Table B.1: Packages used in the iMOD model of the 2021 Zwanburgerpolder situation.

Package	Parameter	Application	Season dependent	Value	Unit	Comment
BND	Model boundary	Per layer	No	Figure B.3	-	0= inactive cell, >0= active cell, <0= fixed for each model layer.
SHD	Starting head	Per layer	No	−1.45	mNAP	To model the pressure head in the first aquifer layer, a constant head of −1.6 mNAP was given to layer 6, the top layer of the aquifer.
KHV	Horizontal permeability	Per layer	No	Table B.2	m/day	
KVA	Vertical anisotropy	Per layer	No	TableB.2	-	KVA = KVV / KHV
KVV	Vertical permeability	Per layer	No	Table B.2	m/day	Not in bottom layer.
SPY	Specific yield	Per layer	No	Table B.2	-	
POR	Porosity	Per layer	No	Table B.2	-	
TOP	Top level	Per layer	No	Every 0.5m from -1m NAP	m NAP	
BOT	Bottom level	Per layer	No	Every 0.5m till -16m NAP	m NAP	
STO	Storage coefficient	Per layer	No	Table B.2	-	Specific storage coefficient x layer thickness
RIV	Conductance of drainage system	Per model	Yes	Table B.3	m^2/day	The RIV package was used to represent the ditches in the polder.
	Elevation of water level	Per model	Yes	Table B.3	m NAP	
	Elevation of bottom level	Per model	Yes	Table B.3	m NAP	
	Infiltration factor	Per model	Yes	Table B.3	-	0 = no infiltration, >0 infiltration allowed
RGH	Recharge strength	For layer 1	Yes	Daily precipitation surplus collected from KNMI	mm/day	

Table B.2: Parameters used per lithology class in the iMOD model of the 2021 Zwanburgerpolder situation. 1 [Morris and Johnson, 1967].

Lithology	Specific yield [-] [1]	Porosity [-][1]	Hor Per [m/day][1]	Ver Per [m/day][1]	Anistropy [-]
Coarse sand	0.30	0.39	30.00	20.000	0.67
Medium sand	0.32	0.39	7.50	5.000	0.67
Fine sand	0.33	0.40	1.50	1.000	0.67
Clayey sand	0.10	0.43	0.50	0.010	0.02
Clay	0.06	0.46	0.01	0.001	0.10
Peat	0.44	0.92	2.00	0.100	0.05

Table B.3: Parameters used for seasonal variables in the iMOD model of the 2021 Zwanburgerpolder situation.

Parameter	Summer	Winter	Unit
Boezem conductance	625.00	625.00	m^2/day
Boezem water level elevation	−0.60	−0.64	m NAP
Boezem bottom level elevation	−4.04	−4.04	m NAP
Boezem infiltration factor	0.30	0.30	-
Main ditches conductance	1.00	1.00	m^2/day
Main ditches water level elevation	−1.71	−1.81	m NAP
Main ditches bottom level elevation	−2.51	−2.51	m NAP
Main ditches infiltration factor	0.30	0.30	-
Side ditches conductance	1.00	1.00	m^2/day
Side ditches water level elevation	−1.71	−1.81	m NAP
Side ditches bottom level elevation	−2.11	−2.11	m NAP
Side ditches infiltration factor	0.30	0.30	-

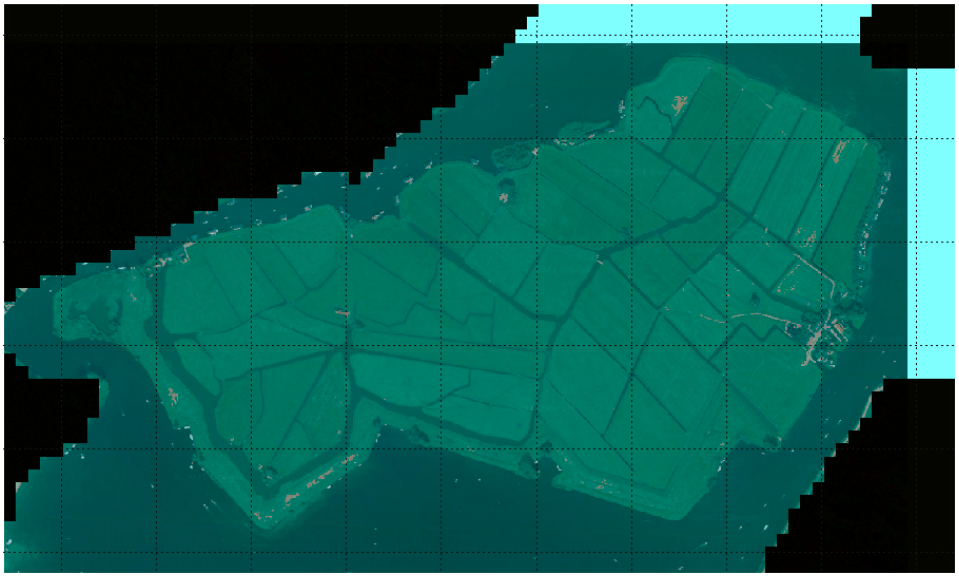

Figure B.3: Model boundary, the blue highlighted region was taken into account for this model. The boezem and the island were set to 1 (active cells) and the black surroundings were set to 0 (inactive cells).

B.3. Future Zwanburgerpolder scenarios

In the section below, the added parameters used in the future models are shown. For all five measures, climate data (precipitation and evaporation) based on the KNMI'14 scenarios [KNMI, 2015] was used for October 1st 2062 till September 30th 2065.

Adding ditches

For this measure, ditches were added along the middle of each parcel. The ditches were added using the RIV package, and got the same characteristics as the side ditches in the 2021 model.

Installing horizontal drains
To model the influence of installing horizontal drains, drains with a drain spacing of 12 m [Pleijter and van den Akker, 2007] were added to each parcel. The drains were added using the iMOD DRN package. For this, two input parameters were needed: the elevation of the drains and the conductance. The drains were installed at -1.76 mNAP and were given a conductance of 1.00 m^2/day.

Temporarily inundating parcels
Here, the recharge between the 10^{th} and the 13^{th} of June was increased to 20 mm/day.

Installing vertical drains
As the vertical drains connect to a horizontal drain installed down the middle of the parcels, this measure was modelled similarly to the horizontal drain measure. Meaning, a horizontal drain was added using the DRN package. The elevation of the drain was put at -1.60 mNAP, the pressure head in the aquifer and the conductance was made 1.00 m^2/day.

Raising the ditch water level
For this final method, the summer ditch water levels were raised from -1.71 mNAP to -1.51 mNAP in the RIV package.

C

Monitored groundwater pressure head time series

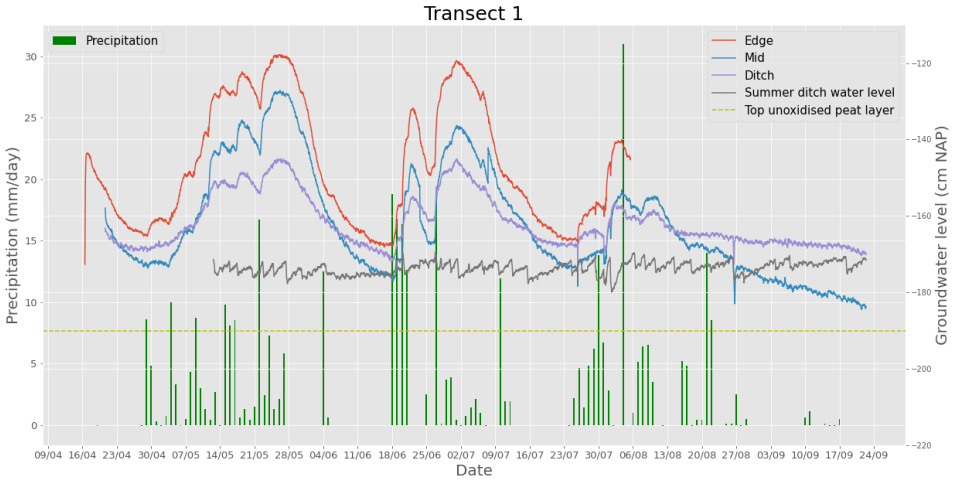

Figure C.1: Pressure monitor data for the boreholes along Transect 1 between the 16th of April and the 23rd of September.

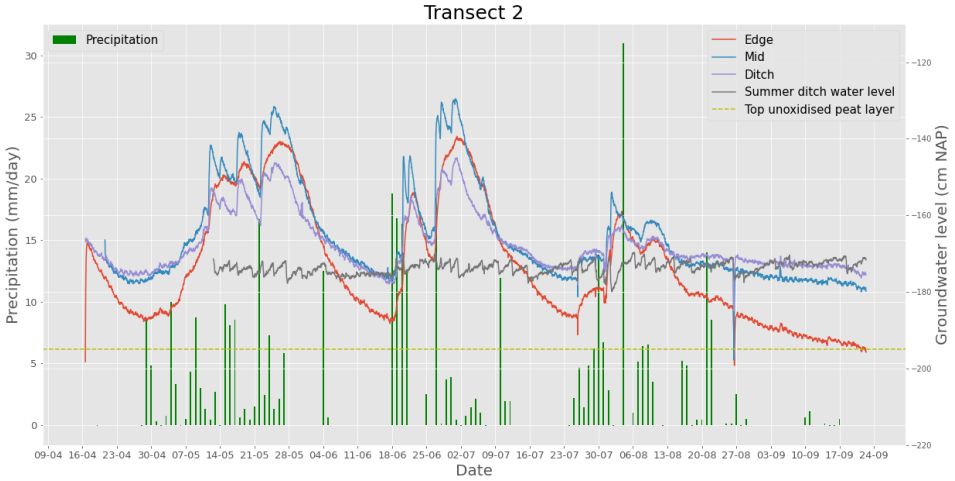

Figure C.2: Pressure monitor data for the boreholes along Transect 2 between the 16th of April and the 23rd of September.

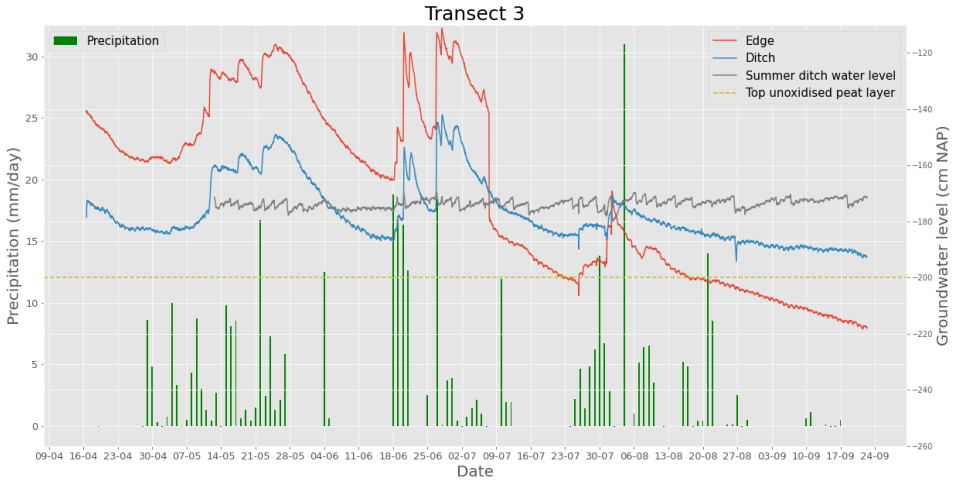

Figure C.3: Pressure monitor data for the boreholes along Transect 3 between the 16th of April and the 23rd of September.

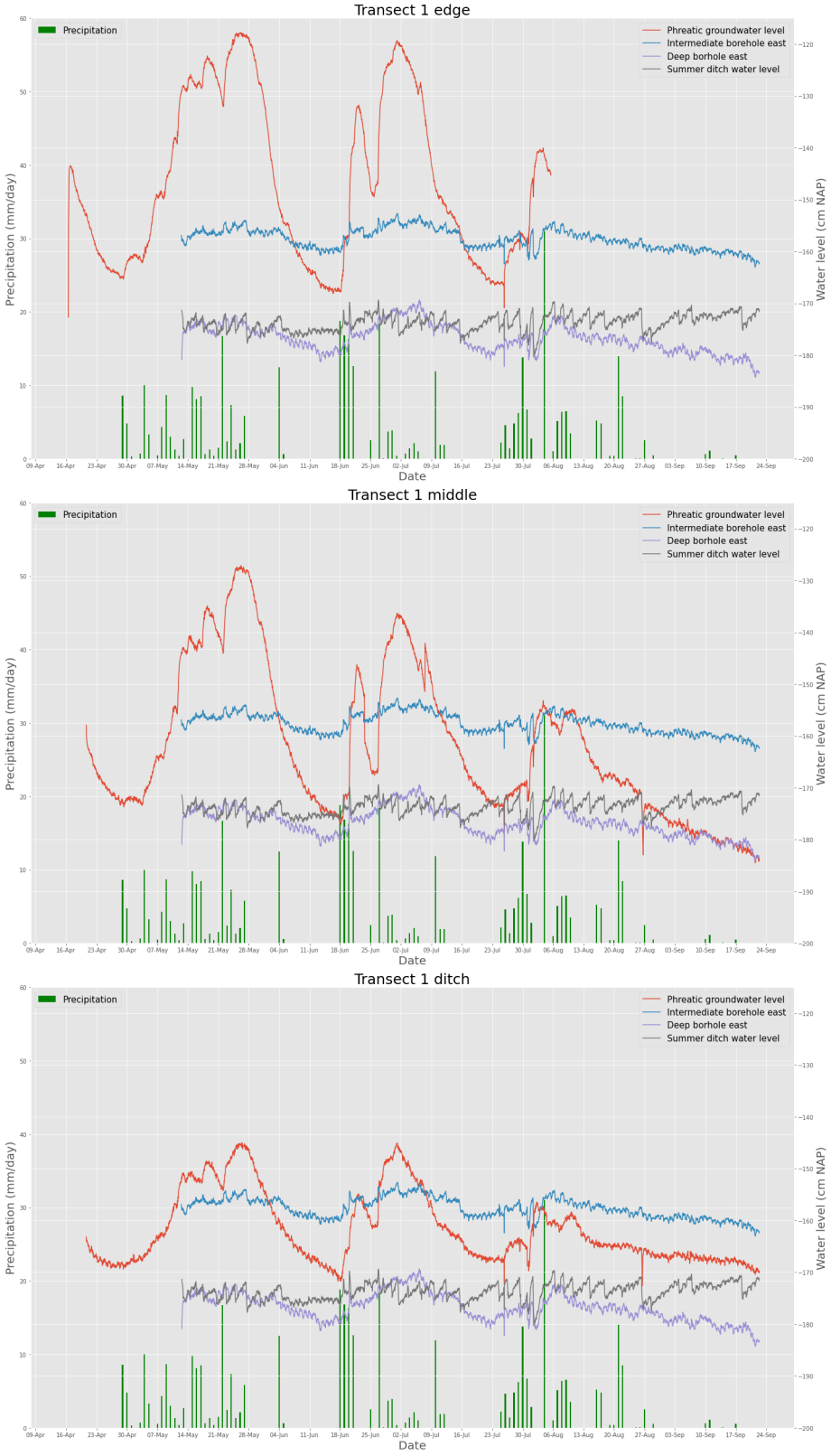

Figure C.4: Pressure monitor data for the boreholes along Transect 1 as well as the deep borehole pressure monitor data between the 16th of April and the 23rd of September.

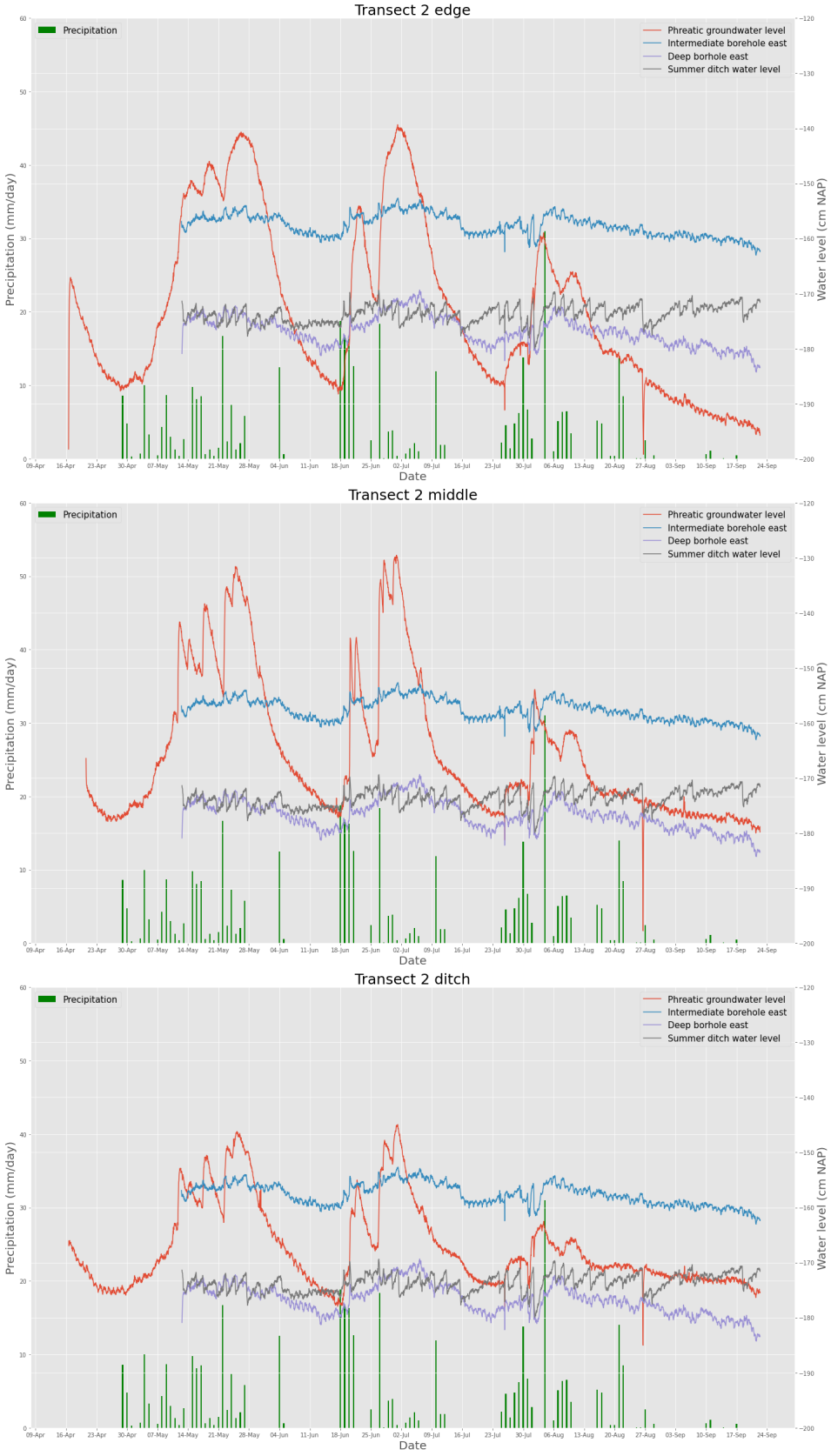

Figure C.5: Pressure monitor data for the boreholes along Transect 2 as well as the deep borehole pressure monitor data between the 16th of April and the 23rd of September.

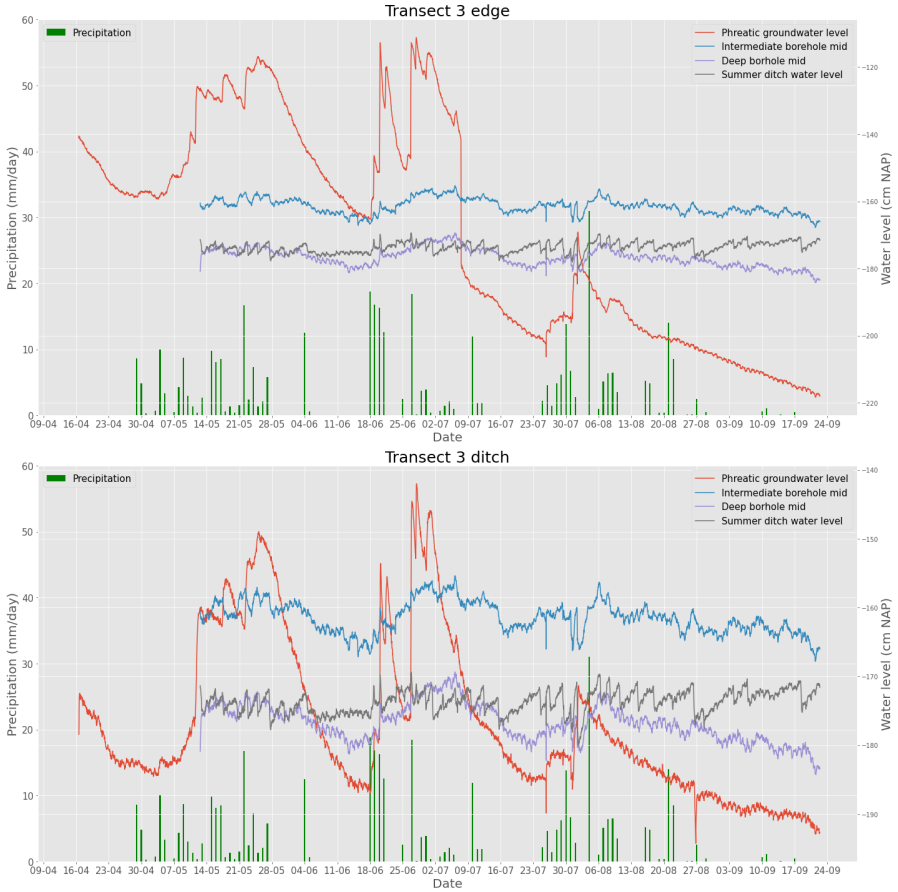

Figure C.6: Pressure monitor data for the boreholes along Transect 3 as well as the deep borehole pressure monitor data between the 16th of April and the 23rd of September.

D

Historical surface water quality data collected by Rijnland

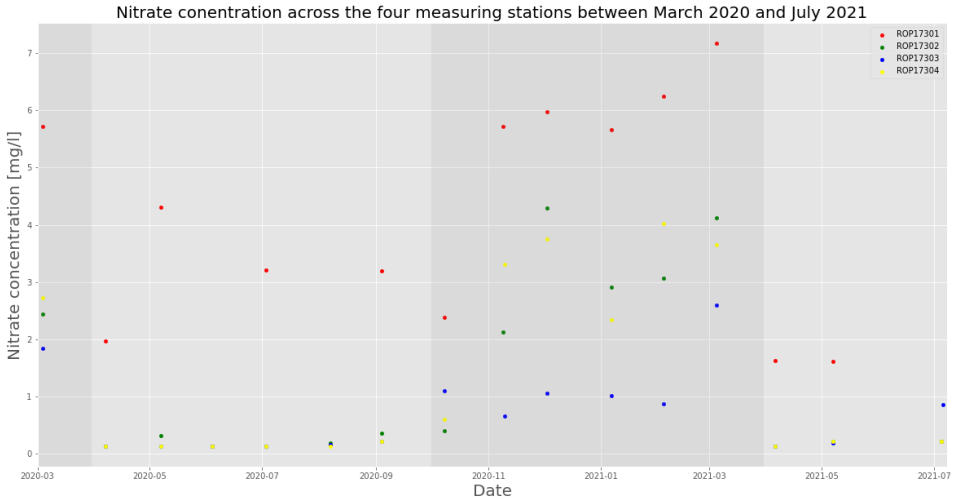

Figure D.1: Monthly variations in nitrate concentrations across the four sample locations for Rijnland's total sampling period.

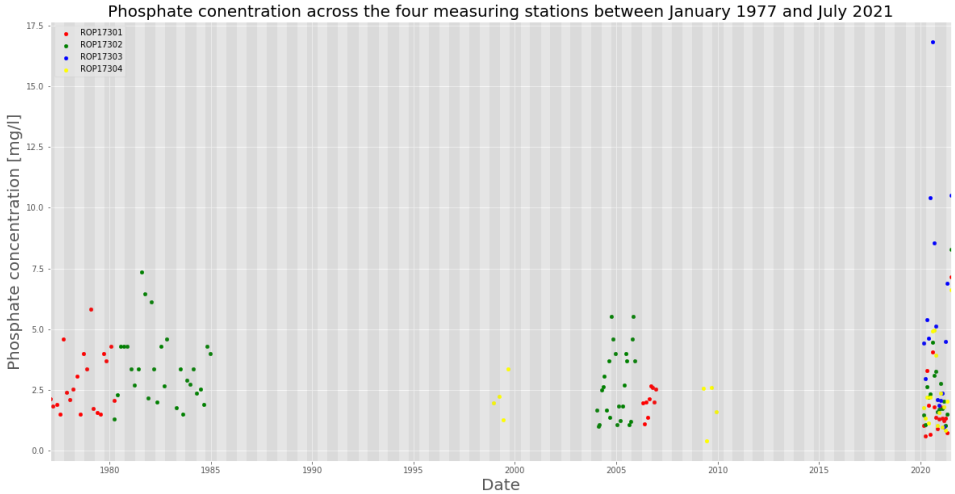

Figure D.2: Monthly variations in phosphate concentrations across the four sample locations for Rijnland's total sampling period.

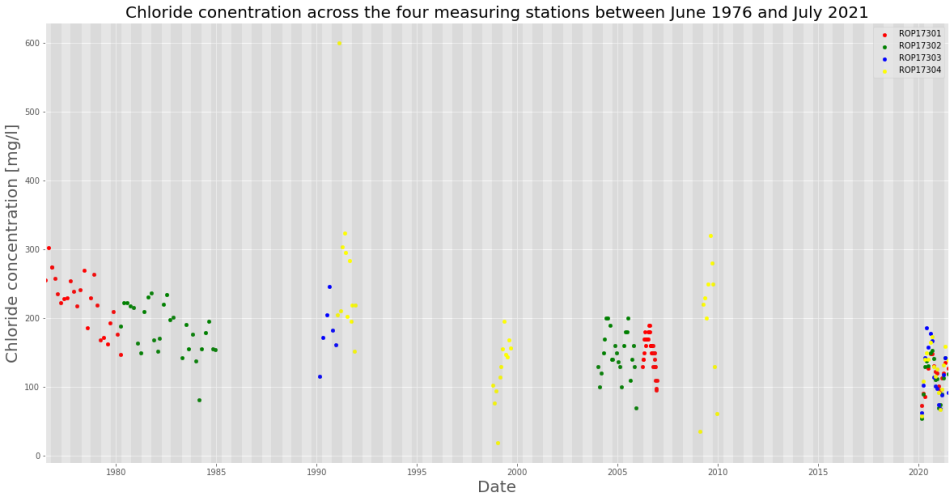

Figure D.3: Monthly variations in chloride concentrations across the four sample locations for Rijnland's total sampling period.

E

GHG conversions from ppm to a rate

To convert the MGGA values found in Chapter 6.2 to a rate, the following steps were undertaken. Firstly, the slope of each graph (CO_2 and CH_4) was calculated. Then certain values needed to be known: the volume of the air in each flux chamber (ZZZ) in liters, the surface area of the flux chambers (YYY) in square meters and the volume of 1 mol ideal gas at the temperature of the measurements (XXX) in liters. For a temperature of 12.8°C, the outside temperature during the measurements, the volume of 1 mol ideal gas is 23.47 l. With the calculated and collected values, the following conversions could be applied:

CH_4 flux
ppm/sec to mmol/sec:

$$\frac{\frac{\text{Slope}}{10^6}}{\text{XXX}} \times 1000 \times \text{ZZZ} \tag{E.1}$$

mmol/sec to *u*mol/h:

$$\text{mmol/sec} \times 1000 \times 60 \times 60 \tag{E.2}$$

*u*mol/h to *u*g/h:

$$u\text{mol/h} \times 16.04 \tag{E.3}$$

*u*g/h to *u*g/m^2/h:

$$\frac{u\text{g/h}}{\text{YYY}} \tag{E.4}$$

CO_2 flux
ppm/sec to mmol/sec:

$$\frac{\frac{\text{Slope}}{10^6}}{\text{XXX}} \times 1000 \times \text{ZZZ} \tag{E.5}$$

mmol/sec to *u*mol/h:

$$\text{mmol/sec} \times 1000 \times 60 \times 60 \tag{E.6}$$

*u*mol/h to mg/h:

$$u\text{mol/h} \times 44.0095 \tag{E.7}$$

mg/h to mg/m^2/h:

$$\frac{\text{mg/h}}{\text{YYY}} \tag{E.8}$$

In the table below, the different slopes, volumes and areas used in this study can be seen along with the results of the conversions described above.

Table E.1: Conversion steps from CO_2 and CH_4 emissions in ppm to a rate in mg/m^2/h.

	Slope [ppm/sec]		Volume gas cylinder	Surface area tube	CH_4 flux				CO_2 flux			
	CO_2	CH_4	[L] (ZZZ)	[m^2] (YYY)	mmol/sec	$u$mol/h	uh/h	ug/m^2/h	[mmol/sec]	[mmol/h]	[mg/h]	[mg/m^2/h]
Undeep	0.0000	0.0000	1.8997	0.0044	0.00000000	0.00	0.00	0.00	0.0000000	0.00	0.00	0.00
Middeep	0.4760	0.0003	1.3696	0.0044	0.00000002	0.06	1.04	235.67	0.0000278	0.10	4.40	996.10
Deep	0.0133	0.0003	3.2693	0.0044	0.00000005	0.17	2.68	606.27	0.0000019	0.01	0.29	66.44
Borehole	0.1000	0.0208	0.0271	0.0001	0.00000002	0.09	1.39	12301.36	0.0000001	0.00	0.02	162.01
Grass	0.4167	0.0000	19.4848	0.0661	0.00000000	0.00	0.00	0.00	0.0003459	1.25	54.81	829.81
Water	0.0642	0.0013	11.6909	0.0661	0.00000062	2.24	35.95	544.34	0.0000320	0.12	5.07	76.71

F

GHG CO_2 equivalent emissions

In a paper written by the Food and Agriculture Organization (FAO) in 2015, it was stated that the amount of methane produced by a cow during enteric fermentation is equal to 80.9 kg CH_4 per year. Further, the FAO also established the percentage of the different sources contributing to GHG emissions in dairy systems, see Figure F.1.

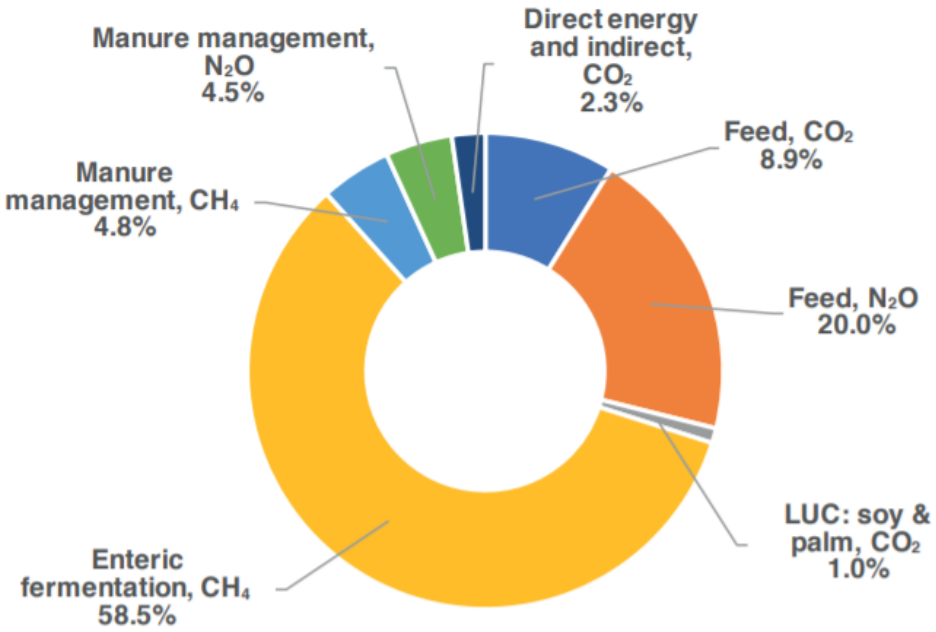

Figure F.1: Emissions sources from global dairy cattle systems in 2015 [Food and of the United Nations, 2019].

Knowing that 58.5 % of the emissions is equivalent to 80.9 kg CH_4 per year [Food and of the United Nations, 2019], it was possible to translate the percentages for feeding, land management and manure management into kg GHG per year, resulting in:

Table F.1: Dairy farming percentage of components translated into kg GHG/year.

Emitter	Process	Percentage CH_4	Percentage N_2O	Percentage CO_2	kg CH_4/year/cow	kg N_2O/year/cow	kg CO_2/year/cow
Cows	Enteric fermentation	58,50	-	-	80,90	-	-
Land management and feed production	Mowing, liming, feed production and importing	-	20,00	8,90	-	27,66	12,31
Manure management	Spreading	4,80	4,50	-	6,64	6,22	-

The next step was to convert the CH_4 and N_2O components into CO_2 equivalent values. To do this, the following conversion factors were used [Kwakernaak et al., 2010]:

Table F.2: GHG to CO_2 equivalent conversion factors [Kwakernaak et al., 2010].

CH_4 factor	N_2O factor	CO_2 factor
23	296	1

By multiplying the values found in Table F.1 by the conversion factors from above and adding the yearly energy consumption for the dairy production obtained through Joost van Schie and the peat oxidation component, the final CO_2 equivalent values for the farm were found and displayed in Table 6.3. These values are the emissions per cow and per hectare. As there are fifty dairy cows at the Eenzaamheid, excluding calves, and 40 ha of land, the total CO_2e emissions created by the Eenzaamheid become:

Table F.3: Total CO_2 e emissions created by the Eenzaamheid.

	t CO_2e
Dairy farming with 50 cows	613.83
Peat oxidation for 40.47ha	1214.10
Total	1827.93